



universität
wien

DIPLOMARBEIT

Titel der Diplomarbeit

Investigation of direct interaction between Myc and the Myc-target BASP1

angestrebter akademischer Grad

Magister der Naturwissenschaften (Mag. rer. nat.)

Verfasserin / Verfasser:	Leonhard Geist
Matrikel-Nummer:	0108014
Studienrichtung (lt. Studienblatt):	Molekulare Biologie
Betreuerin / Betreuer:	Robert Konrat

Wien, am 23.10.2008

Investigation of direct interaction between Myc and the Myc-target BASP1

Diplomarbeit

Vorgelegt am
Institut für biomolekulare Strukturchemie
an der
Universität Wien
2008

Verfasst
von

Leonhard Geist

Betreut
von

**Robert Konrat
und
Bettina Schweng**

Danksagung

An dieser Stelle möchte ich mich bei all denjenigen bedanken, die es mir ermöglicht haben, diese Arbeit zu verfassen.

Mein größter Dank gilt meiner Familie, meinen Eltern Maria und Ernst und meinen Geschwistern Anna-Maria und Clemens, die mich in allen Phasen meines Lebens bestens unterstützt haben und mir nicht nur mein Studium und meine berufliche Laufbahn ermöglicht haben, sondern auch meinen Enthusiasmus für Musik mit mir teilen und mich in meinen musikalischen Aktivitäten immer gefördert und bestärkt haben.

Ich möchte mich auch bei allen meinen Freunden und Bekannten bedanken, die mich besonders während meines Studiums begleitet und unterstützt haben.

Weiters will ich mich bei all jenen bedanken, die mir die nötigen Mittel bereitgestellt und mir bei der Planung und Durchführung meiner Arbeit immer bereitwillig zur Seite gestanden sind. Dies schließt alle Mitglieder der Gruppe für NMR (Robert Konrat) ein. Im Besonderen möchte ich mich bei meinen Betreuern Robert Konrat und Bettina Schweng bedanken und bei Martina Ortbauer, Karin Ledolter und Christoph Kreutz für die technische Unterstützung. Danke auch für die angenehme und lockere Arbeitsatmosphäre, für die gemütlichen (und lehrreichen) Kaffeepausen und den unglaublichen Enthusiasmus und Optimismus, den diese Gruppe auszeichnet. Außerdem will ich mich auch bei allen Mitgliedern der Gruppe für Kristallographie (Kristina Djinovic-Carugo) bedanken, besonders bei Patrizia Abrusci, die mir bei vielen molekularbiologischen Fragestellungen behilflich war.

Auch ein großer Dank gilt der Gruppe Klaus Bister des Instituts für Biochemie der Universität Innsbruck. Besonders will ich mich bei Markus Hartl für sein Engagement und bei Taras Valovka und Theresia Matt für ihre Hilfsbereitschaft bedanken.

Schlussendlich will ich mich auch bei der Gruppe Marc Haenlin des Zentrums für Entwicklungsbiologie an der Universität Paul Sabatier in Toulouse bedanken für die sehr schöne und lehrreiche Zeit in ihrem Team während meines Aufenthalts in Frankreich. Einen besonderen Dank will ich Marc Haenlin, Lucas Waltzer, Benoit Augé und meiner Betreuerin Géraldine Ferjoux für ihre Geduld aussprechen.

Es gibt natürlich noch viele mehr, die ich hier nicht namentlich erwähnt habe, aber die meiner Dankbarkeit bewusst sein sollen.

Zusammenfassung

Brain Acid-Soluble Protein 1 (BASP1) ist ein intrinsisch unstrukturiertes Protein, das in Mechanismen wie dem Auswachsen und der Plastizität von Neuronen involviert ist und vor kurzem als Co-Suppressor des Wilms' tumor suppressor protein 1 (WT1) entdeckt wurde. Diese Co-Suppressor Aktivität wird durch Interaktion von BASP1 mit der WT1 Suppressions-Region vermittelt. Außerdem wurde eine Änderung der subzellulären Lokalisation von BASP1 in HeLa Zellen nach Induktion von Apoptose festgestellt.

Ein neu entwickelter Algorithmus (Robert Konrat), der Proteine aufgrund ihrer so genannten Meta-Struktur untersucht, prognostiziert für eine 20-40 Aminosäuren lange Region von BASP1 eine große Wahrscheinlichkeit für Protein Interaktion. Auch die Sekundärstruktur des interagierenden Proteins (bzw. des relevanten Teils des Proteins) kann durch die Meta-Struktur Analyse vorhergesagt werden. Im Fall von BASP1 interagiert die genannte Region wahrscheinlich mit einem Loop oder einem β -Faltblatt Segment eines anderen Proteins. Damit übereinstimmend, prognostiziert Meta-Struktur Analyse eine Loop oder β -Faltblatt Konformation und eine hohe Wahrscheinlichkeit für Protein Interaktion für die Suppressions-Region von WT1. Folglich stimmt Meta-Struktur Analyse mit der beobachteten Interaktion zwischen BASP1 und WT1 überein.

Aktuelle Studien konstatierten eine differentielle Expression von BASP1 in MC29 transformierten Zelllinien embryonaler Fibroblasten von Huhn und Wachtel. Das MC29 Virus codiert für das onkogene v-Myc Protein, welches nach Infektion der Zelllinie überexprimiert wird und schlussendlich, schon auf Ebene der Transkription, zur Repression von BASP1 führt. Überraschenderweise, hindert ektopische Expression von BASP1 in MC29 infizierten Zellen die Transformation der Zellen durch v-Myc. Andere Studien mit einem so genannten „cell penetrating peptide“ (ein Peptid, das die Zellmembran penetrieren kann), das ein 20 Aminosäuren langes Segment der prognostizierten Protein Interaktions Region von BASP1 beinhaltet, konstatierten einen starken „zell-schwächenden“ Effekt (cytopathic effect) dieses Peptids auf embryonale Hühner-Fibroblasten. Dieser Effekt war weitaus stärker in MC29 transformierten als in untransformierten embryonalen Hühner-Fibroblasten. Dieses Resultat betont die Funktionalität des kleinen interagierenden Segments von BASP1. Die Hypothese wurde aufgestellt, dass die wechselseitige Hemmung der Proteine BASP1 und Myc möglicherweise auf direkter Interaktion zwischen diesen zwei Proteinen basiert.

Obwohl die N-terminale Transaktivierungsdomäne (TAD) von Myc Proteinen sehr unstrukturiert ist, wurden sowohl α -helikale Bereiche als auch β -Faltblatt Segmente

vorausgesagt. Myc TAD kann mit vielen auch strukturell unterschiedlichen Proteinen interagieren. Diese spezifischen Interaktionen werden oft durch unterschiedliche Bereiche von TAD vermittelt.

Das Ziel dieser Studie war die direkte Interaktion zwischen dem bereits genannten Interaktions-Peptid von BASP1 und einem N-terminalen Teil von v-Myc (enthält c-Myc TAD vom Huhn), dem gesamten v-Myc Protein bzw. dem c-Myc Protein (Huhn) zu untersuchen. Dies wurde versucht mittels His6 Pull-Down Experimenten und Bindungsstudien mithilfe analytischer Gelfiltrations-Säulen.

Schlussendlich konnte direkte Interaktion zwischen Myc und BASP1 mit den genannten Methoden nicht nachgewiesen werden. Folglich bleibt der Mechanismus der wechselseitigen Beeinflussung dieser zwei Proteine weiterhin unklar.

Abstract

Brain Acid-Soluble Protein 1 (BASP1) is an intrinsically unstructured protein, which is involved in neuronal sprouting and plasticity and has also been identified as a cosuppressor for the Wilms' Tumor suppressor protein 1 (WT1). This cosuppressor activity is mediated via binding of BASP1 to the WT1 suppression region. Moreover, the subcellular localization of human BASP1 is altered upon induction of apoptosis in HeLa cells.

A novel bioinformatical approach, based on the Meta-structure concept (Robert Konrat), predicts a small stretch of 20-40 amino acids of chicken BASP1 with a high probability for interaction with other proteins, presumably with a loop or β -stranded part of a protein. In agreement with this finding, meta-structure analysis of WT1 predicts for its suppression region a loop or β -stranded conformation and a high probability for protein interaction. Hence, the Meta-structure approach is in agreement with the observed interaction between BASP1 and WT1.

Current studies found chicken BASP1 to be differentially expressed in MC29-transformed avian embryonic fibroblast cell lines. The MC29 virus encodes oncogenic v-Myc, which leads to the repression of BASP1 already at the transcriptional level. Surprisingly, ectopic expression of chicken BASP1 in MC29 infected chicken embryonic fibroblasts hinders the transformation of the cells by v-Myc. In addition, a synthetical cell penetrating peptide comprising a 20 residue long stretch of the predicted protein interaction site of BASP1 led to a cytopathic effect in chicken embryonic fibroblasts (CEF). This effect was more stringent in MC29 transformed than in untransformed CEF, highlighting the functionality of this small interacting stretch of BASP1. It was hypothesized that the mutual suppression of Myc and BASP1 might be a consequence of direct interaction between those proteins.

The N-terminal transactivation domain (TAD) of Myc proteins, although highly unstructured, was proposed to harbour α -helical as well as β -stranded segments. Myc TAD is able to interact with a lot of even structurally different proteins. These specific interactions are often mediated by different parts of Myc TAD.

The aim of this study was to investigate direct interaction between the small interacting peptide of BASP1 and an N-terminal part of v-Myc (harbouring chicken c-Myc TAD), full-length v-Myc and chicken c-Myc, respectively, with the help of His6 pull-down assays and binding studies by analytical size exclusion chromatography.

As a matter of fact, we were not able to observe direct interaction between Myc and BASP1 with the used methods, indicating that the mutual repression between those proteins remains still unclear.

Table of Contents

DANKSAGUNG	2
ZUSAMMENFASSUNG	3
ABSTRACT	5
TABLE OF CONTENTS	7
ABBREVIATIONS	9
INTRODUCTION	11
THE META-STRUCTURE CONCEPT	11
CELL CYCLE CONTROL	12
ONCOGENES AND VIRUSES	13
THE MYC GENE FAMILY	14
<i>The proto-oncogene myc</i>	14
<i>The Myc/Max/Mad network</i>	17
<i>Myc target genes</i>	20
<i>Myc and cellular transformation</i>	21
<i>The Myc protein</i>	22
1. The bHLHZip motif of Myc	23
2. The transactivation domain of Myc	24
THE BRAIN ACID-SOLUBLE PROTEIN 1 (BASP1)	27
THE INTERPLAY BETWEEN BASP1 AND MYC	31
MATERIALS AND METHODS	32
1. Microorganisms	32
2. Media for Bacterial Growth	33
3. Buffers and Solutions	35
4. General Methods: DNA	45
4.1. Agarose Gel Electrophoresis of DNA	45
4.2. Cloning of DNA fragments	46
4.2.1. Digestion of DNA with restriction endonucleases	46
4.2.2. Phosphatase treatment of DNA fragments	47
4.2.3. Ligation of DNA fragments	48
4.2.4. Polymerase Chain Reaction (PCR)	49
4.2.5. Preparation of competent bacteria (Hanahan) [175]	50
4.2.6. Transformation of <i>E. coli</i> bacteria – heat shock protocol	50
4.2.7. Preparation of <i>E. coli</i> starter cultures	51
4.2.8. Preparation of plasmid DNA from bacteria	51
4.2.9. Phenol:Chloroform extraction of DNA	51
4.2.10. EtOH precipitation of DNA	52
4.2.11. iso-Propanol precipitation of DNA	52
4.2.12. Quantification of nucleic acids	53
5. General methods: Protein	54
5.1. Expression of recombinant proteins	54
5.2. Preparation of lysates for protein purification	55
5.3. Enrichment of inclusion bodies	56
5.4. Refolding of proteins using stepwise dialysis	56
5.5. Concentration of protein samples using membrane filters	57
5.6. Chromatographic Methods	58
5.6.1. The Fast Performance Liquid Chromatography (FPLC) System	58

5.6.2.	<i>Immobilized metal ion affinity chromatography IMAC (HiTrap Chelating HP 5ml)</i>	58
5.6.3.	<i>Anion exchange chromatography (Resource Q 6ml)</i>	60
5.6.4.	<i>Preparative size exclusion chromatography (HiLoad 16/60 Superdex 75 prep grade)</i>	61
5.6.5.	<i>Analytical size exclusion chromatography (Superdex 75 10/300 GL)</i>	62
5.7.	<i>Quantification of protein</i>	63
5.8.	<i>TEV protease cleavage of proteins</i>	64
5.9.	<i>SDS Polyacrylamide Gel Electrophoresis (SDS-PAGE) of proteins [177]</i>	65
5.10.	<i>Pull-Down Assay</i>	68
5.11.	<i>Western blot</i>	70
5.12.	<i>Circular dichroism spectroscopy of proteins</i>	72
6.	<i>Cell Culture</i>	74
6.1.	<i>Preparation of cellular extract</i>	74
7.	<i>Specific protocols</i>	75
7.1.	<i>Expression and purification of His6-Carrier-cBASP1 peptide fusion proteins</i>	75
7.1.1.	<i>Construction of expression vectors coding for His6-Carrier-cBASP1 peptide fusion proteins</i>	75
7.1.2.	<i>Expression and purification of His6-Carrier-cBASP1 peptide fusion proteins</i>	77
7.2.	<i>Expression and purification of the MC29EB protein</i>	78
7.2.1.	<i>The expression vector coding for MC29EB protein</i>	78
7.2.2.	<i>Expression and purification of the MC29EB protein</i>	78
7.3.	<i>Expression and purification of His6-Minimax</i>	80
7.3.1.	<i>Construction of the expression vector coding for His6-Minimax</i>	80
7.3.2.	<i>Expression and purification of His6-Minimax</i>	81
RESULTS		82
INVESTIGATION OF DIRECT INTERACTION BETWEEN C-MYC AND THE cBASP1 INTERACTING PEPTIDE		82
1.	<i>Construction of expression plasmids encoding His6-Carrier-cBASP1pep</i>	84
2.	<i>The His6-Carrier-cBASP1 peptide fusion proteins</i>	84
3.	<i>The MC29EB protein</i>	87
4.	<i>Circular Dichroism Spectroscopy of MC29EB</i>	89
5.	<i>Pull-down assay with purified His6-Carrier-cBASP1pep as bait protein and enriched MC29EB as prey protein</i>	90
6.	<i>Binding assay between His6-Carrier-cBASP1pep and MC29EB via analytical gel filtration</i>	93
INVESTIGATION OF DIRECT INTERACTION BETWEEN v-MYC AND THE cBASP1 INTERACTING PEPTIDE		95
1.	<i>MC29 transformed chicken embryonic fibroblasts</i>	95
2.	<i>Pull-down assay with purified His6-Carrier-cBASP1pep as bait protein and cellular extract from MC29 transformed CEF</i>	95
META-STRUCTURE ANALYSIS OF BASP1 AND WT1		98
DISCUSSION		105
THE PULL-DOWN ASSAY AS A METHOD FOR THE INVESTIGATION OF PROTEIN INTERACTION		105
DOES BASP1 BIND DIRECTLY TO MYC TAD?		106
THE MUTUAL SUPPRESSION OF MYC AND BASP1		109
<i>Ectopic expression of BASP1 hinders transformation by v-Myc</i>		109
<i>Transformation by v-Myc leads to BASP1 repression</i>		111
REFERENCES		112
CURRICULUM VITAE		118

Abbreviations

2nd IA	secondary structure of the interactor
Amp	ampicillin
APS	ammoniumperoxodisulfate
BASP	brain acid-soluble protein
BCIP	5-bromo-4-chloro-3-indolyl phosphate p-toluidine salt
BIRPs	BASP1 immunologically related proteins
bHLHZip	basic region/helix-loop-helix/leucine zipper
bp	base pair
CaM	calmoduline
CoA	chloramphenicol
cDNA	complementary DNA
CIP	calf intestinal alkaline phosphatase
C-terminus	carboxy terminus
CV	column volume
Da	dalton (1/12 of the mass of a ¹² C atom)
DNMT	DNA methyl transferase
DTT	dithiothreitol
EDTA	ethylenediaminetetraacetic acid
Fc	fragment crystallizable (base of the antibody)
fw	forward primer
Gag	group-specific antigen
GB1	B1 Ig binding domain of streptococcus
GST	glutathione-S-transferase
HAT	histone acetyl transferase
HDAC	histone deacetylase
His6 tag	six consecutive histidine residues
IMAC	immobilized metal ion affinity chromatography
IPTG	isopropyl-β-D-thiogalactoside
IUP	intrinsically unstructured protein
kb	kilo base
LB media	Luria-Bertani media
MB I-III	Myc (homology) box I-III
MBP	maltose-binding protein
MC29	myelocytomatosis retrovirus 29
MM1	Myc modulator-1
myr	myristoyl-group
NBT	p-nitro blue tetrazoliumchloride
NOE	nuclear Overhauser effect
N-terminus	amino-terminus
OD ₆₀₀	optical density (absorbance) at 600nm
O-GlcNAc	O-linked N-acetylglucosamine monosaccharides
PAGE	polyacrylamide gel electrophoresis
PCR	polymerase chain reaction
PEST	peptide sequence rich in proline (P), glutamic acid (E), serine (S) and threonine (T)
PI3K	phosphoinositide-3-kinase

PKC	protein kinase C
PPI	probability for protein interaction
ppm	parts per million
PtdIns(4,5)P ₂	phosphatidylinositol (4,5)-bisphosphate
rev	reverse primer
rpm	revolutions per minute
RSV	rous sarcoma virus
SDS	sodium dodecyl sulfate
SID	mSin3-interaction domain
TBP	TATA box-binding protein
T-D	T-box DNA binding domain
TAD	transactivation domain
TEMED	N,N,N',N'-tetramethylethylenediamine
TEV	tobacco etch virus
TFE	trifluoroethanol
T _m	melting temperature
TRD	transrepression domain
Tris	trishydroxymethylaminomethane
trx	thioredoxin
U	unit
WT1	Wilms' tumor suppressor protein 1

Introduction

The Meta-Structure Concept

The Meta-Structure Concept was developed by Robert Konrat with the aim to extract information about protein structure and function out of the primary sequence of a protein without the help of 3D structural information, which often, even at high resolutions, is insufficient to predict protein function or functional sites. Individual residues are treated as tightly interacting chemical entities and their mutual interdependences can be quantified using parameters borrowed from network theory. Finally meta-structure analysis from the primary sequence of a protein gives information about the compactness of a protein (whether proteins are highly structured, unstructured or partially folded). It can be used for the search of protein fold topology similarities (meta-structure homologues), which are not necessarily visible in the primary sequence of proteins. Furthermore, it is able to predict protein interaction and ligand binding sites [2].

Cell Cycle Control

The homeostasis of a multicellular organism depends on a tight control of the cellular behaviour of single cells. Each cell corresponds to a complex mixture of extracellular as well as intracellular signals, which regulates processes as cell growth, cell proliferation, cell differentiation and apoptosis. Multiple interconnected signal transduction pathways transfer information to the nucleus, where a network of proteins (transcription factors, chromatin remodelling complexes, proteins of the basic transcriptional machinery, etc.) lead to the transcription of genes in response to those signals. A number of pathways exist, which ensure the integrity of the cell, especially the genome of the cell before cell division. Those internal checkpoint control mechanisms are triggered by events as DNA damage and can stop the cell cycle at certain checkpoints. The ability to repair those damages decides the fate of the cell. Fig. 1 shows a schematic representation of the cell cycle.

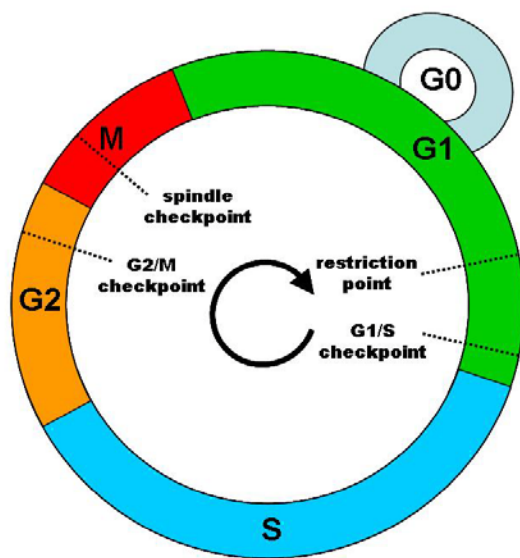


Fig. 1. The cell cycle. G1: Gap 1 phase; S: Synthesis phase; G2: Gap 2 phase; M: Mitosis; G0: resting phase. During the Gap phases and Synthesis phase the cell is producing proteins, RNA, etc. (G1, G2) and replicates its genome (S). The G0 phase indicates a resting phase, where the cell no longer divides (e.g. after terminal differentiation). Dotted lines indicate certain checkpoints during the cell cycle, at which the cell cycle can be halted, e.g. to repair possible damages. At those checkpoints the cell might decide to undergo apoptosis.

If constituents of those pathways are deregulated, the reception and transmission of signals are disturbed; hence there is no proper response. As a result, the balance between cell division and cell death is affected and may eventually – if not recognized – lead to uncontrolled cell proliferation and tumor growth. The so-called transformation of cells to a tumorigenic state can be caused by the activation of proto-oncogenes as well as the deactivation of tumor suppressor genes. The products of proto-oncogenes are important constituents of signaling pathways regulating cell proliferation and therefore have oncogenic potentials. Important proto-oncogenes, which are deregulated in many human tumors, are

myc, *ras* and *jun*. A lot of these proto-oncogenes have been discovered as the cellular homologues of viral oncogenes.

Oncogenes and Viruses

Oncogenes were first discovered in DNA tumor viruses as the genes responsible for *in vivo* and *in vitro* neoplastic transformation observed with such viruses. Examples of such oncogenes are the *large T* (tumor) antigen, '*middle*' *T* antigen, *E7* gene and *E1A* gene of polyoma, SV40, papilloma and adenoviruses, respectively. The products of those genes rely on the cooperation of other cellular oncogenes to establish a fully transformed phenotype [3].

Another group of oncogenes had been identified as transforming alleles in the genomes of replication defective RNA tumor viruses. Interestingly, these genes do not exist in replication competent RNA tumor viruses, although they may induce neoplastic tumor formation *in vivo* by a distinct mechanism [3]. Oncogenes from replication defective RNA tumor viruses have homologous genes in cells, called proto-oncogenes. Therefore it was hypothesized that those viruses picked up a cellular gene via recombination during their evolution and that this gene was altered either by subsequent mutation or already at the recombination event, possibly leading to the fusion of a viral protein with the cellular proto-oncogene. One of the first oncogenes characterized was the *v-src* gene of Rous Sarcoma virus (RSV) [4]. The *v-myc* oncogene was discovered in the acute Myelocytomatosis retrovirus MC29 as being responsible for transformation [5-7]. The Harvey murine sarcoma virus (Ha-MuSV) RNA genome has been shown to contain an approximately 4.5 kb insert of rat genetic sequences, which codes for the nonvirion phosphoprotein p21 (*v-ras*) [8, 9]. The Avian Sarcoma virus 17 (ASV17) carries the *v-jun* oncogene [10].

A lot of oncogenes from tumor viruses as well as from tumors have been characterized so far. Moreover, the functions of the respective proto-oncogenes in 'healthy' cells are of great interest in order to better understand the mechanisms underlying neoplastic transformation and also normal cell physiology.

Proto-oncogenes have all in common that they encode proteins, which are members of the signaling cascade regulating genes and proteins involved in cellular proliferation and differentiation. If proto-oncogenes transform to oncogenes via different mechanisms (e.g.: mutation, translocation, etc.), cells are not able to respond or not properly respond to signals, which control these processes, anymore, consequently leading to a cancerous state.

The *myc* gene family

The *myc* gene family encodes transcription factors, which are implicated in a lot of different pathways controlling cell behaviour and therefore have a high oncogenic potential. A lot of research is interested in the structural features of Myc proteins leading to their tremendous functional diversity. Myc transcription factors interact with a lot of different proteins in a specific manner either via their N-terminal transactivation domain (TAD) or the C-terminal 'basic region/helix-loop-helix/leucine zipper' motif (bHLHZip) and are able to either activate or repress transcription of different genes depending on the cellular context.

The research on *myc* genes started with the discovery of the highly oncogenic *v-myc* encoded in the proviral genome of the acute transforming Myelocytomatosis retrovirus (MC29), which was isolated in 1964 from a chicken with spontaneous myelocytomatosis [11]. The protein encoded by *v-myc* induces tumor formation in MC29 infected chicken [12, 13] and can transform several different lineages of mammalian and avian cells either alone or in cooperation with other oncogenes [14]. The *v-myc* sequence was later on found to occur also in other retroviral isolates CMII, MH2, OK10 and FTT [15-19].

The proto-oncogene myc

The *c-myc* proto-oncogene, which is the cellular homolog of *v-myc*, was discovered in chicken [20, 21], what led to the conclusion, that *v-myc* was derived from the cellular *c-myc* by retroviral transduction. In fact, sequence alignments of the MC29 proviral genome with the nondefective helper virus (MC29-associated virus) and cellular chicken *c-myc*, showed that the MC29 virus arose by recombination of the nondefective helper virus with cellular sequences present within the normal chicken genome [1]. Fig. 2 shows an alignment of MC29 *v-myc*, chicken *c-myc* and RSV *gag* and *env* sequences indicating the 5' and 3' recombination junctions between *v-myc* and *c-myc*.



Fig. 2. The 5' and 3' recombination junctions between *v-myc* and chicken *c-myc* indicating the recombination event between the nondefective helper virus and chicken *c-myc*. RSV *gag* and *env* sequences were used for the alignment to chicken *c-myc* and MC29 *v-myc*. Vertical lines indicate homologous sequences (adapted from Reddy et al. 1983 [1])

In mammals, the *myc* gene family comprises 5 related genes, *c-myc*, *N-myc*, *L-myc*, *S-myc* and *B-myc*. *c-myc*, *N-myc* and *L-myc* all have the same three-exon and two-intron structure, where the first exon appears to have regulatory function, whereas polypeptide coding regions lie in exons 2 and 3. Interestingly, removal of the first exon/intron enhances the oncogenic potential [22]. The *S-myc* gene is an intronless gene, which is most similar to the second and third intron of *N-myc* [23]. *B-myc* consists only of second exon sequence and is most homologous to *c-myc* [24].

As *c-Myc* is involved in so many fundamental processes regulating cell behaviour, the expression of *c-myc* is tightly regulated by different transcription factors, signal transduction pathways and feedback loops that activate or repress *c-myc* transcription [25]. The promoter region of *c-myc* harbours two transcription initiation sites upstream of exon 1, together with regulatory sequences, which are necessary for normal promoter function in eukaryotes [26]. A short region of 40 base pairs – highly homologous to *N-Myc* – lies proximal to the second promoter P2 of *c-myc* and harbours an E2F-site bound by E2F transcription factors, which is overlapping with a transforming growth factor TGF β inhibitory element (TIE), which mediates down-regulation of *c-myc* via Smad proteins [27-29]. In addition, several proteins including the zinc finger protein MAZ, the homeodomain protein CUT and Sp1 can bind to a GC-rich element termed ME1a1 [30-32]. Moreover, *c-myc* is target of NF κ B [33, 34] and can be repressed as well as activated by the WT1 tumor suppressor protein [35, 36]. Multiple mitogenic signals activate *c-myc* expression, for example v-Abl via the Ras/Raf2-signaling cascade and PDGF via Src/Vav2/Rac [37-40], whereas anti-mitogenic signals as TGF β , APC, glucocorticoids and interferon γ (IFN γ) repress *c-myc* expression [41-45].

Other mechanisms of *c-myc* regulation involve DNA stretches that are bound by different proteins in their single-stranded and double-stranded state, respectively. The CT element just upstream of promoter P1 consists of 5 imperfect repeats of the sequence

CCCTCCCCA. It is bound by Sp1 when double stranded, but when single stranded, the pyrimidine-rich strand is bound by heterogeneous nuclear ribonucleoprotein K (hnRNP K), while the purine-rich strand is bound by the cellular nucleic acid binding protein (CNBP) [46]. In addition, a 27-bp region of this purine-rich strand located -142 to -115 upstream of promoter P1, the nuclease hypersensitivity element III1 (NHEIII1) [47], comprises guanine-rich tracts capable of forming G-quadruplexes that function as silencer element [48]. G-quadruplexes have been found in a lot of promoter regions spanning 1 kb upstream of transcription start sites of genes [49]. Interestingly, systematic algorithmic searches for guanine-rich tracts found putative G-quadruplex-forming sequences to be prevalent in proto-oncogenes but essentially lack in tumor-suppressor genes [50]. Moreover, an increasing number of proteins have been identified that is able to interact with G-quadruplexes as well as promote or non-catalytically disrupt G-quadruplex formation [51-53]. The NHE III1 in the *c-myc* promoter has been shown to control 80-90% of its transcriptional activity [54].

The Far UpStream Element (FUSE) of the *c-myc* gene is an extended, largely AT-rich segment, which is located more than 1500 base pairs upstream of the *c-myc* promoter. It is bound by FUSE binding proteins (FBPs), which bind sequence-specifically to single-stranded DNA [55]. FBPs act as transcriptional activators via interaction with the subunits of TFIIF p62, p80/XPD and p89/XPB [56]. The FBP interacting repressor (FIR) is a repressor of activated transcription and binds to FBP as well as single-stranded DNA. FIR, like FBP, interacts with the TFIIF subunit p89/XPB but opposes FBP function [57]. The Myc target gene p38 is another FBP binding partner [58], which targets FBP for ubiquitylation and subsequent degradation; hence the FBP/Myc/p38 system is an example for a classical homeostatic end-product feedback loop [59]. The FBP/FIR system together with melted FUSE might be a possible control mechanism for the intensity of on-going transcription [59] considering the fact that torsional forces generated by the RNA polymerase are powerful enough to melt susceptible sequences such as FUSE [60].

c-myc is expressed in practically all cells of embryonic and adult tissues during proliferation, as well as in a wide variety of malignancies of different cell types. Contrary, the expression patterns of *N-myc* and *L-myc* appear to be more restricted to certain types of tissues and depending on the developmental stage. Consistent with this, they were found to be expressed only in a restricted set of tumors. *N-myc* was found in neuroblastomas, whereas *L-myc* was isolated from small-cell lung carcinomas [61-63].

The study of the *myc* gene family intensified after the realization that these genes are not only key regulators of cell proliferation, differentiation and apoptosis, but they decisively

regulate many different aspects of cell behaviour. This potency requires a highly controlled expression of the members of this gene family. Deregulation of *myc* genes contributes to the genesis of many human tumors, in which an elevated expression level of *myc* mRNAs has been stated [64]. Most striking, it was discovered that enhanced expression of Myc proteins contributes to almost every aspect of tumorigenesis [65]. It had long been recognized, that Myc proteins can drive unrestricted cell proliferation [66] and inhibit cell differentiation [67], but recently it was shown, that deregulated expression of *myc* can drive cell growth [68, 69] and vasculogenesis [70], reduce cell adhesion [71, 72], and promote metastasis [65] and genomic instability [73]. There are several different molecular mechanisms underlying a deregulated state of *myc* genes, as gene amplification, gene translocation or mutations affecting for example post-translational modification of the N-terminal transactivation domain (TAD). For example, *c-myc* gene translocations and substitution mutations of residue Thr58 in c-Myc TAD are often found in Burkitt's lymphoma [74, 75]. Thr58 is an *in vivo* phosphorylation site and the major O-GlcNAc glycosylation site of c-Myc. Moreover, it is altered to a methionine or alanine in four different retroviral strains [76, 77]. Mutation of Thr58 therefore prevents regulation by posttranslational modification [78, 79]. Amplification of *N-myc* is associated with neuroblastoma [80].

The Myc/Max/Mad network

The common feature of proteins of the Myc/Max/Mad network is the 'basic region/helix-loop-helix/leucine zipper' (bHLHZip) motif, which allows DNA binding, dimerization with other members of the network as well as interaction with other proteins. Myc has not been found as a monomer *in vivo* but bound to its partner protein Max (Myc-associated factor X). The characterization of Max initiated the search for other proteins with a bHLHZip domain and led to the identification of the Mad proteins Mad1, Mxi1, Mad3 and Mad4 [81, 82] and two additional proteins Mnt and Mga [83, 84], which are able to heterodimerize with Max. Mad proteins and Mnt share, apart from the bHLHZip motif, an mSin3 interaction domain (SID), which mediates transcriptional repression [85-87]. Mlx, a Max-like protein, was identified soon afterwards and is able to heterodimerize with Mad1, Mad4 and Mnt [88, 89] and further extends the network to the Mlx binding proteins MondoA

and WBSCR14 [90, 91]. Functional homodimerization is only observed with Max and Mix. Homodimers and heterodimers of the network function as DNA binding competent complexes and recognize the same DNA sequence (CACCA/GTG), which is a subset of the general E-box DNA sequence (CANNTG) that is bound by all bHLH proteins [92, 93]. The currently known proteins of the Myc/Max/Mad network are depicted in Fig. 3 with Max and Mix as central components.

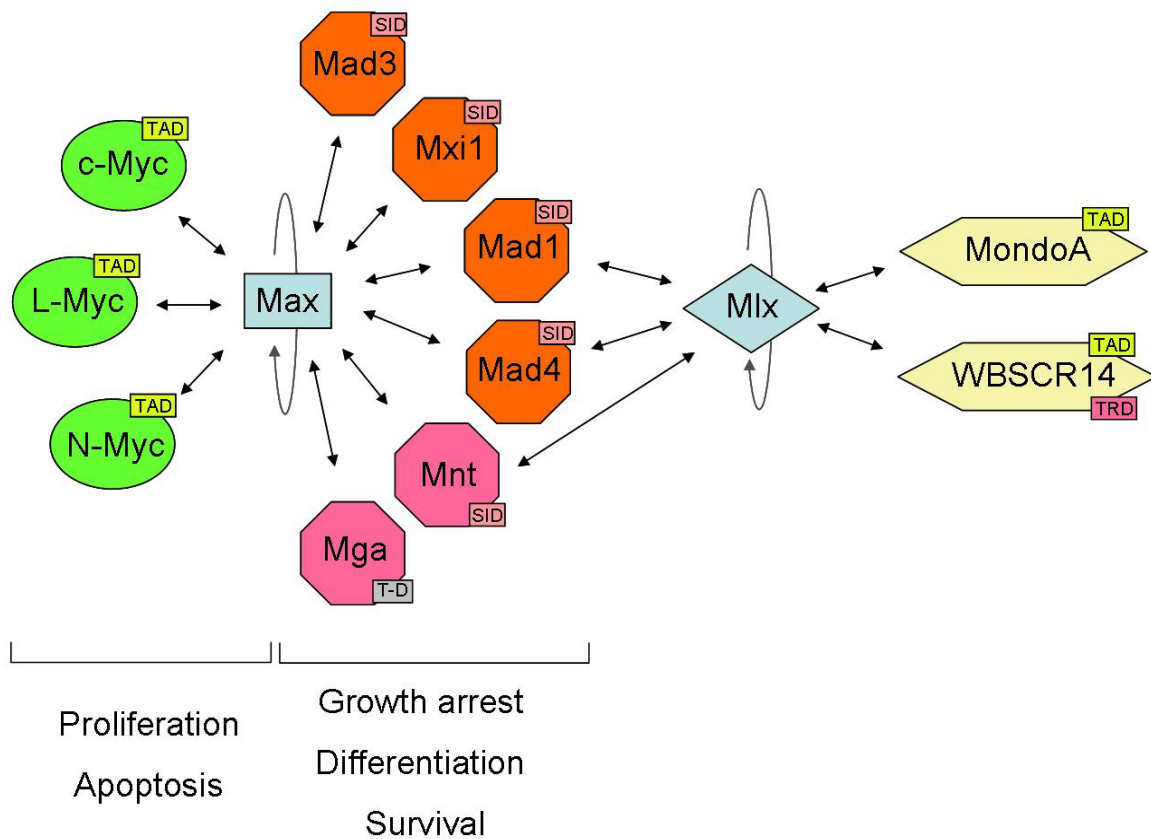


Fig. 3. The Myc/Max/Mad network. All constituents of the network have a bHLHZip domain, which is needed for homo- and heterodimerization. Arrows indicate the known interactions between the network members. Heterodimerization is marked by double arrows. Homodimerization of Max and Mix is marked by grey curved arrows. Additional domains are indicated by small boxes. TAD: transactivation domain; SID: mSin3-interaction domain; T-D: T-box DNA binding domain; TRD: transrepression domain. The TAD of Myc proteins is also involved in transcriptional repression. As far as characterized the members of the network function as regulators of different aspects of cell behaviour as indicated.

Transcriptional regulation of Myc/Max/Mad network proteins is thought to affect the chromatin structure of gene loci and a lot of proteins have already been described to interact with Myc, which are parts of chromatin remodelling complexes (e.g. TRRAP, TIP48, TIP49, etc.). TRRAP is a core subunit of the TIP60 and GCN5 histone acetyltransferase (HAT)

complexes [94] and its interaction with Myc is dependent on the integrity of a conserved domain in c-Myc TAD, Myc box II. Subsequent histone acetylation of responsive promoters leads to enhanced gene expression [95, 96]. Interestingly, TRRAP is also a constituent of a complex containing the p400 E1A-binding protein, whose *Drosophila* and yeast homologues, Domino and Swr1, are histone exchange factors [97, 98]. Conversely, Mad proteins recruit repressor complexes, which contain histone deacetylase (HDAC) activity, through their SID domain. The antagonism of Myc and Mad proteins is supported by the fact that Myc proteins are present in proliferating cells, whereas Mad proteins are expressed in non-proliferating, differentiated cells [81, 82].

As a matter of fact, an increasing number of studies find Myc also to repress transcription of certain genes. For example, Miz1 can tether the Myc/Max heterodimer to core promoters devoid of E-boxes, what eventually leads to gene repression [99-104]. Furthermore, Myc has been found at other core promoters that lack E-box sequences and not in combination with Miz1. Therefore it is hypothesized that Myc can be recruited by other proteins to their cognate DNA-binding sites [105]. Possible candidate proteins, which might act as Myc tethering factors, are specificity protein-1 (Sp1) [106], nuclear factor Y (NF-Y) [107], transcription factor II-I (TFII-I) [108] and yingyang-1 (YY1) [109].

Furthermore, proteins exist that influence activator and/or repressor roles of Myc. p19^{ARF} is able to bind to Myc and inhibits its ability to activate transcription, but seems to leave repression by Myc unaffected [110, 111].

The list of proteins directly interacting with Myc is growing and strikingly, it's not possible to separate Myc domains into classical DNA-binding domain and transcriptional-effector domain, as interaction with proteins does occur at the N-terminal TAD as well as at the C-terminus. Prominent proteins that interact with the C-terminus of Myc and lead to transcriptional activation are CREB-binding protein (CBP) and p300 that have histone acetyltransferase activity [112]. Moreover, recruitment of the DNA methyltransferase 3a (DNMT3a) to Myc-Miz1 complexes has been observed, suggesting a possible Myc induced repression mechanism via DNA methylation of target promoters [113].

Myc target genes

A lot of genes harbour E-box sequences in their promoter sequence and are therefore potential Myc target genes. As Myc is even recruited to core promoters lacking E-box sequences the list of potential target genes becomes even greater. The question is now, which genes influenced by Myc are crucial targets. Furthermore to consider is the fact that Myc influences indirectly the expression of genes through the transcriptional activation of factors which themselves regulate gene expression.

Myc target genes have been identified in developmental pathways. Myc regulates the transcription of cyclin D2 and the cell-cycle inhibitor p18^{INK4c} (might not be a direct target by Myc), which regulate the proliferation and differentiation of neuronal precursor cells [114]. Cyclin D1, cyclin D2 and E2F2 are regulated by N-Myc via the sonic hedgehog pathway [115]. Finally, the cell-cycle inhibitor p15^{INK4b} is suppressed by Myc what leads to the release of cell-cycle arrest mediated by the transforming growth factor- β (TGF β) [102, 103, 116].

Other Myc target genes are found in specific metabolic pathways. Myc activates the expression of lactate dehydrogenase A (LDHA), which seems to be required for Myc-induced transformation of fibroblasts [117, 118]. LDHA plays a role in glucose uptake and glycolysis, what might explain the 'Warburg effect' observed with tumor cells. The 'Warburg effect' describes the observation of tumor cells showing enhanced rates of glycolysis under aerobic conditions [119]. Myc also leads to enhanced iron availability via the induction of the transferrin receptor and iron-responsive-element-binding protein-2 (IRP2) as well as the repression of H-ferritin and NRAMP1, which counteract the former proteins [120, 121]. Furthermore, Myc upregulates metabolic enzymes required for folate metabolism, which is important for cell growth and metabolism [122].

Finally, Myc directly binds to promoters and activates transcription of genes implicated in ribosome biogenesis [123-126]. Interestingly, Myc even regulates the transcription of ribosomal RNA genes [127-129].

Other Myc targets were found in the course of differential expression screens comparing v-Myc transformed chicken embryonic fibroblasts (CEF) with untransformed CEF. Some genes were found to be enhanced after v-Myc transformation, as Osteopontin (OPN), which is homologous to human Secreted Phosphoprotein 1 (SPP1), lipocalin Q83, which is possibly involved in iron metabolism and was currently found to be able to bind arachidonic acid, and WS5, which is meta-structurally homologous to semaphorins. Other

genes were repressed after v-Myc transformation including BASP1 and CRP2 (unpublished data).

Those are only a few important Myc target genes. A list of putative Myc target genes is found at www.myccancergene.org and already comprises ~ 1700 genes.

Myc and cellular transformation

A deregulated state of *myc* alone is not sufficient for transformation or tumorigenesis and additional mutations are required for tumor formation. There are two main mechanisms known that limit cellular transformation by Myc. First, Myc network proteins are controlled post-transcriptionally by Ras-dependent signaling pathways. Second, cells have fail-safe mechanisms that protect them from transformation by Myc. Those mechanisms need to be inactivated for the cells to adopt a transformed state [130].

For example, Myc cooperates with oncogenes from the Ras pathway to establish a transformed state [131-133]. Ras signaling influences the Myc network by the following mechanisms:

First, Ras regulates the phosphorylation of Myc on Thr58 and Ser62 via activation of mitogen-activated kinases and inhibition of glycogen synthase kinase-3 (GSK3) [134-136], consequently stabilizing Myc. In many lymphomas, Thr58 of Myc is mutated rendering Myc resistant to degradation by the ubiquitin E3 ligase SCF^{FBW7}, which recognizes phospho-Thr58 [75].

Second, active Ras leads – via activation of the AKT protein kinase – to the phosphorylation of FoxO family transcription factors, which in their non-phosphorylated state directly bind to and repress many Myc target genes involved in cell proliferation [137]. Additionally, AKT kinase phosphorylates Miz1, which is subsequently bound by 14-3-3 proteins and released from the p21^{CIP1} promoter. Thereby Miz1 is no longer able to inhibit cell proliferation [138].

Third, transcriptional repression by Myc is regulated through the PI3K pathway. Phosphorylation at Ser71 of Myc by a Rho-dependent kinase (downstream of PI3K) leads to enhanced repression of thrombospondin-1 [139].

The Myc protein

The *v-myc* oncogene codes for a Gag-Myc fusion protein consisting of 453 N-terminal residues encoded by the 5' end of the viral *gag* gene fused to a short stretch of six amino acids encoded by the 5' untranslated region of the *c-myc* gene plus 416 residues encoded by the exons 2 and 3 of chicken *c-myc* [1]. Substitution mutations in the v-Myc protein compared to its cellular counterpart c-Myc have been found in both the N-terminal and C-terminal regions, which contain domains necessary for transformation.

The N-terminus of Myc proteins harbours the transactivation domain (TAD), which is a major protein interaction platform, whereas the C-terminus contains the 'basic region/helix-loop-helix/leucine zipper' (bHLHZip) motif, which is necessary for DNA binding, dimerization and protein interaction. The N-terminal TAD and C-terminal bHLHZip motif are connected via a suggested flexible linker region, which is less conserved between different species. Fig. 4 shows a schematic representation of the human c-Myc protein.

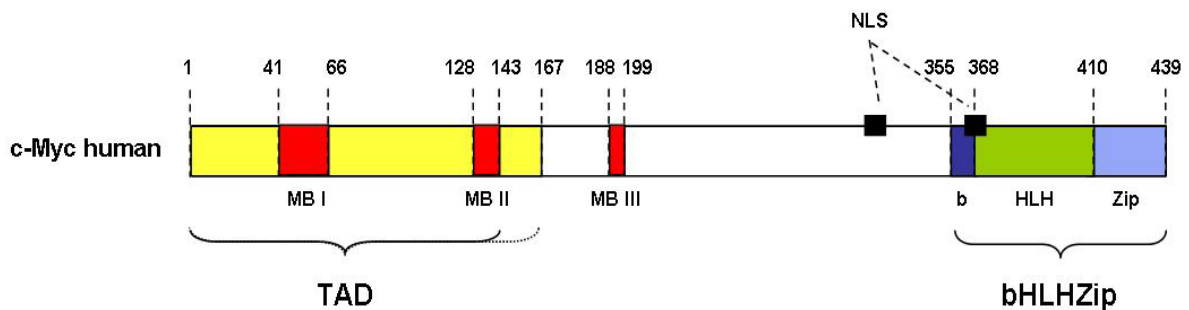


Fig. 4. Schematic representation of human c-Myc. TAD: transactivation domain (yellow); MB I-III: Myc boxes I-III (red); b: basic region (dark blue); HLH: helix-loop-helix motif (green); Zip: leucine zipper (light blue); NLS: nuclear localization signal (black). The extended bracket indicating TAD reminds for the recent finding that a C-terminally prolonged region of TAD is binding with higher affinity to interactors, than the previously described "minimal region" of TAD.

1. **The bHLHZip motif of Myc**

The bHLHZip motif spanning residues 355 to 439 of human c-Myc comprises three distinct domains, which are found in other transcription factors as well. The N-terminal basic region (b) makes unspecific and specific contacts with the DNA phosphate backbone and nucleotides of the E-box sequence. The helix-loop-helix domain (HLH) and the leucine Zipper (Zip) with its typical heptad pattern $(abcdefg)_n$ are needed for protein dimerization. Information about the three-dimensional structure is provided for Mad/Max and Myc/Max heterodimers in complex with their cognate DNA sequence from X-ray crystallographic data [140]. NMR studies together with other techniques as CD spectroscopy elucidated solution structural and dynamic properties of monomeric v-Myc and described a beads-on-a-string motional behaviour of the v-Myc bHLHZip domain in solution [141]. Moreover, some X-ray crystal structure observations of bHLHZip proteins suggested that those proteins might be able to form antiparallel tetramers. Such an arrangement was for instance observed in the crystal structure of the c-Myc/Max/DNA complex [140] and the Max homodimer bound to its DNA [142]. Tetramerization of proteins of the Myc/Max/Mad network raises the possibility of DNA looping, which is a ubiquitously found mechanism fundamental to a lot of different processes including transcription, recombination and replication [143]. As a matter of fact, tetramers are not formed in solution and there is no evidence of specific interaction between two Myc/Max heterodimers. Still, at high concentrations of Myc and Max, a head-to-tail arrangement of Myc/Max heterodimers could be observed, which is due to dipole-dipole interactions between two heterodimers. The long coiled-coil structure of the Myc/Max bHLHZip heterodimer results in the formation of a large dipole moment due to the alignment of the dipoles of the individual peptide units. Binding of a Myc/Max heterodimer to DNA enhances dipole-dipole interaction with another DNA bound Myc/Max heterodimer, possibly leading to DNA looping (Bettina Schweng, doctoral thesis). Fig. 5 shows the heterodimers formed by the bHLHZip domains of Myc, Max and Mad bound to DNA.

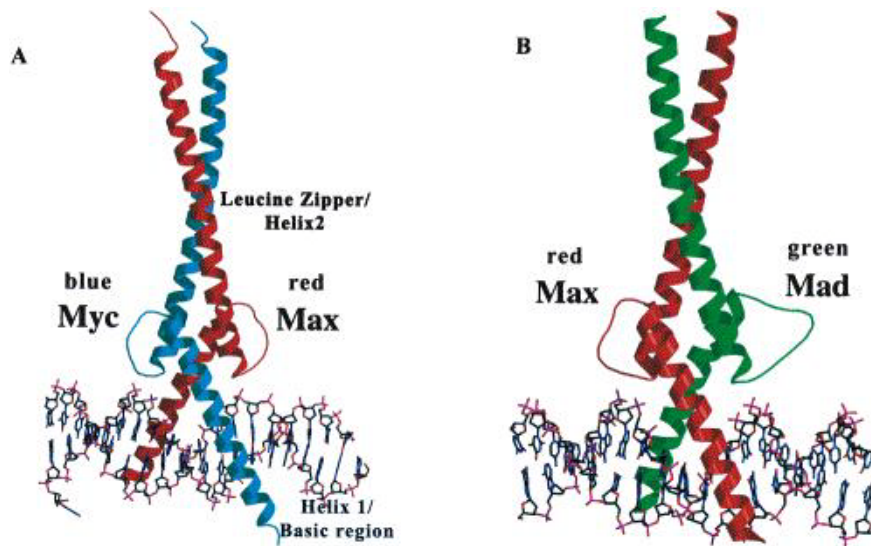


Fig. 5. Heterodimers formed by the bHLHZip domains of Myc, Max and Mad. Myc/Max (A) and Mad/Max (B) heterodimers bound to DNA. The basic region (b) is involved in DNA binding. The HLH and Zip motives are needed for dimerization.

2. *The transactivation domain of Myc*

The N-terminal transactivation domain of Myc proteins is of special interest, as it is capable of binding functionally and specifically to a wide range of target proteins. Not only do these interactors often differ in secondary structure but also binding may result in opposing functions of the TAD region. The TAD harbours two highly conserved regions, Myc box I (MBI) and Myc box II (MBII), spanning residues 41 to 66 and 128 to 143, respectively, which share 80% sequence similarity with N- and L-myc [144, 145]. The Myc boxes are thought to be the major recognition sites for regulating proteins interacting with c-Myc. It appears, that most of these proteins need both Myc boxes for interaction (TRRAP, P-TEFb, NF-Y, TBP, Bin1, p107, Yaf2 and p21; reviewed by [64]). Recently, a third conserved region Myc box III (MBIII) spanning c-Myc residues 188 to 199 was described to be involved in Myc proteolysis. Deletion of the so-called D-element, which includes MBIII, stabilized the Myc protein without affecting its ubiquitylation [146]. Furthermore, MBIII is important for transcriptional repression and transformation by Myc. Interestingly, disruption of MBIII increases the efficiency of Myc to induce apoptosis [147]. Fig. 6 shows an alignment between c-Myc TAD of different species and v-Myc from the MC29 virus indicating the highly conserved Myc boxes I-III and regions with predicted secondary structural elements [145].

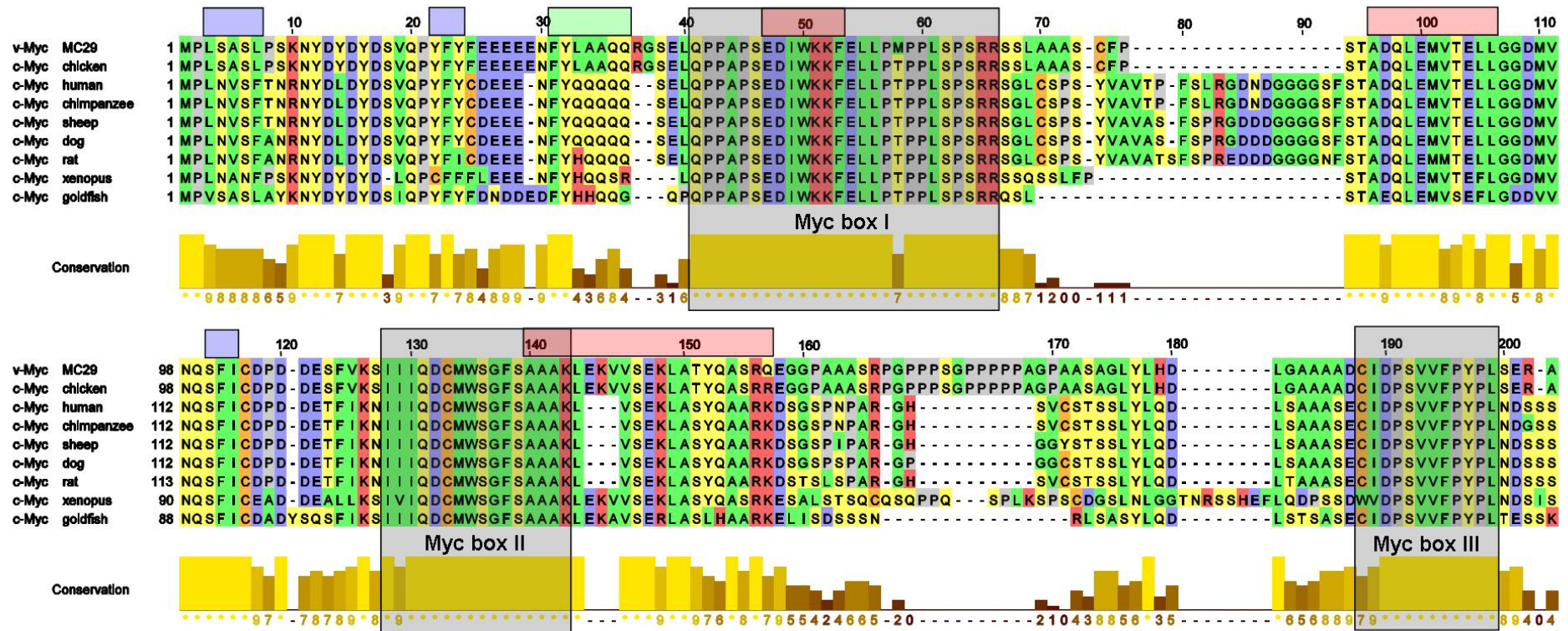


Fig. 6. Alignment of v-Myc TAD and c-Myc TAD amino acid sequences from different species. The Myc boxes I-III are indicated by grey boxes. The colour code outlines roughly amino acid properties: acidic (blue), basic (red), hydrophobic (green), polar (yellow) as well as cysteine (orange) and proline (grey). The histogram below gives a measure of conservation between the sequences of the different species. Red boxes indicate regions, which are predicted to form amphipathic α -helices in human c-Myc TAD. The green box indicates a predicted α -helix. Blue boxes indicate predicted β -strands. Upper numbers correspond to human c-Myc residue numbers.

Former studies quoted a minimal region of Myc residues 1 to 143 being sufficient for transactivation in neoplastic transformation [148] and for binding to the basal transcription factor TBP (TATA box-binding protein) [149, 150]. Very recently studies revealed some information about the structure of the transactivation domain and how interaction with other proteins might occur. Nevertheless, very little is known about the molecular mechanisms leading to either transcriptional activation or repression. It was discovered that the two structurally and functionally orthogonal target proteins, TBP and MM1 (Myc modulator-1) are bound with highest specificity and affinity only by a prolonged c-Myc TAD region (residues 1 to 167). The additional C-terminal stretch (residues 143-167) appears to promote increased folding. Interestingly, already the conserved C-terminal region of human c-Myc TAD spanning residues 92-167 is able to bind TBP and MM1, but with less affinity. It was suggested, that N- and C-terminal parts of c-Myc TAD, harbouring MBI and MBII, respectively, act in concert during binding, possibly involving a folding-on-binding mechanism and a molten globule like-state [145].

Likewise, NMR analysis of rat B-Myc, which is most homologous to the N-terminus of c-Myc but being devoid of C-terminal parts, depicted a neither completely unfolded nor a folded protein with NOE values similar to that of molten globule proteins [151]. Interestingly, in the study using human c-Myc₁₋₁₆₇ an increase in α -helical content has been observed upon binding to MM1 [145]. Contrary, an increase in secondary structural content was not observed upon interaction between rat B-Myc and MM1, although interaction was confirmed by NMR [151]. However, both studies describe that interaction between the respective Myc protein and MM1 or TBP differs in regard to specific TAD residues or domains that are used for interaction. Worth to notice is that MM1 is predicted to be helical and appears to hinder transactivation by c-Myc, while TBP, a major c-Myc target in transcriptional activation, consists of predominantly β -sheets [152, 153].

These recent findings highlight the enormous potential of Myc TAD to interact with different proteins in a specific manner and underline the functional advantage of intrinsically disordered proteins. The possibility of NMR techniques to provide residue-level structural information even of unstructured proteins make it an indispensable tool for the investigation of this tantalizing class of proteins [154-157].

The brain acid-soluble protein 1 (BASP1)

BASP1 (brain acid-soluble protein 1, brain abundant-membrane attached signal protein 1) is a fascinating protein in the sense that it seems to have quite different functions. On the one hand it is described as a protein involved in neurite outgrowth and plasma membrane organization [158-160]. On the other hand it seems to play a certain role in regulation of transcription [161, 162]. Finally, it belongs to the class of intrinsically unstructured proteins, which became of greater interest after techniques were developed, especially in the field of NMR, that are able to extract structural information even from quite disordered proteins or proteins that exist in equilibrium between folded and unfolded states.

The homologues of human BASP1 were first identified as the brain-specific proteins CAP-23 (cortical cytoskeleton-associated protein of 23 kDa) in chicken brain [163] and its rat homologue NAP-22 (neuron-specific acidic protein of 22 kDa) [164]. Later, a group of brain acid soluble proteins (BASPs) were described in mammals and birds in the course of the search for participants in signal recognition and information transfer to the components controlling synaptic vesicle behaviour and neurotransmitter release in nerve endings. Four proteins had been identified BASP1, BASP2-1, BASP2-2 and BASP3. BASP2-1 and BASP2-2 were confirmed as the two forms of the prominent neuronal growth-associated protein GAP-43 (B-50, pp46, F1, neuromodulin) [165]. BASP1, despite showing a number of similar physico-chemical properties in common with GAP-43, belongs to a different protein family, the BASP1 family. Members of this protein family, as bovine BASP1, rat brain protein NAP-22 and chicken brain protein CAP-23, show 80%, 70% and 45% sequence identity, respectively, to human BASP1. Several PEST sequences are found in all members of the BASP1 family, which are characteristic of short-living proteins. The conservation of PEST sequences in BASP1 of different species suggests a high significance of those sequences for BASP1 function [166].

BASP1 was identified as a myristoylated protein that is highly expressed in nerve terminals. It is able to bind calmodulin (CaM), despite being devoid of any canonical calmodulin-binding domain [167]. N-myristoylation is important not only for BASP1 binding to a lipid membrane but also for interaction with CaM and protein kinase C (PKC). As a matter of fact, BASP1 devoid of the N-terminal myristoyl moiety is not bound by CaM; neither is myristic acid or a short myristoylated peptide, myr-GKK. The minimal fragment able to bind to Ca^{2+} -CaM with high affinity is the myristoylated nine-amino-acid N-terminal peptide of BASP1 (myr-G₁GKLSKKKK) [168]. After co-crystallization of this peptide in

complex with CaM, it could be seen that the myristoyl moiety extends into a hydrophobic tunnel created by the hydrophobic pockets of the N- and C-terminal lobes of CaM. Moreover, several N-terminal residues play important roles in BASP1-CaM interaction. BASP1 Leu4 interacts with CaM Phe12 and Met144, BASP1 Lys3 interacts with CaM Glu7 and the C-terminal basic cluster of the myristoylated BASP1 peptide is surrounded by many acidic residues of CaM [169]. One mode of function of BASP1-CaM complex formation is the regulation of phosphorylation of BASP1 Ser5 by PKC [167].

At least six BASP1 immunologically related proteins (BIRPs), which represent a set of myristoylated BASP1 N-terminal fragments lacking C-terminal parts, have been found in different species. Interestingly, BASP1 proteins and BIRPs are also found in significant amounts in non-nervous tissues as testis, kidney and lymphoid organs (spleen, thymus), suggesting that they might provide different physiological functions. Interestingly, it has been observed, that in a definite species, the same set of BASP1 fragments is present in different tissues, BASP1 fragments comprising about 50% of the total BASP1 amount in a tissue [170].

A lot of studies deal with the role of BASP1 in nervous tissue. It has recently been shown, that overexpression of BASP1 induces neurite outgrowth in neuronal cell lines. Interestingly, GAP-43 could substitute for BASP1 function with respect to neural cell adhesion molecule (NCAM)-independent neurite outgrowth. On the contrary, NCAM-mediated neurite outgrowth could only be stimulated by GAP-43, indicating overlapping but not similar roles of BASP1 and GAP-43. Mutation at the serine-5 phosphorylation site of BASP1 appears to have no adverse effect on this function, whereas the myristoyl moiety of BASP1 is indispensable for BASP1-mediated neurite outgrowth [159].

Other studies revealed that a myristoylated 19 amino terminal residues long fragment of BASP1 interacts with lipid membranes in a concentration dependent manner and is able to sequester PtdIns(4,5)P₂ and cholesterol into lipid rafts [158, 160]. PtdIns(4,5)P₂ is implicated in the attachment of the cytoskeleton to the plasma membrane as well as in the regulation of actin dynamics [171-174]. As BASP1 is able to influence the distribution of PtdIns(4,5)P₂ and cholesterol in the membrane, it therefore might indirectly influence actin cytoskeleton behaviour, explaining its involvement in neuronal sprouting and plasticity.

Considering these findings, a main function of BASP1 seems to be the regulation of the organization and morphology of the plasma membrane.

Strikingly, recent studies shed “different” light on BASP1 function, possibly being implicated in transcriptional regulation. BASP1 was discovered as transcriptional cosuppressor for the Wilms’ tumor suppressor protein 1 (WT1), which is a transcriptional regulator with putative target genes including those for growth factors and regulators of cell division. WT1 plays a key role in kidney development. Wilms’ tumor, a pediatric malignancy of the kidneys, has been found to either contain mutations in WT1 or aberrantly express WT1. BASP1 interacts with an N-terminal suppression region of WT1 (WT1 residues 92-101), which regulates the transcriptional activation domain. The elimination of endogenous BASP1 expression leads to augmentation of WT1 transcriptional activation [161].

Moreover, human BASP1 (hBASP1) was discovered in the search for apoptosis-specific antigens. In HeLa cells hBASP1 is located in the nucleus. After induction of apoptosis hBASP1 is cleaved and transported into the cytoplasm in a caspase-dependent manner [162]. These findings, together with the identified cosuppressor activity of BASP1 on WT1 function, raise the possibility that the caspase-dependent change of subcellular localization of hBASP1 might influence the transcriptional machinery.

Structurally, only very little is known about BASP1. As a matter of fact, crystallographic data exists only of the myristoylated N-terminal 19 amino acids in complex with CaM [169]. The meta-structure approach places BASP1 into the group of intrinsically unstructured proteins (IUPs), predicting very low compactness values and a low degree of secondary structural content (Fig. 7). Compactness values are below 200 and sometimes even below 0. For comparison, lowest compactness values of WT1 are around 150 and highest values around 600 (→ “Results” Fig. 22). This lack of secondary structure associated with BASP1 could also be confirmed by NMR-analysis (unpublished data). Interestingly, the meta-structure approach further predicts a relatively small region of chicken BASP1 spanning residues 42 to 80 as well as human BASP1 spanning residues 42 to 90 as being highly probable for interaction with other proteins, presumably with an extended, loop or β -stranded region of a protein.

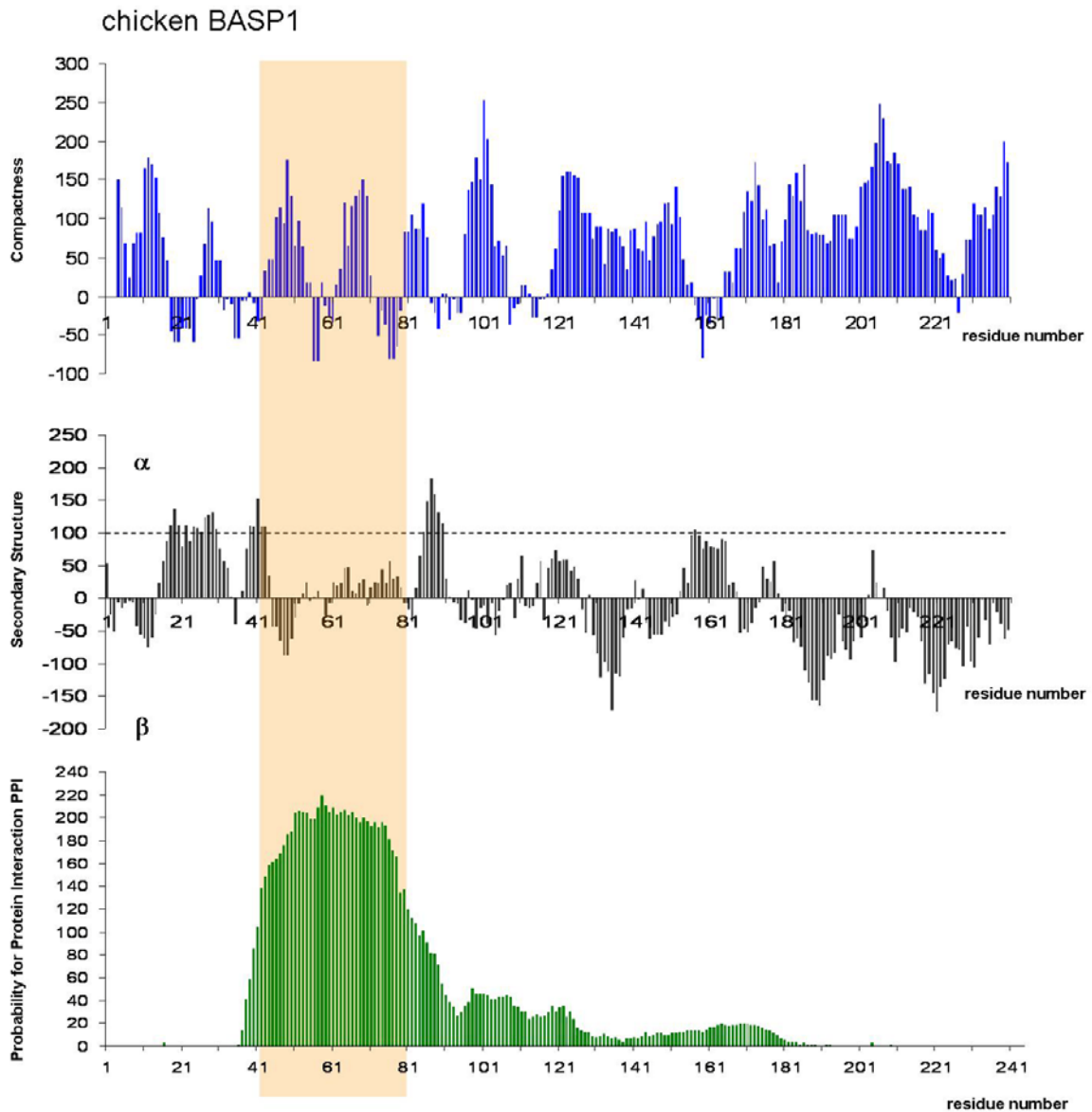


Fig. 7. Meta-structure analysis of chicken BASP1 yielding residue-based Compactness values and Secondary Structure probabilities as well as Probabilities for Protein Interaction (PPI). Ad Secondary Structure prediction: probabilities for α -helical segments are typically above 100 (dashed line); probabilities for extended conformations and β -strands are typically below 100. The region with highest probability for protein interaction is indicated by a red box (residues 42-80).

The interplay between BASP1 and Myc

The list of target genes regulated by the transcription factor Myc is long, as Myc is implicated in a lot of different processes controlling cell behaviour. The chicken *BASP1* gene (*cBASP1*) has been found to be specifically downregulated in MC29 transformed chicken embryonic fibroblasts (unpublished data). Current research tries to elucidate the mechanism how *cBASP1* is regulated by Myc proteins.

Interestingly, transformation by v-Myc is hindered by ectopic expression of *cBASP1*, suggesting that downregulation of *cBASP1* is a necessary step in transformation mediated by v-Myc (unpublished data). It is of special interest, to solve the question how transformation by v-Myc is regulated by cBASP1. One possibility is that cBASP1 interacts directly with Myc and consequently hinders transactivation of Myc target genes. In favour of this hypothesis are the findings that BASP1 is able to act as a cosuppressor.

Additionally, a small stretch of cBASP1 residues 60-80, which is predicted to be highly probable for protein interaction, has already been shown to lead to a cytopathic effect specifically in v-Myc transformed cells.

This study tries to elucidate, if the proteins cBASP1 and v-Myc or chicken c-Myc interact directly.

Materials and Methods

1. Microorganisms

<i>Organism</i>	<i>Strain</i>
<i>Escherichia (E.) coli</i>	DH5 α
	BL21(DE3)
	BL21(DE3)pLysS
	Rosetta(DE3)
	Rosetta(DE3)pLysS
<i>all strains derived from novagen</i>	
<hr/>	
<i>Chicken embryonic fibroblasts (CEF)</i>	
<i>Quail embryonic fibroblasts (QEF)</i>	

2. Media for Bacterial Growth

LB

Luria bertani medium

10 g (bacto-)tryptone
5 g yeast extract
10 g NaCl
(dissolve in app. 950 ml H₂O, adjust pH to 7.4 with NaOH)
H₂O to a final volume of 1 l
→ autoclave at 121°C
→ store at 4°C

LB

Luria bertani medium
(recipe with LB-Broth)

20 g LB-Broth
→ add H₂O to a final volume of 1 l
→ autoclave at 121°C
→ store at 4°C

LB selective media

LB_{Amp} 1 l LB
LB_{CoA} → add 1 ml of ampicillin (100 mg/ml) and/or chloramphenicol
LB_{Kan} (25 mg/ml) and/or kanamycin (25 mg/ml) just before use
→ prepare fresh

LB selective agar

for ~ 20 plates

500 ml LB
7.5 g agar agar
→ autoclave at 121°C for 15 min, cool to 55°C,
add 500 µl of appropriate antibiotics, pour into plates
→ store at 4°C

M9 medium

6 g Na₂HPO₄·x2H₂O

3 g KH₂PO₄

0.5 g NaCl

1 g NH₄Cl

→ dissolve in 1 l H₂O, autoclave at 121°C for 15 min

Prior to use add:

20 ml of 20% glucose → filtrated (0.2 µm)

2 ml of 1 M MgSO₄ → autoclaved

10 ml trace elements solution → filtrated (0.2 µm)

0.3 ml 1 M CaCl₂ → filtrated (0.2 µm)

antibiotics

optional: 1 ml biotin, 1 ml thiamine

→ store at 4°C

M9 medium

for ¹⁵N-labelling of proteins

s. M9 medium

use ¹⁵NH₄Cl instead of NH₄Cl

M9 medium

for ¹⁵N, ¹³C-labelling of proteins

s. M9 medium

use ¹⁵NH₄Cl instead of NH₄Cl

use 2 to 4 g ¹³C-Glucose instead of Glucose (add after autoclaving)

M9 medium

for ¹⁵N, ¹³C, ²H-labelling of proteins

6 g Na₂HPO₄·x2H₂O

3 g KH₂PO₄

0.5 g NaCl

1 g ¹⁵NH₄Cl

496 mg MgSO₄

2 to 4 g ¹³C-Glucose

add D₂O to a final volume of 1 l

100 mg ampicillin

12 mg Chloramphenicol

1 mg biotin

1 mg thiamine

0,3 ml CaCl₂

→ sterile filtrate and use immediately

→ use 190 mg IPTG for induction of protein expression

TY 2x

16 g (bacto-) tryptone
10 g yeast extract
5 g NaCl
H₂O to a final volume of 1 l
→ autoclave at 121°C for 15 min
→ store at 4°C

3. Buffers and Solutions

**Acrylamide/bisacrylamide
(separation gel)**

33 % (w/v) acrylamide

0.9 % (w/v) bisacrylamide

33 g acrylamide
0.9 g bisacrylamide (N,N'-methylene bisacrylamide)
H₂O to a final volume of 100 ml
→ sterilize by filtration (0.2 µm)
→ store light-protected at 4°C

**Acrylamide/bisacrylamide
(stacking gel)**

20 % (w/v) acrylamide

1 % (w/v) bisacrylamide

20 g acrylamide
1 g bisacrylamide (N,N'-methylene bisacrylamide)
H₂O to a final volume of 100 ml
→ sterilize by filtration (0.2 µm)
→ store light-protected at 4°C

**Ammoniumperoxodisulfate
(APS)**

10 % (w/v)

1 g ammoniumperoxodisulfate
H₂O to a final volume of 10 ml
→ store at -20°C

Ampicillin

100 mg/ml (≅0.27 M)

1 g ampicillin
H₂O to a final volume of 10 ml
→ sterilize by filtration (0.2 µm)
→ store at -20°C

AP buffer

100 mM Tris×HCl (pH 9.5)	6.06 g tris base
100 mM NaCl	2.92 g NaCl
5 mM MgCl ₂	0.51 g MgCl ₂ ×6H ₂ O
	→ dissolve in H ₂ O
	→ adjust to desired pH
	H ₂ O to a final volume of 500 ml

Blocking solution

10 mM Na ₂ H _(3-x) PO ₄ (pH 7.4)	5 g non fat dry milk
150 mM NaCl	PBS-T buffer to a final volume of 100 ml
0.1 % v/v Tween 20	→ make fresh before use
5 % w/v non fat dry milk	

Bradford reagent

1 ml ethanol abs.
2 ml H ₃ PO ₄
21 ml H ₂ O
1ml <i>Serva Blue G</i> solution
→ let stand for 30 min at room temperature before use

Bromphenol blue

0.5%	5 mg bromphenol blue
	H ₂ O to a final volume of 1 ml

BSA solution

1 mg/ml	10 mg bovine serum albumin
	H ₂ O to a final volume of 10 ml
	→ store at -20°C

CaCl₂

1 M	14.7 g CaCl ₂ ×2H ₂ O
	H ₂ O to a final volume of 100 ml
	→ autoclave at 121°C for 15 min

Chloramphenicol

25 mg/ml	250 mg chloramphenicol
	EtOH to a final volume of 10 ml
	→ store at -20°C

Coomassie staining solution

0.5% (w/v) Coomassie	2.5 g Coomassie Brilliant Blue R-250
50% (v/v) EtOH	250 ml EtOH (98%)
10% (v/v) HOAc	50 ml HOAc (99%)
	H ₂ O to a final volume of 500 ml
	→ store light protected

Destaining solution

for protein gels	300 ml EtOH (98%)
30% (v/v) EtOH	100 ml HOAc (99%)
10% (v/v) HOAc	H ₂ O to a final volume of 1 l

Dialysis buffer

20 mM Tris×HCl (pH 7.4)	2.42 g tris base (121.14 g/mol)
1 mM EDTA	1ml 1 M EDTA pH 8.0
1mM β-Mercaptoethanol	144µl β-Mercaptoethanol
4 M Urea	240.24 g Urea (60.06 g/mol)
	→ dissolve in H ₂ O (!! volume !!)
	→ adjust to desired pH (with HCl _{conc})
	H ₂ O to a final volume of 1 l

Dithiothreitol (DTT)

1 M	1.54 g dithiothreitol
	H ₂ O to a final volume of 10 ml
	→ sterilize by filtration (0.2 µm)
	→ store at -20°C

DNA sample buffer (5x)

for agarose gel electrophoresis	100 µl EDTA 1 M (pH 8.0)
20 mM EDTA	5 mg bromphenol blue
30 % (w/v) Glycerine	1.7 ml glycerine
0.5 % (w/v) SDS	125 µl SDS 20 %
0.1 % (w/v) Bromphenol blue	H ₂ O to a final volume of 5 ml
	→ store at 4°C

dNTP Mix (2mM each)

2 mM dATP	10 µl dATP 100 mM
2 mM dCTP	10 µl dCTP 100 mM
2 mM dGTP	10 µl dGTP 100 mM
2 mM dTTP	10 µl dTTP 100 mM
	H ₂ O to a final volume of 500 µl
	→ aliquote and store at -20°C

EDTA buffer

1 M EDTA pH 8.0 186.1 g Titriplex III (372.2 g/mol)
20 g NaOH
H₂O to a volume of about 400 ml
→ adjust pH with 5 M NaOH
H₂O to a final volume of 500 ml
→ autoclave at 121°C for 15 min

Ethidium bromide

10 mg/ml (BioRad)
→ store light protected at 4°C

Glucose

1 M 19.8 g Glc×H₂O
H₂O to a final volume of 100 ml
→ sterilize by filtration (0.2 µm)
→ store at 4°C

HCl

1 M 50 ml HCl_{conc} (32 %, ρ=1.16)
H₂O to a final volume of 500 ml

High imidazole buffer

20 mM Tris×HCl (pH 7.4) 2.42 g tris base
0.5 M Imidazole 17.02 g imidazole (68.08 g/mol)
→ dissolve in H₂O
→ adjust pH
H₂O to a final volume of 0.5 l

Inclusion bodies washing buffer (IBW)

50 mM Tris×HCl pH 8.0 25 ml Tris×HCl 1 M (pH 8.0)
2 mM EDTA 1 ml EDTA 1 M (pH 8.0)
5% (v/v) Glycerine 25 ml 100% glycerine
1% (v/v) Triton X-100 5 ml Triton X-100
(1 mM DTT or 1 mM β-Mercaptoethanol) H₂O to a final volume of 500 ml
optional: add prior to use: DTT or β-Mercaptoethanol

IPTG

1 M
2.4 g IPTG (238.25 g/mol)
H₂O to a final volume of 10 ml
→ sterilize by filtration (0.2 µm)
→ store at -20°C

Kanamycin

25 mg/ml
250 mg Kanamycin monosulfate
H₂O to a final volume of 10 ml
→ sterilize by filtration (0.2 µm)
→ store at -20°C

KCl

1 M
7.46 g KCl (74.55 g/mol)
H₂O to a final volume of 100 ml
→ autoclave at 121°C for 15 min

K₂HPO₄

50 mM
11.4 g K₂HPO₄×3H₂O (228.23 g/mol)
H₂O to a final volume of 1 l

KH₂PO₄

50 mM
6.8 g KH₂PO₄ (136.09 g/mol)
H₂O to a final volume of 1 l

KOAc buffer pH 6.0

3 M
29.45 g KOAc (98.15 g/mol)
H₂O to a volume of about 90 ml
→ adjust pH (with HOAc)
H₂O to a final volume of 100 ml

Laemmli buffer

(Tris-glycine electrophoresis buffer)

25 mM Tris
190 mM Glycine
0.1 % SDS
6 g tris base
28.75 g glycine
2 g SDS
H₂O to a final volume of 2 l

Low imidazole buffer

20 mM Tris×HCl (pH 7.4)	2.42 g tris base
10 mM Imidazole	0.68 g imidazole (68.08 g/mol)
	→ dissolve in H ₂ O
	→ adjust pH
	H ₂ O to a final volume of 1 l

Lysis buffer**'NaP_i NaCl pH 7.4'**

20 mM Na _x H _(3-x) PO ₄ (pH 7.4)	5.48 g NaCl
100 mM NaCl	1 ml 1 M EDTA pH 8.0
1 mM EDTA	144 µl β-Mercaptoethanol
1 mM β-Mercaptoethanol	NaP buffer to a final volume of 1 l

Lysis buffer**'Tris pH 7.4'**

20 mM Tris×HCl (pH 7.4)	2.42 g tris base
1 mM EDTA	1 ml 1 M EDTA pH 8.0
1 mM β-Mercaptoethanol	144 µl β-Mercaptoethanol
	H ₂ O to a final volume of 1 l

MgCl₂

1 M	20.33 g MgCl ₂ ×6H ₂ O
	H ₂ O to a final volume of 100 ml
	→ autoclave at 121°C for 15 min

MgSO₄

1 M	24.78 g MgSO ₄ ×7H ₂ O (246.48 g/mol)
	H ₂ O to a final volume of 50 ml
	→ autoclave at 121°C for 15 min

MnCl₂

1 M	3.96 g MnCl ₂ ×4H ₂ O
	H ₂ O to a final volume of 20 ml
	→ sterilize by filtration (0.2 µm)
	→ store at -20°C

MOPS buffer

1 M pH 7.0

20.93 g MOPS

→ dissolve in H₂O

adjust pH with NaOH

H₂O to a final volume of 100 ml

→ sterilize by filtration (0.2 µm)

→ store at -20°C

Na₂HPO₄

20 mM

3.55 g Na₂HPO₄×2H₂O (177.99 g/mol)H₂O to a final volume of 1 l

NaH₂PO₄

20 mM

2.76 g Na₂HPO₄×H₂O (137.99 g/mol)H₂O to a final volume of 1 l

NaCl

2 M

58.44 g NaCl

H₂O to a final volume of 500 ml→ autoclave at 121°C for 15 min

NaOAc buffer

for DNA precipitation

3 M

24.6 g NaOAc

H₂O ad about 80 ml

adjust to desired pH with HOAc

H₂O to a final volume of 100 ml→ autoclave at 121°C for 15 min

NaOH

1 M

20.00 g NaOH

H₂O to a final volume of 500 ml

NaP buffer

20 mM sodium phosphate pH 7.4

adjust pH by mixing

20 mM NaH₂PO₄ 100 mM NaCl20 mM Na₂HPO₄ 100 mM NaClto a final volume of 1 l

PBS buffer10 mM $\text{Na}_x\text{H}_{(3-x)}\text{PO}_4$ (pH 7.4)

150 mM NaCl

10 ml 1 M $\text{Na}_x\text{H}_{(3-x)}\text{PO}_4$ (pH 7.4)

75 ml 2 M NaCl

→ dissolve in H_2O

→ adjust pH with NaOH

 H_2O to a final volume of 1 l→ autoclave at 121°C for 15 min

PBS-T buffer10 mM $\text{Na}_x\text{H}_{(3-x)}\text{PO}_4$ (pH 7.4)

150 mM NaCl

0.1 % v/v Tween 20

1 ml Tween 20

PBS buffer to a final volume of 1 l

→ autoclave at 121°C for 15 min

Ponceau-S staining solution

0.1 % Ponceau S

5 % acetic acid

(Sigma Aldrich)

**2x Protein sample buffer
(SDS-PAGE)**

120 mM Tris×HCl, pH 6.8

6 % (w/v) SDS

20 % (v/v) Glycerine

0.01 % (w/v) Bromphenol blue

10 % (v/v) β -Mercaptoethanol

1.2 ml Tris×HCl 1 M (pH 6.8)

3 ml SDS 20 %

2 ml glycerine

1 mg Bromphenol blue

 H_2O to a final volume of 9 ml→ store in 900 μ l aliquots at -20°C

→ thaw only once

Add 100 μ l of β -mercaptoethanol to 900 μ l of buffer→ store at 4°C

RbCl

4 M

9.67 g RbCl

 H_2O to a final volume of 20 ml→ sterilize by filtration (0.2 μ m)

SDS 20%

20% SDS (w/v)

20 g SDS

 H_2O to a final volume of 100 ml

Stop Mix (5x)**for DNA restriction**

20 mM EDTA	0.1 ml 1 M EDTA (pH 8.0)
30 % Glycerine	1.7 ml glycerine
0.5 % SDS	0.125 ml 20 % SDS
0.1 % bromphenol blue	2 ml 0.5% bromphenol blue
	H ₂ O to a final volume of 5 ml

Stripping buffer

20 mM Tris×HCl (pH 7.4)	2.92 g NaCl
10 mM Imidazole	5 ml 0.5 M EDTA
1 M NaCl	Low imidazole buffer to a final volume of 50 ml
50 mM EDTA	

TBE buffer (10x)

pH _{calc} 8.3	108 g tris base
0.89 M Tris	55 g H ₃ BO ₃
0.89 M Boric acid	7.44 g EDTA Na ₂ ×2H ₂ O
0.02 M EDTA	H ₂ O to a final volume of 1 l
	→ autoclave at 121°C for 15 min

TE buffer

20 mM Tris×HCl (pH 7.4)	2.42 g tris base
1 mM EDTA	1 ml 1 M EDTA pH 8.0
	→ dissolve in H ₂ O
	→ adjust to desired pH (with HCl _{conc})
	H ₂ O to a final volume of 1 l

TEU buffer

20 mM Tris×HCl (pH 7.4)	2.42 g tris base
1 mM EDTA	1ml 1 M EDTA pH 8.0
7 M Urea	420.42 g Urea (60.06 g/mol)
	→ dissolve in H ₂ O (!! volume !!)
	→ adjust to desired pH (with HCl _{conc})
	H ₂ O to a final volume of 1 l

TEUS buffer

20 mM Tris×HCl (pH 7.4)	2.42 g tris base
1 mM EDTA	1ml 1 M EDTA pH 8.0
7 M Urea	420.42 g Urea (60.06 g/mol)
1 M NaCl	58.44 g NaCl (58.44 g/mol)
	→ dissolve in H ₂ O (!! volume !!)
	→ adjust to desired pH (with HCl _{conc})
	H ₂ O to a final volume of 1 l

TFB II solution

10 mM MOPS, pH 7.0	50 µl MOPS 1 M (pH 7.0)
75 mM CaCl ₂	375 µl CaCl ₂ 1 M
10 mM NaCl	25 µl NaCl 2 M
15 % (v/v) Glycerine	0.75 ml glycerine
	H ₂ O to a final volume of 5 ml
	→ prepare fresh
	→ sterilize by filtration (0.2 µm)

TFB I solution

100 mM RbCl	1.25 ml RbCl 4 M
50 mM MnCl ₂	2.50 ml MnCl ₂ 1 M
10 mM CaCl ₂	0.50 ml CaCl ₂ 1 M
30 mM KOAc pH 6.0	0.50 ml KOAc 3 M (pH 6.0)
15 % (v/v) Glycerine	7.50 ml glycerine
	H ₂ O to a final volume of 50 ml
	→ prepare fresh
	→ sterilize by filtration (0.2 µm)

**10x Transfer buffer
(without Methanol)**

tris base	30 g tris base
glycine	144 g glycine
	H ₂ O to a final volume of 800 ml

Transfer buffer

tris base	100 ml 10x Transfer buffer (without methanol)
glycine	200 ml methanol
20 % v/v methanol	H ₂ O to a final volume of 1 l

Urea

8 M	6 g Urea
	H ₂ O to a final volume of 100 ml

4. General Methods: DNA

4.1. Agarose Gel Electrophoresis of DNA

A DNA fragment migrates at different rates through gels containing different concentrations of agarose. By varying agarose concentration, it is possible to resolve a wide range of DNA fragments.

<i>agarose concentration % (w/v)</i>	<i>range of separation (bp)</i>	<i>agarose for 10 ml gel (g)</i>	<i>agarose for 30 ml gel (g)</i>
0.3	5000 – 60000	0.03	0.09
0.6	1000 – 20000	0.06	0.18
0.7	800 – 10000	0.07	0.21
0.9	500 – 7000	0.09	0.27
1.2	400 – 6000	0.12	0.36
1.5	200 – 3000	0.15	0.45
2.0	100 – 2000	0.20	0.60
3.0	50 - 1000	0.30	0.90

- Add the appropriate amount of agarose to an appropriate amount of 1xTBE buffer.
 - For high percentage gels (3-5%) add an excess amount of distilled H₂O to increase the weight by 10-20% (or preferentially use a vertical polyacrylamide gel for tiny fragments).
- Heat the suspension in the microwave to the boiling point.
 - For high percentage gels (3-5%): check (by weighing) that the excess 10-20% of water has evaporated and, if needed, continue boiling to remove the excess water, or add hot distilled water to restore the initial weight.
- Cool to ~ 50°C in a water bath, add 1 µl of Sybr-Safe 1:1000 dilution (invitrogen) per 10 ml of gel.
- Pour agarose into a prepared gel tray with a comb.
- Let the gel polymerize at room temperature (protect from light, when using Sybr-Safe).
- Put the gel in a horizontal gel chamber, fill with 1xTBE and remove the comb.
- Load DNA sample dissolved in DNA sample buffer, run gel at 40-60 V for 1 hr or 90-100 V for 30 min.

- Detect bands with the help of a UV-transilluminator.
- Elute DNA from gels using the QIAEXII Gel Extraction Kit (Qiagen).

4.2. Cloning of DNA fragments

4.2.1. Digestion of DNA with restriction endonucleases

Depending on subsequent experiments, an appropriate amount of DNA has to be digested. For analytical purposes (verification of constructs by restriction digest) only minor amounts of DNA may be used. (Typically, a band is easily visible, if it contains about 20 ng of DNA. The detection limit for SYBR Safe stain as well as ethidium bromide is roughly 0.5 ng/band in a minigel for fragments larger than 200 bp viewed on a 300 nm transilluminator).

If follow-up experiments include gel extraction of specific bands, purification of DNA fragments and ligation, the amount of DNA used for digestion has to be adapted to a minimal amount, which will be needed for ligation, bearing in mind, that DNA might be lost during successive experimental steps.

By definition, 1 unit of restriction enzyme will completely digest 1 µg of substrate DNA in a 50 µl reaction in 60 minutes.

		e.g.: for analytical purpose $V_{\text{final}} = 10 \mu\text{l}$
DNA (plasmid or PCR product)	0.5-3 µg	5 µl (~ 0.1 µg/µl)
10x restriction buffer		1 µl
10x BSA (optional)		1 µl
H ₂ O	to appropriate volume	2.5 µl
Restriction enzyme	5-10 U	0.5 µl (10 U/µl)

→ Incubate at the recommended temperature for 2 hrs (up to o/n). With some enzymes star activity has been observed, i.e. time of digestion must not be too long.

→ If necessary terminate the reaction by incubation of the solution at the inactivation temperature for 10 to 20 min or by adding 1/4 of the total volume of 5x DNA sample buffer.

→ Store at 4°C or directly load onto a gel.

Additional information:

- *The volume of the enzyme added must not exceed more than 10% of the total volume, as the glycerine within the enzyme buffer may inhibit restriction.*
- *If the DNA has to be cleaved with two restriction enzymes or modified with other enzymes e.g. alkaline phosphatase or blunt ending enzymes, the reactions can be carried out simultaneously if both enzymes are active in the same buffer. Alternatively, the enzyme with the buffer of lower ionic strength should be used first. The appropriate amount of salt and the second enzyme can be added subsequently. Another way is to precipitate DNA after the first digestion and then perform the second one.*

4.2.2. Phosphatase treatment of DNA fragments

Alkaline Phosphatases (AP) catalyze the removal of 5' phosphate groups from DNA, RNA, ribo- and deoxyribonucleoside triphosphates. They can even remove phosphate groups from proteins. There are different sources of alkaline phosphatase. Most widely used is calf intestinal alkaline phosphatase (CIP), which can be inactivated by heat. One application of alkaline phosphatase in nucleic acid manipulation is the removal of 5' phosphates from plasmid or bacteriophage vectors that have been cut with restriction enzymes. This prevents religation of vectors, if only one restriction enzyme was used, and insertion of unwanted DNA fragments, if two restriction enzymes were used, respectively. As alkaline phosphatases are very active, they have to be either inactivated or quantitatively removed before proceeding to subsequent experiments (e.g.: ligation).

1 µl of CIP was added directly to the digestion mixture (35 µl) and incubated for ~ 1 h at 37°C. The reaction mixture was subsequently purified using a PCR purification kit (Qiagen) to remove enzymes and other contaminants. The digested and CIP-treated vector DNA was dissolved in H₂O.

Additional information:

- *The DNA fragment, which is inserted into the vector, is NOT to be treated with phosphatase.*

4.2.3. Ligation of DNA fragments

Depending on the ligation conditions (sticky end or blunt end ligation, CIP-treatment of vector DNA, etc.) the insert:vector molar ratio may be differently chosen (3:1, 1:1, 1:3). Usually 100ng of vector DNA in a final volume of 10-20 µl is used in a standard ligation protocol.

Molar Ratio of Insert to Vector:

$\frac{\text{length of insert (in kb)}}{\text{length of vector (n kb)}} \times \text{ng of vector} = \text{ng of insert needed for a 1: 1 ratio}$

		e.g.: molar ratio insert:vector = 3:1 $V_{\text{final}} = 20\mu\text{l}$ insert → 737 bp vector → 5350 bp
Vector DNA	100ng	5 µl (20 ng/µl)
Insert DNA	according to molar ratio	3 µl (14 ng/µl)
5x T4 DNA Ligase buffer		4 µl
H ₂ O	to appropriate volume	6.8 µl
T4 DNA Ligase	0.1-1.0 U	0.2 µl (5U/µl)

→ Incubate at 16°C o/n.

→ Inactivate DNA Ligase at 65°C for 10 min or directly transform bacteria with ligation mix.

4.2.4. Polymerase Chain Reaction (PCR)

Standard PCR mixture

		e.g.: $V_{\text{final}} = 20\mu\text{l}$
Vector DNA	1-50 ng	0.25 μl (0.2 $\mu\text{g}/\mu\text{l}$)
10x Taq Pol buffer (MgCl ₂ free)		2 μl
MgCl ₂ 50mM	1-6 mM	1.2 μl (\triangleq 3mM)
dNTP mix (2mM each)	0.2 mM	2 μl
forward primer 10 μM	10-50 pmol	1 μl (\triangleq 10 pmol)
reverse primer 10 μM	10-50 pmol	1 μl (\triangleq 10 pmol)
H ₂ O	to appropriate volume	12.35 μl
T4 Taq polymerase (1U/ μl)	0.2 U	0.2 μl

Standard PCR program

			e.g.: for ~100bp PCR product	
denaturation/activation	95°C	00:05:00	95°C	00:05:00
30x	denaturation	95°C	95°C	00:00:20
	annealing	55 – 65°C	53°C / 56°C / 60°C	00:00:20
	elongation	72°C	72°C	00:00:20
final elongation	72°C	00:05:00	72°C	00:05:00
	4°C	hold	4°C	hold

- Either add the appropriate amount of DNA sample buffer (5x) and purify PCR product by agarose gel electrophoresis using low melting agarose (BIORAD) and the QIAEXII Gel Extraction Kit (Qiagen) or purify it via PCR purification kit (Qiagen) without running a gel.
- Very small PCR-products are purified by phenol:chloroform extraction and subsequent iso-propanol precipitation.

4.2.5. Preparation of competent bacteria (Hanahan) [175]

- Prepare an overnight culture of the respective *E. coli* strain; inoculate LB medium supplemented with the appropriate antibiotics with cells from the bacterial stock solution.
- Inoculate 100 ml of 2x TY medium with 1 ml of the overnight culture.
- Let the bacteria grow at 37°C and 225 rpm until an OD₆₀₀ = 0.4-0.5.
- Cool the flask for 10-15 min on ice.
- Pour the culture into ice-cold 50 ml conical tubes.
- Centrifuge at 4°C for 10 min at 4000 x g and discard the supernatant.
- Resuspend gently the pellet in 100 ml ice-cold TFB I solution.
- Incubate on ice for 10 min.
- Centrifuge as above and discard supernatant.
- Resuspend the pellet in 4 ml of ice-cold TFB II solution.
- Immediately prepare 100 µl aliquots in pre-chilled 2 ml tubes and store them at -80°C
- Recommended: *test the transformation efficiency by transforming 10 ng of pUC19 plasmid DNA according to the heat-shock protocol. The efficiency should be about 1x10⁶ to 1x10⁷ pfu per µg of DNA.*

4.2.6. Transformation of *E. coli* bacteria – heat shock protocol

- Thaw a 100 µl aliquot of competent cells on ice.
- Add ~ 10 ng of plasmid DNA and incubate the mixture on ice for 2-30 min.
- Incubate the mixture at 42°C in a water bath for 90 sec.
- Cool 2 min on ice.
- Add 300 µl of LB medium and incubate at 37°C for 45 min at 225 rpm.
- Plate 50 to 400 µl of bacterial suspension on an agar plate containing the appropriate antibiotics.
- Place the plate in an incubator at 37°C for 10 to 15 hrs.

4.2.7. Preparation of *E. coli* starter cultures

Starter cultures for plasmid midi preparations

- Inoculate 50-100 ml of LB medium supplemented with the appropriate antibiotics with a single colony from a transformation plate using a sterile pipette tip. Alternatively, use 1 μ l of a glycerol stock for inoculation.
- Incubate at 37°C and 225 rpm for at least 12 hrs.

Starter cultures for recombinant protein expression

- inoculate 20 ml of LB medium (*optional: supplemented with 2 g/l glucose to prevent that galactose from the medium induces the IPTG system*) containing the appropriate antibiotics with one or more colonies from a transformation plate
- incubate at 37°C and 225 rpm over night (or until OD₆₀₀ reaches 1.0 to 1.5)

4.2.8. Preparation of plasmid DNA from bacteria

- Plasmid DNA from bacteria was obtained using Plasmid Mini or Midi Kits (Qiagen) according to the manufacturer's instructions.

4.2.9. Phenol:Chloroform extraction of DNA

Phenol:chloroform extraction is a way to remove proteins from nucleic acid solutions. A subsequent extraction with chloroform is performed to remove traces of phenol.

- The phenol has to be adequately equilibrated to a pH of 7.8-8.0.
- Add H₂O to the DNA solution to a final volume of 200 μ l.

1. Add an equal volume of phenol:chloroform.
 2. Mix until an emulsion forms → vortexing is possible when isolating small DNA molecules (<10 kb).
 3. Centrifuge at maximum speed in a table-top centrifuge for 1 min at room temperature.
→ organic and aqueous phase should be separated.
 4. Transfer the aqueous phase to a fresh tube and discard interface and organic phase.
→ *optional: interface and organic phase may be “back-extracted”.*
- Repeat steps 1-4 until no protein is visible at the interface.
 - Add an equal volume of chloroform and repeat steps 2-4.
 - Recover the nucleic acid by EtOH or iso-propanol precipitation.

4.2.10. EtOH precipitation of DNA

- Start with a total volume of 100 to 200 µl of DNA solution, pre-chill on ice.
- Add 1/10 of the total volume of 3 M NaOAc (pH 5.2).
- Add 2.5 volumes of ice cold EtOH_{abs}, mix and incubate at –20°C for 30 min.
- Centrifuge at 4°C for 30 min at 13000 rpm.
- Wash the pellet with 150 µl of ice cold 70% EtOH, centrifuge briefly.
- Discard supernatant and air-dry the pellet (or dry carefully with a Speed Vac).

4.2.11. iso-Propanol precipitation of DNA

- Add 1/10 of the total volume of 3 M NaOAc (pH 5.2) to the DNA solution.
- Add 1 volume of iso-propanol, mix and incubate at –20 °C o/n.
- Centrifuge at 4°C for 30 min at 13000 rpm.
- Wash the pellet with 150 µl of ice cold 70% EtOH, centrifuge briefly.
- Discard supernatant and air-dry the pellet (or dry carefully with a Speed Vac).

4.2.12. Quantification of nucleic acids

- Prepare 100 μl dilutions of DNA in H_2O in concentrations of about 5 to 50 $\mu\text{g}/\text{ml}$.
- Measure the absorbance at 260 and 280 nm in a UV Spectrophotometer.
- The following assessments can be used for quantification:
 - DNA: $A_{260} = 1$ at a concentration of 50 $\mu\text{g}/\text{ml}$
 - RNA: $A_{260} = 1$ at a concentration of 40 $\mu\text{g}/\text{ml}$
- A ratio of A_{260}/A_{280} between 1.6 and 2.0 indicates pure DNA or RNA without significant protein contamination.

5. General methods: Protein

5.1. Expression of recombinant proteins

- Plasmid DNA from bacteria was obtained using Plasmid Mini or Midi Kits (Qiagen).
- Transform the respective *E. coli* strain with the expression plasmid containing the gene sequences of the protein of interest (→ section 4.2.6: “Transformation of *E. coli* bacteria – heat shock protocol”).
- Prepare a starter culture in LB medium as described.
- When the starter culture has reached optimal OD₆₀₀ dilute 1/10 to 1/30 with expression medium containing the appropriate antibiotics.
- Incubate at 20 to 37°C and 225 rpm until OD₆₀₀ reaches 0.5 to 0.9 (*depending on the protein to be expressed*).
- **Control 1:** Pipet 1 ml of the culture into a 1.5 ml tube, centrifuge at 4000 rpm for 5 min, remove the supernatant and suspend the pellet in 50 µl of 1x protein sample buffer, store at –20°C.
- Induce protein expression by adding IPTG. *Exact conditions for induction and further incubation depend on the nature of the expressed protein; final IPTG concentration ranges from 0.4 to 2 mM, incubation temperature and time range between 37°C for several hours and 18°C over night.*
- **Control 2:** Measure OD₆₀₀ of the culture. Pipet 1 ml of the culture into a 1.5 ml tube and centrifuge at 4000 rpm for 5 min. Remove the supernatant and resuspend the pellet in 200 µl of lysis buffer and lyse the cells, e.g. by sonication. Take a sample and mix 1:1 with 2x protein sample buffer. Centrifuge at 18000 rpm for 10 min, take a sample from the supernatant and mix 1:1 with 2x protein sample buffer. Store the samples at –20°C.

Harvesting:

- Cool the flask with the expression culture for 15 min on ice.
- Centrifuge for 15 min at 4000 rpm at 4°C.
- Remove the supernatant and dissolve the pellet in 30 ml of ice-cold lysis buffer per liter of bacterial culture. *The optimal buffer conditions depend on the properties of the protein of interest and have to be optimized for every purification. E.g. use Tris×HCl buffer for acidic proteins (purified by anion exchange chromatography), or a sodium phosphate buffer for basic proteins (purified by cation exchange chromatography). Lysis buffers can also contain various amounts of salt (10 to 500 mM), reductants as 0.1% (w/v) β-mercaptoethanol or 0.5 to 10 mM DTT, and metal ions if the protein is a metal binding protein.*
- Freeze the bacterial suspension in liquid nitrogen and store at –20°C o/n or –80°C for long term storage.
- Check the expression of the recombinant protein using SDS-PAGE. Load 10 to 20 μl of the control samples and compare the amount of insoluble and soluble protein fraction.

5.2. Preparation of lysates for protein purification

- Thaw the bacterial suspension on ice or in a room tempered water bath.
- If the recombinant protein is expressed in pLysS strains incubate the suspension on ice for 1 hr. *These strains contain lysozyme and will lyse during thawing.*
- Sonicate the lysate for 10 min on ice (sonicator-conditions: sonicator tip should reach at least 5mm beneath the surface; 40-60% power; 30-50% of a second pulse-length). *This breaks the cells and fragments the bacterial DNA.*
- Centrifuge the lysate at 4°C and 18000 rpm for 15-30 min. *This should result in a compact pellet and a clear supernatant.*
- *If not previously done, analyze aliquots of the supernatant and the pellet (soluble vs. insoluble protein fractions) equivalent to 50 μl of bacterial culture by SDS-PAGE.*

5.3. Enrichment of inclusion bodies

If a recombinant protein is expressed in inclusion bodies this has both, advantages and disadvantages. As an advantage, inclusion bodies are mostly free of other components, so they can be treated as almost pure protein. However, inclusion bodies are insoluble and the protein has to be denatured and refolded to obtain viable samples. Anyway, the inclusion bodies have to be washed to get rid of cell fragments and other remainders of bacterial cells, and afterwards a special denaturing/renaturing protocol has to be established for each protein.

- After lysis resuspend the pellet (from 1 l expression culture) in 3.5 ml IBW buffer.
→ sonicate briefly to destroy cell clumps and for resuspension.
- Centrifuge at 4°C and 18000 rpm for 10-15 min.
- Discard supernatant and resuspend the pellet in 3.5 ml of IBW buffer.
→ sonicate briefly to destroy cell clumps and for resuspension.
- Centrifuge at 4°C and 18000 rpm for 10-15 min.
- Discard supernatant and resuspend the pellet in 3.5 ml of NaP buffer.
→ sonicate briefly to destroy cell clumps and for resuspension.
- Centrifuge at 4°C and 18000 rpm for 10-15 min.
- Discard supernatant and solubilize the pellet in a suitable buffer for subsequent purification steps (e.g. 8 M Urea or TEU buffer).

5.4. Refolding of proteins using stepwise dialysis

- Dissolve the pellet in an appropriate denaturing agent, e.g. 8M Urea or TEU buffer.
→ to dissolve the protein more easily, the suspension can be heated to 37°C.
- Centrifuge at 4°C and 18000 rpm for 10 min to remove insoluble particles.
- Equilibrate a dialysis bag with a cut off value smaller than the molecular weight of the protein in about 50 ml of dialysis buffer or water.
- Fill the denatured protein sample in the dialysis bag and close with clamps.
- Dialyze into 200 ml of dialysis buffer (target buffer + 4M Urea) at 4°C for 30 to 40 min under stirring.

- Add 66 ml of target buffer to give a final concentration of 3 M Urea.
→ Continue dialysis at 4°C for 30 to 40 min.
- Add 132 ml of target buffer to give a final concentration of 2 M Urea.
→ Continue dialysis at 4°C for 30 to 40 min.
- Add 400 ml of target buffer to give a final concentration of 1 M Urea.
→ Continue dialysis at 4°C for 30 to 40 min.
- Add 800 ml of target buffer to give a final concentration of 0.5 M Urea.
→ Continue dialysis at 4°C for 30 to 40 min.
- Dialyze into 1000 ml target buffer over night at 4 °C.

5.5. Concentration of protein samples using membrane filters

Centriprep or Centricon filters (Amicon) are suitable to generate highly concentrated protein samples, e.g. to obtain protein samples of high concentration for NMR analysis under native conditions.

- Transfer the protein solution to a centriprep (up to 15 ml volume) or a centricon (up to 2 ml volume) with a cut off value smaller than the molecular weight of the protein.
- Centrifuge at 4000 rpm at 4°C; the buffer will pass the filter, while the protein will be retained.

5.6. Chromatographic Methods

5.6.1. The Fast Performance Liquid Chromatography (FPLC) System

Protein purification was performed using the FPLC system *Äktaexplorer* from amersham pharmacia biotech. Chromatographic methods used were affinity, ion exchange and size exclusion chromatography. All FPLC purification steps were performed either at room temperature or at 4°C.

5.6.2. Immobilized metal ion affinity chromatography IMAC (HiTrap Chelating HP 5ml)

HiTrap Chelating HP 5ml is a pre-packed column from amersham pharmacia. The matrix is composed of iminodiacetic acid coupled via a spacer arm of seven atoms to highly crosslinked agarose beads. Several residues, for example histidine, form complexes with many metal ions. Charged with suitable ions (e.g.: Ni²⁺, Co²⁺,...) this column will selectively retain proteins with complex forming amino acids exposed on the surface. Chelating agents, as EDTA, should be avoided. Don't use DTT as a reducing agent in protein samples, use β-mercaptoethanol instead. His6-tagged proteins can be purified directly from pre-treated bacterial lysates.

- Wash the sample pump with H₂O to ensure that it is free of air.
- Wash the column with 5 CV of H₂O to wash away the 20% ethanol solution.
- Load the column with 0.5 CV of 0.1 M NiCl₂ or 0.1 M NiSO₄.
- Wash the column with 5 CV of H₂O.
- Choose a buffer system that is suitable for the analysis following the purification.
- Degas the buffer solutions using a water jet pump and filtrate through a ZapCapS bottle top filter (0.2-0.45 μm).

- Flush the pumps, the valves and the sample applicator of the FPLC system with the buffer solutions.
- Equilibrate the column with 5 CV of binding buffer (low imidazole buffer) until the base line is stable.
- *Optional: Wash the column with 5 CV elution buffer to elute unspecifically bound metal ions and re-equilibrate with 5 CV of binding buffer.*
- Centrifuge the bacterial lysate at 4°C and 18000 rpm for at least 10 min to remove insoluble particles.
- Load the supernatant onto the column using the sample pump. Be careful to load the sample at slow flow rates or alternatively more than once, to ensure binding of the His6-tagged protein.
- Wash with 5-10 CV of binding buffer.
- *Optional: Wash with 5 CV high salt buffer (binding buffer + 0.5-1 M NaCl) to eliminate ion exchange effects. Wash again with 5 CV of binding buffer.*
- Elute the protein with 2-5 CV (usually sufficient) of elution buffer (high imidazole buffer).
 - *also possible: linear gradient from 0-100% elution buffer of e.g. 10-20 CV.*
- Collect fractions of the flow through and the eluate and analyse the samples by SDS-PAGE.
- After the purification, flush the FPLC system, strip the column with 5 CV stripping buffer, wash with 5-10 CV of H₂O and eventually with 4 CV of 20% of ethanol for storage. From time to time wash the column with 2 CV of 0.5 M NaOH.

5.6.3. Anion exchange chromatography (Resource Q 6ml)

Resource Q is a pre-packed column from pharmacia biotech. The matrix is composed of monodisperse polystyrene/divinyl benzene beads with quaternary ammonium as anion exchanger. It is suitable for purification of acidic proteins ($pI < 7$). The pH of the buffer should be at least 1 pH unit above the pI of the protein of interest so that it is negatively charged and will bind to the matrix. Anionic detergents should be avoided as they bind to quaternary ammonium. The practical protein loading range is up to 150 mg, whereas the sample volume is of minor importance.

- Choose a buffer system that is not bound by the exchanger (e.g.: Tris×HCl) and prepare two buffer solutions, one with low ionic strength (e.g. 10 mM NaCl) and one with high ionic strength (e.g. 0.5 to 1 M NaCl).
- Degas the buffer solutions using a water jet pump and filtrate through a ZapCapS bottle top filter (0.2 μm).
- Flush the pumps, the valves and the sample applicator of the FPLC system with the buffer solutions.
- Equilibrate the column with at least 2 CV of start buffer (low ionic strength buffer).
- Run 2 CV of elution buffer (high ionic strength buffer) through the column.
- Re-equilibrate the column with 5 CV of start buffer.
- Centrifuge the bacterial lysate at 4°C and 18000 rpm for at least 10 min to remove insoluble particles.
- Load the supernatant onto the column using the sample pump.
- Wash with 5 CV of start buffer.
- Elute the protein via gradient elution by mixing start and elution buffer over e.g. 20 CV.
→ lower flow rates and more shallow gradients improve resolution.
- Collect fractions of the flow through and the eluate and analyse the samples by SDS-PAGE.
- After the purification, flush the FPLC system, wash the column with 5-10 CV of H₂O and eventually with ~ 5 CV of 20% ethanol for storage. From time to time clean the column with 5 CV 1 M NaCl, 5 CV 1 M NaOH, 5 CV 1 M HCl and 5 CV 1 M NaCl, before washing with H₂O and storing in 20% ethanol.

5.6.4. Preparative size exclusion chromatography (HiLoad 16/60 Superdex 75 prep grade)

HiLoad 16/60 Superdex 75 prep grade is a pre-packed column from amersham pharmacia biotech. The matrix is produced by covalent bonding of dextran to highly cross-linked agarose. The separation range of this column lies in the molecular weight range between 3 000 to 70 000, the bed volume is approximately 120 ml. Proteins applied to this column are separated according to their size. Large proteins elute first, while small proteins can enter the pores of the matrix and are thus retarded. This polishing step is mostly used as a last step in protein purification to achieve final high-level purity.

- Choose a buffer system that is suitable for the analysis following the purification (e.g. sodium phosphate or Tris buffer at appropriate pH).
- Degas the buffer solutions using a water jet pump and filtrate through a ZapCapS bottle top filter (0.2 µm).
- Equilibrate the column with at least 2 CV of running buffer until the base line is stable.
- Flush the pumps, the valves and the sample applicator of the FPLC system with the buffer solutions.
- Dissolve the protein sample in 1 to 2% of the bed volume (up to 5 ml) of running buffer or concentrate to this volume.
- Centrifuge the protein sample at 4°C and 18000 rpm for at least 10 min to remove insoluble particles.
- Load the protein solution onto the column using a syringe (loop sample injection).
- Elute the column with 1.5 CV of running buffer.
- Collect fractions of the flow through and the eluate and analyse the samples by SDS-PAGE.
- *If the resolution is low, decrease the flow rate or the sample volume or sample amount. To avoid nonspecific ionic interactions with the matrix, use buffers with ionic strength of at least 150 mM NaCl. Alternatively, gel filtration can be performed under denaturing conditions with buffers containing up to 8 M urea or up to 6 M guanidinium hydrochloride.*
- After the purification, flush the FPLC system and wash the column with a minimum of 3 CV of water and eventually with 4 CV of 20% of ethanol (wash the column from time to time with 0.5 CV of 0.5 M NaOH).

5.6.5. Analytical size exclusion chromatography (Superdex 75 10/300 GL)

Superdex 75 10/300 GL is a pre-packed column from GE Healthcare. The matrix consists of a composite of cross-linked agarose and dextran. The separation range of this column lies in the molecular weight range between 3 000 to 70 000, the bed volume is approximately 24 ml. The column efficiency, expressed as the number of theoretical plates per meter is > 30 000 N/m. Proteins applied to this column are separated according to their size. This column is for analytical purposes, the amount of protein loaded onto the column should be ≤ 10 mg in a volume of 25-500 μ l.

- Choose a buffer system that is suitable for the analysis.
- Degas the buffer solutions using a water jet pump and filtrate through a ZapCapS bottle top filter (0.2 μ m).
- Wash the column with at least 2 CV of H₂O.
- Equilibrate the column with at least 2 CV of running buffer until the base line is stable.
- Flush the pumps, the valves and the sample applicator of the FPLC system with the buffer solutions.
- Centrifuge the protein sample at 4°C and 18000 rpm for at least 10 min to remove insoluble particles.
- Load 25-500 μ l protein solution onto the column using a syringe (loop sample injection).
→ not more than 10 mg protein.
- Elute the column with 1.5 CV of running buffer.
- Collect fractions of the flow through and the eluate and analyse the samples by SDS-PAGE.
- After the purification, flush the FPLC system and wash the column with a minimum of 3 CV of water and eventually with 4 CV of 20% of ethanol (wash the column from time to time with 1 CV of 0.5 M NaOH).

5.7. Quantification of protein

Bradford assay (Coomassie Blue protein assay)

The absorbance maximum of the dye in an acidic solution shifts from 465 to 595 nm after adding protein due to stabilization of the anionic form of the dye by both hydrophobic and ionic interactions. The dye principally reacts with arginine residues and to a lesser extent with histidine, lysine, tyrosine, and phenylalanine residues.

Preparation of a calibration curve:

- Prepare a 0.1 $\mu\text{g}/\mu\text{l}$ BSA solution in H_2O .
- Prepare 11 aliquots with 0 μg , 1 μg , 2 μg , 3 μg , 4 μg , 5 μg , 6 μg , 7 μg , 8 μg , 9 μg and 10 μg of BSA in 100 μl H_2O and transfer to polystyrene cuvettes for measurement in a photometer.
- Mix each aliquot with 1ml of Bradford reagent and let stand for ~ 2 min.
- Measure the absorbance at 595 nm.
- Establish the calibration curve.

Measurement of protein samples:

- 5 μl of protein sample are diluted with H_2O to a final volume of 100 μl .
- Add 1ml of Bradford reagent and let stand for ~ 2 min.
- Measure the absorbance at 595 nm.
- Calculate protein concentration with the help of the calibration curve.

5.8. TEV protease cleavage of proteins

TEV protease is the name for the 27 kDa catalytic domain of the Nuclear Inclusion a (NIa) protein of the tobacco etch virus (TEV). TEV protease recognizes highly specific a linear epitope of the general form EXXYXQ'(G/S), with the cleavage occurring between Q and G or S. The most efficient and most commonly used substrate is ENLYFQS. TEV protease is maximally active at 34°C, but it is recommended to perform digests at room temperature or at 4°C overnight. The “standard” reaction buffer for TEV protease is 50 mM Tris×HCl (pH 8.0), 0.5 mM EDTA and 1 mM DTT, but it tolerates a range of buffers, including phosphate, MES and acetate. The cleavage can be inefficient, if the cleavage site is too close to ordered structures or the substrate exists in the form of soluble aggregates [176].

Initial screen for TEV protease – substrate ratio determination:

- Measure protein concentrations of TEV protease and protein sample.
- Mix TEV protease and the protein sample in the ratios 1:50, 1:100, 1:250 and 1:500 in a fixed volume of TE buffer (e.g.: 20 µl) and a fixed amount of protein (e.g.: 20 µg per digest).
- Mix the digestion mixture carefully.
- Cleave at 4°C o/n.
- Analyze the samples by SDS-PAGE.
- Depending on the outcome of the cleavage, enhance or reduce the amount of TEV protease.
- If the perfect conditions are found, scale up the experiment.

5.9. SDS Polyacrylamide Gel Electrophoresis (SDS-PAGE) of proteins [177]

SDS-PAGE is used for the investigation of protein samples in terms of contained proteins. Gels containing sodium dodecyl sulfate (SDS) provide dissociating conditions, where proteins are separated strictly according to polypeptide size. A discontinuous buffer system [178, 179] and polyacrylamide (PAA) concentrations from 10%-20% were used. As molecular weight markers served Unstained Protein Molecular Weight Marker SM0431 (Fermentas) (14.4, 18.4, 25, 35, 45, 66.2, 116 kDa), SDS7 (Sigma Aldrich) (14.2, 20.1, 24, 29, 36, 45, 66 kDa), SDS6H2 (Sigma Aldrich) (29, 45, 66, 97, 116, 200 kDa) and the Ultra-low Range Molecular Weight Marker M3546 (Sima Aldrich) (1.060, 3.496, 6.5, 14.2, 17.0, 26.6 kDa).

15% gels were used most often and cast using the Mini-PROTEAN 3 Multi-Casting Chamber (BIORAD).

	12 resolving gels	12 stacking gels
Tris (pH 9.0)	8 ml	-
Tris (pH 6.8)	-	3.5 ml
40% PAA (37.5 : 1)	24 ml	-
40% PAA (19 : 1)	-	3.5 ml
H ₂ O	32 ml	21 ml

	<i>degas</i>	
20% SDS	320 µl	70 µl
TEMED	20 µl	35 µl
APS	200 µl	140 µl

Protocol for gels with specific percentage:

- Clean glass plates, spacers and combs with iso-propanol to remove contaminants (proteins and lipids) and let them dry.
- Assemble the glass plates separated by spacers leakproof according to the manufacturer's instructions.
- Mark the height of the separating gel (~ 1 cm beneath the comb teeth)

Separation gel:

[10 % – 20 % acrylamide, 0.27 % – 0.55 % bisacrylamide, 390 mM Tris×HCl (pH 9.0), 0.1 % SDS]

- Mix acrylamide solution (33%) with H₂O according to the table (*in a 100ml suction flask, if you want to degas → not necessary*) and add solutions given below.

separation gel	acrylamide/bisacrylamide (separation gel)	H ₂ O
10%	5.3 ml	9.9 ml
11%	5.8 ml	9.4 ml
12%	6.4 ml	8.9 ml
13%	6.9 ml	8.3 ml
14%	7.4 ml	7.8 ml
15%	8.0 ml	7.3 ml
16%	8.5 ml	6.7 ml
17%	9.0 ml	6.2 ml
18%	9.6 ml	5.7 ml
19%	10.1 ml	5.2 ml
20%	10.6 ml	4.6 ml

Tris×HCl 3 M (pH 9.0)	2.28 ml
20% SDS	90µl
TEMED	10µl
APS	67µl

- Mix thoroughly and pipete the solution between the glass plates up to the marked line, overlay with ~ 1 ml H₂O saturated butanol and let the gel polymerize (~ 20 min, *check excess solution*).

Stacking gel:

[4.5 % acrylamide, 0.22 % bisacrylamide, 125 mM Tris×HCl (pH 6.8), 0.15 % SDS]

- *before adding TEMED and APS decant the butanol from the polymerized separation gel, wash with deionized H₂O and get rid of excess H₂O using a paper towel*

acrylamide/bisacrylamide (stacking gel)	2.25 ml
H ₂ O	6.25 ml
Tris×HCl 1 M (pH 6.8)	1.25 ml
20% SDS	75µl
TEMED	20µl
APS	100µl

- Mix thoroughly and pipete the solution onto the separation gel.
- Immediately insert a comb (avoid trapping air bubbles) and let the gel polymerize (*~ 1 h, check excess solution*).
- Mount the gel into a vertical electrophoresis chamber filled with Laemmli buffer, remove the comb and flush the wells.
- Load the samples (in 1x protein sample buffer) onto the gel (0.5-5 µg protein/sample).
→ *optional: samples (in 1x protein sample buffer) might be heated to 95°C for ~ 3 min to fully denature proteins; centrifuge briefly before loading.*
- Run the gel at 200 V for ~ 40 min (until the bromphenol blue reaches the bottom of the separating gel).
→ *optional: nicest results (less 'smiley' effect, sharper bands) are observed, applying 8 V/cm voltage for the stacking gel and 15 V/cm voltage for the separating gel. Be aware that the running time is highly prolonged.*
- Incubate the gel in Coomassie staining solution for at least 30 min.
→ *for observing very small peptides (< 5 kDa) the gel has to be washed for 5-10 min in H₂O, fixed in freshly prepared 5 % glutaraldehyde for 1 h (to prevent small peptides from diffusing out) and washed 3 times for 5 min in H₂O before incubation in Coomassie staining solution.*
- Destain the gel in destaining solution until the gel is colourless again, except the protein bands.
- Take a picture of the gel with a Gel Doc System (Sony).

5.10. Pull-Down Assay

One way to determine physical interaction between two or more proteins is the pull-down technique, which resembles immunoprecipitation, except that a tagged bait protein is used instead of an antibody. Usually His6 and GST (glutathione S-transferase) are used as fusion tags. The tagged bait protein is then bound by an immobilized affinity ligand specific for the tag, glutathione agarose for GST-tagged proteins or immobilized bivalent metal ion matrices for His6-tagged proteins. A solution containing potential interaction partners (prey proteins) is subsequently applied on the immobilized bait protein.

Two different approaches:

- a) The hypothetical prey protein is expressed and purified in an artificial protein expression system and tested for binding to the immobilized His6-tagged bait protein. Usually, the large amount of purified protein allows confirmation of the pull-down by SDS-PAGE and conventional Coomassie staining. This type of pull-down strategy is usually used to confirm a suspected interaction.
- b) Cellular lysate containing the suspected endogenous prey protein is used during the pull-down assay. In this case, pull-down is confirmed by SDS-PAGE and subsequent western blot using antibodies directed against the prey protein.

ad a)

The pull-down assay was performed on HiTrap Chelating HP 5ml:

- Prepare the column as described above (→ section 5.6.2: “Immobilized metal ion affinity chromatography (HiTrap Chelating HP 5ml)”)
- After equilibration of the column centrifuge the His6-tagged bait protein sample at 4°C and 18000 rpm for at least 10 min to remove insoluble particles.
- Load the supernatant onto the column using the sample pump.
 - *load the sample at slow flow rates or alternatively more than once, to ensure binding of the His6-tagged protein.*
- Wash with 5-10 CV of binding buffer.
- Centrifuge the purified prey protein sample at 4°C and 18000 rpm for at least 10 min to remove insoluble particles.
- Load the supernatant onto the column using the sample pump

→ load the prey protein sample at slow flow rates or alternatively let incubate for a certain time (1 h) to allow interaction.

- Elute the proteins with 2-5 CV of elution buffer (high imidazole buffer).
- Collect fractions of the flow through and the eluate and analyse the samples on an SDS-PAGE.
- After the pull-down assay, flush the FPLC system, strip the column with 5 CV stripping buffer, wash with 5-10 CV of H₂O and eventually with 4 CV of 20% of ethanol for storage. From time to time wash the column with 2 CV of 0.5 M NaOH.

ad b)

The pull-down assay was performed on HiTrap Chelating HP 1ml:

- Co²⁺ was used, instead of Ni²⁺, as it seems to be less prone to unspecific binding of proteins
- usually, a small peristaltic pump was used for this experiment

- Prepare the column as described above (→ section 5.6.2: “Immobilized metal ion affinity chromatography (HiTrap Chelating HP 5ml)”)

- **Optional: Pre-clearing of the cell lysate:**

As there are proteins in a cellular lysate, which are able to interact with bivalent ions by themselves, it might be of interest to pre-clear the lysate. Alternatively, buffers with high ionic strength can be used to inhibit unspecific binding. A drawback of high ionic strength is that it might interfere with the specific interaction between the bait and the prey protein.

- Centrifuge the cell lysate at 4°C and 18000 rpm for at least 10 min to remove insoluble particles.
 - Load the supernatant of the cell lysate onto the column.
 - Elute with ~ 5 CV of binding buffer and collect the flow through
 - this flow through fraction is the pre-cleared cell lysate and should be devoid of proteins that bind unspecifically to the Co²⁺ column.
 - Elute with ~ 5 CV of elution buffer
 - contains proteins that bind unspecifically to the Co²⁺ column.
 - Re-equilibrate the column with 5-10 CV binding buffer
 - optional: recharge the column with Co²⁺
- After equilibration of the column centrifuge the His6-tagged bait protein sample at 4°C and 18000 rpm for 10 min or more.

- Load the supernatant onto the column.
→ *load the sample at slow flow rates (or alternatively more than once, to ensure binding of the His6-tagged protein).*
- Wash with 5-10 CV of binding buffer.
- Centrifuge the cell lysate at 4°C and 18000 rpm for 10 min or more.
- Load the supernatant of the cell lysate onto the column or – **with additional pre-clearing – load the pre-cleared cell lysate onto the column.**
→ *load the cell lysate at very slow flow rates or alternatively let incubate for a certain time (1 h) to allow interaction.*
- Elute the proteins with 2-5 CV of elution buffer (high imidazole buffer).
- Collect fractions of the flow through and the eluate and analyse the samples via SDS-PAGE and subsequent western blot with antibodies directed against the prey protein.
- After the pull-down assay strip the column with 5 CV stripping buffer, wash with 5-10 CV of H₂O and eventually with 4 CV of 20% of ethanol for storage. From time to time wash the column with 2 CV of 0.5 M NaOH.

5.11. Western blot

The western blot (alternatively, immunoblot) is a method of detecting specific proteins within a mixture of proteins with the help of specific antibodies. Depending on the method of detection very little amounts of protein can be detected.

Samples, to be tested for containing the protein in question, are separated by SDS-PAGE and subsequently blotted onto a nitrocellulose membrane by applying an electric current orthogonal to the gel and membrane. The negatively charged proteins (SDS) migrate out of the gel and are bound by the nitrocellulose membrane via hydrophobic as well as charged interactions, maintaining the migration pattern of the polyacrylamide gel. Subsequently, a specific protein can be detected with primary antibodies directed against that protein. Methods of detection are colorimetric, chemiluminescent, radioactive and fluorescent detection and often involve enzymes fused to the secondary antibody directed against the Fc domain of the primary antibody. The reaction catalyzed by the bound enzyme is used to detect specific bands corresponding to the protein in question.

Transfer (Tank Blot system):

- Run a gel suitable for Western blotting.
 - *optional: run at the same time a second gel for Coomassie staining.*
- Submerge a nitrocellulose membrane of suitable size shortly in H₂O.
- Equilibrate the nitrocellulose membrane in transfer buffer.
 - work with gloves as the transfer buffer contains methanol; touch the membrane only with forceps (*be aware that the nitrocellulose strongly binds proteins*).
- Soak 2 sponges and 4 sheets of Whatman paper (same size as sponges) in transfer buffer.
- Cut upper right edge of gel and nitrocellulose membrane to remember orientation.
- Set up the transfer sandwich (from anode to cathode):
 - *!! no bubbles !!*
 - Sponge
 - 2x Whatman paper
 - Nitrocellulose membrane
 - Gel
 - 2x Whatman paper
 - Sponge
- Blot at a constant current of 60 mA at 4°C o/n.
- On the next day increase current to 250 mA and blot for additional 2 h.
 - *for high percentage gels (> 15 %) blot ~ 3.5 h.*
- *Optional: stain the gel from the transfer with Coomassie staining solution to check effectiveness of the blotting.*
- Wash the nitrocellulose membrane with H₂O.
- Stain for 2 min in Ponceau-S staining solution, rinse with H₂O and mark the protein marker bands with a ball pen.
- Destain with 1x PBS for 30 min.

Detection with the AP-system (alkaline phosphatase):

- **Blocking** → put the membrane in 100 ml blocking solution at 4°C o/n (or 1 h at room temperature).
- **1st antibody** → apply first antibody (1:200 to 1:1000 diluted in 5 ml blocking solution) in a conical tube on a stirrer for 1 h at room temperature or 4°C o/n.
- **Washing** → wash 3 x 10 min with PBS-T.
- **2st antibody** → apply second antibody (alkaline phosphatase coupled; 1:1000 anti-mouse or 1:5000 anti-rabbit diluted in 1 part blocking solution and 2 parts PBS-T) in a conical tube on a stirrer for 1.5 h at room temperature.
- **Washing** → wash 3 x 10 min with PBS-T and rinse briefly with H₂O.
- **Detection** → detect with 10 µl NBT solution, 5 µl BCIP solution in 10 ml AP-buffer for ~ 10 min.
- **Wash** → wash with H₂O to stop the reaction and store light-protected.

5.12. Circular dichroism spectroscopy of proteins

Circular dichroism (CD) is defined as the difference in absorption of left and right handed circular-polarized light $\Delta A = A_L - A_R$ by chromophores in an asymmetrical environment, resulting in elliptically polarized light. CD spectroscopy can be used to get information about the structure of macromolecules (including the secondary structure of proteins and the handedness of DNA). The most commonly used unit in CD spectroscopy of proteins is the mean residue ellipticity [degree cm² dmol⁻¹], which is obtained by normalization with sample concentration, path length of the cell and with the number of residues. The mean residue ellipticity is measured as a function of wavelength.

For gaining information about the secondary structure of proteins, CD spectra need to be recorded from about 260 nm to ~ 185 nm (far UV). At these wavelengths the amide groups of the peptide backbone interact with the entering circularly-polarized light. Spectra can be analyzed for different secondary structural types: alpha helix, parallel and antiparallel beta sheet, random coil, etc.

Fig. 8 shows typical CD spectra of different secondary structural elements.

Experimental conditions:

- **Buffer:**

Buffers must be as transparent as possible and should exhibit low absorbance in the region of interest (260-180 nm). Sodium or potassium phosphate buffers are suitable for CD measurement. Try to avoid organic buffers and detergents (e.g.: imidazole, DTT, histidine), as they absorb below 220 nm. Chloride ions (e.g.: HCl, NaCl) interfere with CD measurement and should be avoided.

- **Sample concentration:**

Accurate CD measurements are not possible at an absorbance above 1.0. For calculation of the starting molar concentration the following equation is useful:

$$c = 115 / (\text{molecular weight} \times \text{cell length [cm]} \times 7000)$$

- **Path length:**

The smaller the path length of the cell, the lower is the absorption by the solvent. Small path lengths will permit scanning down to lower wavelengths.

- **Filtration:**

Filtering the samples and the buffer through a 0.2-0.45 μm filter will remove dust, aggregated protein and other particles that interfere with CD measurements.

- **CD Spectrometer:**

CD spectra were recorded on a spectropolarimeter (Applied Photophysics π^* -180).

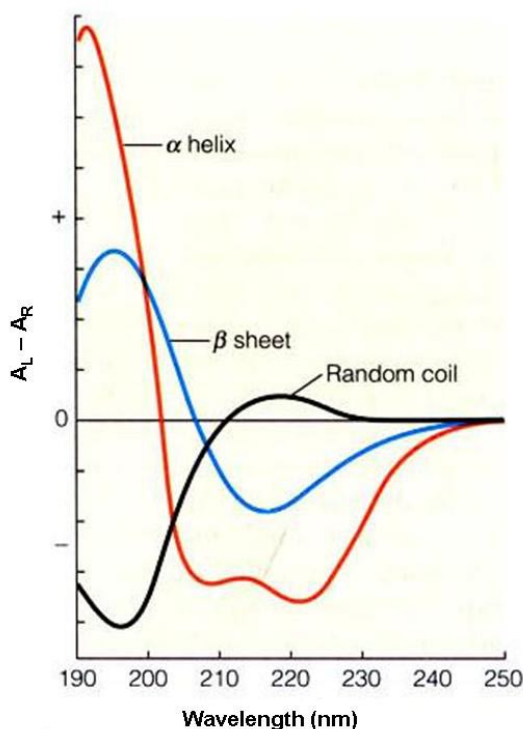


Fig. 8. Typical CD spectra of different secondary structural elements (far UV). Spectrum α -helix (red); β -sheet (blue); random coil (black). The ordinate shows the difference in absorption of left and right handed circular-polarized light $\Delta A = A_L - A_R$ as a function of the wavelength in nm.

6. Cell Culture

6.1. Preparation of cellular extract

- Discard the medium from the cells in the cell culture plates (→ 100 mm culture dishes).
→ *suck off with a water jet pump.*
- Wash the cells with 3-5 ml of PBS and discard PBS completely.
- Cover the cells with 1 ml NDL buffer per plate.
- Pivot the plates on ice for 15-20 min.
- Scrape the cells from the plate floor and pipette the lysate into 2 ml Eppendorf tubes.
- Centrifuge at 4°C and 15000 rpm for 60 min.
- Transfer the supernatant (containing cellular proteins) into a new tube.
- Quantify the protein content (use 2.5 µl cellular extract for the Bradford assay).
- Store the cellular extract at -80°C.

7. Specific protocols

7.1. Expression and purification of His6-Carrier-cBASP1 peptide fusion proteins

7.1.1. Construction of expression vectors coding for His6-Carrier-cBASP1 peptide fusion proteins

pETGB_1a, pETMBP_1a, pETNus_1a, pETtrx_1a and pETZ2_1a were kindly provided by Günter Stier. They code for His6-Carrier-GFP fusion proteins including a TEV cleavage site between the Carrier and GFP. During the cloning procedure, the DNA stretch coding for GFP is cleaved out and substituted by the DNA sequence of interest. The features of this expression system are listed below.

Features:	
His6	N-terminal His6 tag; binds bivalent ions (Ni^{2+} , Co^{2+} ,...); for purification on metal chelating columns
TEV cleavage site	Between the carrier and the target protein; allows cleavage of the target protein from the carrier with a TEV protease.
T7 promoter	For expression systems using T7 RNA polymerase
Kan ^R	Kanamycin resistance
GFP	Green fluorescent protein; default protein
Carriers (solubility enhancement tags):	
GB1	B1 Ig binding domain of Streptococcus; can stabilize aggregation prone proteins; binds independently to secondary antibodies, which can be used for detection of passenger protein in the fusion state; in NMR studies used as myristoylated product via coexpression of a modifying coenzyme to anchor in lipid bilayers [His6-GB1-TEV after Tev cleavage Mw = 8575.6 Da]
MBP	Maltose-binding protein; chaperone function; binds independently to amylose columns [His6-MBP-TEV after Tev cleavage Mw = 42947.65 Da]
NusA	Highly soluble protein [His6-NusA-TEV after Tev cleavage Mw = 57264.51 Da]
trx	Thioredoxin protein; highly stable and soluble [His6-trx-TEV after Tev cleavage Mw = 14213.21 Da]
Z2	Gene fragment of staphylococcal protein A; IgG binding; highly stable and soluble [His6-Z2-TEV after Tev cleavage Mw = 10172.15Da]

To construct the expression vectors coding for the His6-Carrier-cBASP1 peptide fusion proteins, pA-cBASP1 (kindly provided by T. Matt), containing cBASP1 cDNA, was used as a template to subclone the cBASP1 peptide (cBASP1 residues 60 – 80: KVEKDAQVSANKTEEKEGEKE) C-terminally to the respective carrier protein. To stay in frame with the carrier protein, two additional bases had to be introduced, resulting in an additional glutamic acid residue, which corresponds to residue 59 of cBASP1. PCR was performed using primers, which recognize the DNA stretch coding for the target cBASP1 peptide and added at the 5' end an NcoI and at the 3' end a stop-codon and a NotI restriction site [gradient PCR: 5' at 95°C; 30 cycles of (20'' at 95°C; 20'' at 53°C / 56°C / 60°C; 20'' at 72°C); 5' at 72°C; hold at 4°C]. The PCR-product was directly NcoI/NotI digested and purified by phenol:chloroform extraction and subsequent iso-propanol precipitation. The expression vectors were digested with the same enzymes, treated with CIP, to remove 5' phosphate groups, and purified (QIAGEN PCR purification kit). Finally, the digested PCR-product was ligated with the digested and CIP treated expression vector. All constructs (pET-His6-GB1-cBASP1pep, pET-His6-MBP-cBASP1pep, pET-His6-NusA-cBASP1pep, pET-His6-trx-cBASP1pep and pET-His6-Z2-cBASP1pep) were verified by sequencing (VBC biotech sequencing service → www.vbc-biotech.at). As a matter of simplicity, in the following text the term 'Ca' will substitute for each individual Carrier protein (GB1, MBP, NusA, trx, Z2).

Primers:

fw(Nco1)BASPfrag: 5' TAAATACCATGGAGAAGGTTGAGAAGGATGCTCAGGTC

rev(Not1)BASPfrag: 5' ATTAATGCGGCCGCTCACTCTTTCTCCCCTTCTTTTCTTC

- XXX → buffer bases, to ensure high restriction efficiency
- XXX → restriction enzyme recognition site
- XXX → stop codon
- XXX → additional bases to stay in frame with the carrier protein

7.1.2. Expression and purification of His6-Carrier-cBASP1 peptide fusion proteins

pET-His6-‘Ca’-cBASP1pep was transformed into the *E. coli* strain Rosetta(DE3)pLysS. A 20 ml overnight culture prepared in LB-medium supplemented with chloramphenicol (25 µg/ml) and kanamycin (25 µg/ml) was diluted 1:100 in 1 l LB-medium (+ CoA + Kan) or in M9 minimal medium (+ CoA + Kan). M9 minimal medium substituted with ¹³C-glucose and/or ¹⁵NH₄Cl is used for ¹³C and ¹⁵N labelling necessary for NMR analysis. In this study, unlabeled M9 minimal medium was used just to test, if transformed bacteria grow and express recombinant proteins also under minimal conditions. Bacteria were grown at 37°C and 225 rpm in 2 l baffled Erlenmeyer flasks until an OD₆₀₀ of 0.5 to 1.0. Recombinant protein synthesis was induced by the addition of 1 ml 0.4 M IPTG (final concentration 0.4 mM IPTG) and incubation was continued for 3 h. Subsequent steps were carried out at 4°C. Bacteria were collected by centrifugation and the pellet was resuspended in 30 ml lysis buffer (20mM Tris×HCl pH 7.4, 1mM EDTA, 1mM β-mercaptoethanol). The bacterial suspension was frozen in liquid nitrogen and stored at -20°C. For purification, the frozen suspension was thawed carefully, sonicated (to lyse the cells and fragment the DNA) and centrifuged. The clear solution containing soluble proteins was loaded onto a Ni²⁺ column (HiTrap Chelating HP 5ml amersham pharmacia) equilibrated in low imidazole buffer, washed with low imidazole buffer and eluted with high imidazole buffer. Depending on the carrier protein, the recombinant protein was eluted more or less clean from the Ni²⁺ column deduced from Coomassie stained SDS-polyacrylamide gels. For example, His6-NusA-cBASP1pep was still quite contaminated compared to His6-GB1-cBASP1pep, which was already eluted very clean. Therefore, an additional preparative gel filtration step (HiLoad 16/60 Superdex 75 prep grade) was performed, depending on the outcome of the Ni²⁺ affinity chromatography.

a) The protein sample was pure after Ni²⁺ affinity chromatography.

The protein sample was transferred to a Centriprep filter (Amicon) with a cut off value smaller than the molecular weight of the protein. The high imidazole buffer was exchanged by buffer suitable for following experiments (Tris×HCl 20 mM pH 7.4) by 3 to 4 times of concentrating the protein sample and subsequent dilution in the target buffer. Finally the protein sample was concentrated to 0.5-1.5 ml (Centriprep), substituted with EDTA (1 mM) and β-mercaptoethanol (1 mM) and stored at -20°C.

b) The protein sample is not pure enough, additional gel filtration is required.

The protein sample was concentrated to 0.5-1 ml by centrifugation through a Centriprep filter with a cut off value smaller than the molecular weight of the protein, centrifuged and loaded onto a HiLoad 16/60 Superdex 75 prep grade gel filtration column equilibrated in target buffer (Tris×HCl 20 mM pH 7.4). Protein containing fractions were analyzed by SDS-PAGE. Pure fractions were pooled, concentrated to 0.5-1.5 ml (Centriprep), substituted with EDTA (1 mM) and β-mercaptoethanol (1 mM) and stored at -20°C.

7.2. Expression and purification of the MC29EB protein

7.2.1. The expression vector coding for MC29EB protein

pET3d-MC29EB was constructed by T. Matt (diploma thesis, 1997) and encodes a part of the v-Myc oncogene from the MC29 virus corresponding to residues 440-453 of the viral Gag protein – plus an N-terminal methionine – fused to six amino acids encoded by the 5' untranslated region of the chicken *c-myc* gene plus a stretch of 140 residues corresponding to the N-terminus of chicken c-Myc (residues 1-140). Residue 140 (Thr) of chicken c-Myc corresponds to residue 151 (Ser) of human c-Myc.

Recombinant MC29EB has a molecular weight of 17.8 kDa, but migrates at an apparent molecular weight of ~ 21 kDa.

7.2.2. Expression and purification of the MC29EB protein

MC29EB was purified in principle according to the protocol described (T. Matt, diploma thesis, 1997). pET3d-MC29EB was transformed into the *E. coli* strain Rosetta(DE3)pLysS. A 20 ml overnight culture prepared in LB-medium supplemented with chloramphenicol (25 µg/ml) and ampicillin (100 µg/ml) was diluted 1:100 in 1 l LB-medium (+ CoA + Amp) or in M9 minimal medium (+ CoA + Amp). Bacteria were grown at 37°C and 225 rpm in 2 l baffled Erlenmeyer flasks until an OD₆₀₀ of 0.5 to 1.0. Recombinant protein synthesis was induced by the addition of 1 ml 0.4 M IPTG (final concentration 0.4 mM IPTG)

and incubation was continued for 3 h. Subsequent steps were carried out at 4°C. Bacteria were collected by centrifugation and the pellet was resuspended in 30 ml lysis buffer (20mM Tris×HCl pH 7.4, 1mM EDTA, 1mM β-mercaptoethanol). The bacterial suspension was frozen in liquid nitrogen and stored at -20°C. For purification, the frozen suspension was thawed carefully, sonicated (to lyse the cells and fragment the DNA) and centrifuged. MC29EB is insoluble expressed in inclusion bodies; hence, after centrifugation, MC29EB is in the pellet. The supernatant was discarded, the inclusion bodies enriched (→ section 5.3: “Enrichment of inclusion bodies”) and dissolved in 5 ml TEU buffer.

a) The sample still suffering from impurities is later used for pull-down assays.

MC29EB dissolved in TEU buffer was stepwise dialyzed into the target buffer (20 mM Tris×HCl pH 7.4) (→ section 5.4: “Refolding of proteins using stepwise dialysis”), concentrated to 0.5-1.5 ml (Centriprep), substituted with EDTA (1 mM) and β-mercaptoethanol (1 mM) and stored at -20°C.

b) The protein sample needs to be further purified for e.g. CD measurement.

MC29EB was purified via anion exchange chromatography under denaturing conditions. Therefore the protein sample (in TEU buffer) was loaded onto an anion exchange column (Resource Q 6 ml) equilibrated in TEU buffer, washed with TEU buffer and eluted via gradient elution from 0-30% TEUS buffer over 20 CV. MC29EB was eluted from ~ 40 mM NaCl to ~ 200mM NaCl, but was predominantly eluted in 2 peaks. As a matter of fact, the sharp elution in 2 peaks at 53 mM NaCl and 179 mM NaCl as described before (T. Matt, diploma thesis, 1997) could not be reproduced. In fact, the elution of those 2 major peaks seemed to be dependent on the steepness of the gradient (see table below). Usually MC29EB was eluted purer in peak 2.

	Peak 1 at	Peak 2 at	
0-50% TEUS over 20 CV	75 mM NaCl	175 mM NaCl	
0-30% TEUS over 20 CV	50 mM NaCl	149 mM NaCl	Best resolution and best purity of MC29EB in peak 2
0-30% TEUS over 5 CV	152 mM NaCl	230 mM NaCl	Worst resolution and comparably small peak 2

Alternatively, a stepwise gradient was tried for elution, which didn't seem to produce better results:

Linear gradient	0-4% TEUS	2 CV
Constant elution	4% TEUS	2 CV
Linear gradient	4-10% TEUS	2 CV
Constant elution	10% TEUS	2 CV
Linear gradient	10-15% TEUS	2 CV
Constant elution	15% TEUS	2 CV
Linear gradient	15-20% TEUS	2 CV
Constant elution	20% TEUS	2 CV

Purest fractions were pooled, optionally concentrated to a volume suitable for dialysis (Centriprep filter), stepwise dialyzed into the target buffer (20 mM Tris×HCl pH 7.4) (→ section: “Refolding of proteins using stepwise dialysis”) and concentrated to 0.5-1.0 ml (Centriprep filter). Subsequently, the protein sample was centrifuged and loaded onto a HiLoad 16/60 Superdex 75 prep grade gel filtration column equilibrated in target buffer (20 mM Tris×HCl pH 7.4). Protein containing fractions were analyzed by SDS-PAGE. Nearly pure MC29EB was observed at a retention volume of 56-58 ml ($K_{av} = 0.200-0.225$). Pure fractions were pooled, concentrated to 0.5-1.5 ml (Centriprep), substituted with EDTA (1 mM) and β -mercaptoethanol (1 mM) and stored at -20°C .

7.3. Expression and purification of His6-Minimax

7.3.1. Construction of the expression vector coding for His6-Minimax

pET3d-p14max was constructed by Martin Schneider (doctoral thesis, 2002). This expression vector encodes a 92 amino acids peptide termed Minimax (p14max) encompassing amino acid residues 22-113 of chicken Max with an additional N-terminal methionine residue. pET-His6-Minimax was constructed using pET3d-p14max as a template to subclone the Minimax peptide C-terminally to the His6 tag encoded by the expression vector pET-M11. pET-M11 was kindly provided by Günter Stier. It codes for a His6-MAD fusion protein

including a TEV cleavage site between the His6 tag and MAD. During the cloning procedure, the DNA stretch coding for MAD is cleaved out and substituted by the DNA sequence of interest. pET3d-p14max was BamHI/NcoI digested, separated on a preparative agarose gel and the DNA band corresponding to the Minimax sequence was gel extracted (QIAGEN gel extraction). pET-M11 was digested with the same enzymes, treated with CIP, to remove 5' phosphate groups, and purified (QIAGEN PCR purification kit). Finally, the digested and gel extracted Minimax sequence was ligated with the digested and CIP treated pET-M11 vector. The resulting pET-His6-Minimax expression plasmid was verified by sequencing (VBC biotech sequencing service → www.vbc-biotech.at). The His6-Minimax protein encoded by pET-His6-Minimax is cleavable by TEV protease to allow cleavage of the Minimax protein from the His6 tag.

7.3.2. Expression and purification of His6-Minimax

pET-His6-Minimax was transformed into the *E. coli* strain BL21(DE3)pLysS. A 20 ml overnight culture prepared in LB-medium supplemented with chloramphenicol (25 µg/ml) and kanamycin (25 µg/ml) was diluted 1:100 in 1 l LB-medium (+ CoA + Kan). Bacteria were grown at 37°C and 225 rpm in 2 l baffled Erlenmeyer flasks until an OD₆₀₀ of 0.5 to 1.0. Recombinant protein synthesis was induced by the addition of 1 ml 0.4 M IPTG (final concentration 0.4 mM IPTG) and incubation was continued for 3 h. Subsequent steps were carried out at 4°C. Bacteria were collected by centrifugation and the pellet was resuspended in 30 ml lysis buffer (20mM Tris×HCl pH 7.4, 10mM imidazole, 1mM EDTA, 1mM β-mercaptoethanol). The bacterial suspension was frozen in liquid nitrogen and stored at -20°C. For purification, the frozen suspension was thawed carefully, sonicated (to lyse the cells and fragment the DNA) and centrifuged. The clear solution containing soluble proteins was loaded onto a Ni²⁺ column (HiTrap Chelating HP 5ml amersham pharmacia) equilibrated in low imidazole buffer, washed with low imidazole buffer and eluted with high imidazole buffer. The protein sample was transferred to a Centriprep filter (Amicon) with a cut off value smaller than the molecular weight of the protein. The high imidazole buffer was exchanged by buffer suitable for following experiments (20 mM Tris×HCl pH 7.4) by 3-4 times of concentrating the protein sample and subsequent dilution in the target buffer. Finally the protein sample was concentrated to 0.5-1.5 ml (Centriprep), substituted with EDTA (1 mM) and β-mercaptoethanol (1 mM) and stored at -20°C.

Results

Investigation of direct interaction between c-Myc and the cBASP1 interacting peptide

We hypothesized that chicken BASP1 (cBASP1) directly interacts with the transactivation domain (TAD) of c-Myc via a small stretch of amino acids comprising cBASP1 residues 60-80, based on the following observations:

- Transformation of chicken embryonic fibroblasts (CEF) by the MC29 virus (encoding oncogenic v-Myc) is followed by the downregulation of cBASP1 already at the transcriptional level (unpublished data).
- Ectopic expression of cBASP1 in CEF is counteracting transformation by the MC29 virus and leads to the downregulation of endogenous c-Myc (unpublished data).
- Meta-structural data of the cBASP1 protein predicts a peptide comprising amino acid residues 60-80 with a high probability for protein interaction – probably with an extended or β -stranded part of a protein (Fig. 9)
- A synthetic cell penetrating peptide comprising cBASP1 residues 60-80 C-terminally to a peptide stretch enabling penetration of the cell membrane (GRKKRRQRRR-G-KVEKDAQVSANKTEEKEGEKE) lead to a cytopathic effect in MC29 transformed CEF, which is not observed with a control cell penetrating peptide harbouring cBASP1 residues 15-30 (GRKKRRQRRR-G-NDEKAKDKDKKAEGAA) and a random control peptide lacking a cell penetration sequence (unpublished data).

- The cytopathic effect induced by the noted cBASP1 cell penetrating peptide is less stringent in untransformed CEF (unpublished data).
- The transactivation domain (TAD) of c-Myc has already been shown to be bound and thereby regulated by different proteins (TRRAP, P-TEFb, NF-Y, MM1, TBP, Bin1,...) [64].
- The TAD of c-Myc, despite being mostly unfolded, was predicted by secondary structure prediction software (DSC, PHD and PREDATOR) to contain α -helical stretches, as well as β -stranded regions. Two of the predicted α -helices lie – at least partly – in Myc box I (MBI) and Myc box II (MBII), the regions described to be essential for binding of c-Myc TAD to other proteins [145]. On the contrary, Phe104 of rat B-Myc (corresponding to Phe115 of human c-Myc) seems to be involved in interaction with MM1 [151] and lies in a region predicted to be a β -strand [145].

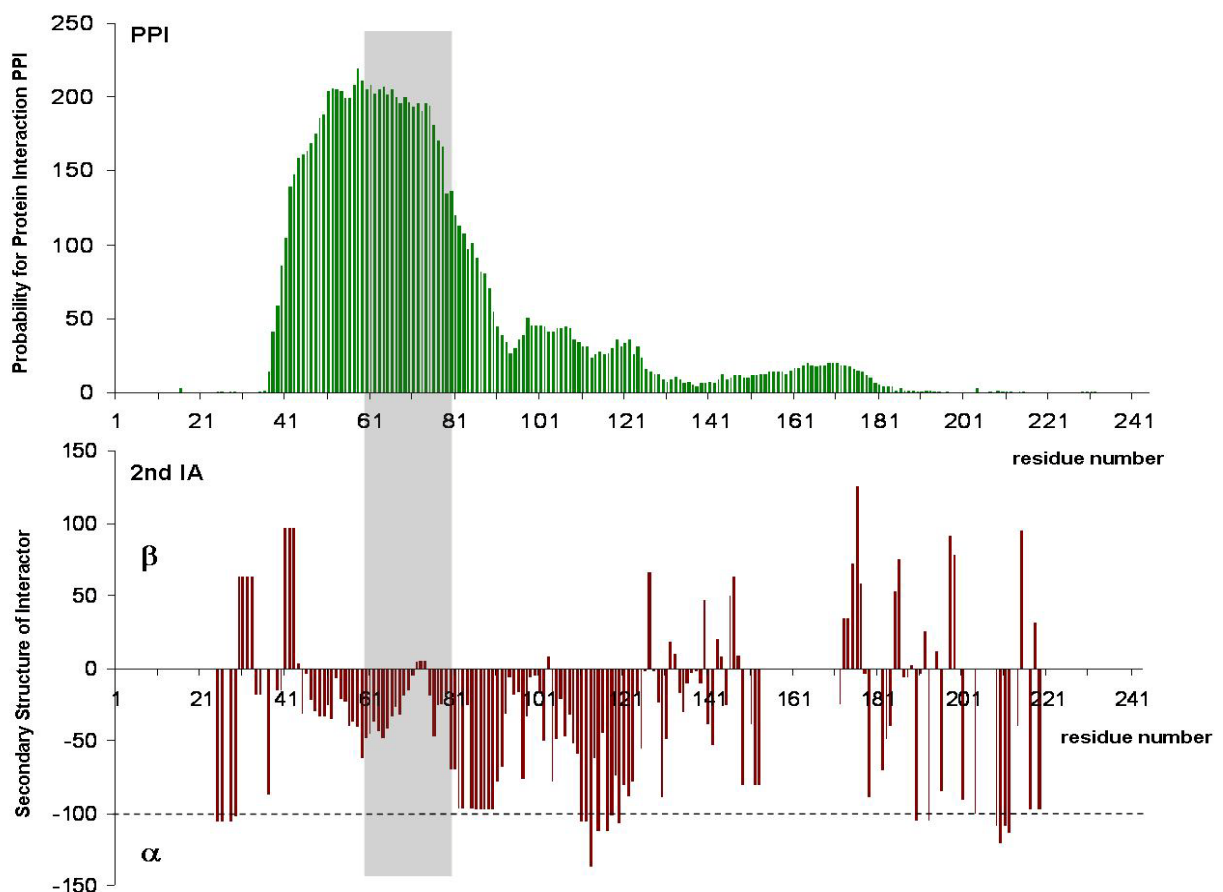


Fig. 9. Residue-based Probability for Protein Interaction (PPI) and probable Secondary Structure of the Interactor (2nd IA) based on the Meta-structure analysis of chicken BASP1 (cBASP1). Ad 2nd IA: Probabilities for α -helical segments are typically below -100 (dashed line); probabilities for extended conformations and β -strands are typically above -100. The cBASP1 peptide (residues 60-80) is indicated by a grey box.

1. Construction of expression plasmids encoding His6-Carrier-cBASP1pep

A possibility by means of testing the interaction between the cBASP1 peptide (residues 60-80) and c-Myc is the pull-down technique. We decided to try out a His6 pull-down method in combination with Ni²⁺ (or Co²⁺) affinity columns.

Expression vectors were constructed encoding an N-terminally His6 tagged version of the cBASP1 peptide including a Carrier protein for solubility reasons and a TEV cleavage site between the Carrier and the N-terminal cBASP1 peptide to allow cleavage of the peptide from the His6-Carrier moiety. Fig. 10 shows a schematic representation of the 5 different encoded His6-‘Ca’-cBASP1 peptide fusion proteins. Construction of the pET-His6-‘Ca’-cBASP1pep expression vectors and properties of the different carrier proteins are described in section: “Construction of expression vectors coding for His6-Carrier-cBASP1 peptide fusion protein”.

MKHHHHHHPMKQ..GB1-carrier...VTEGSGSGSENLYFQ`GAMEKVEKDAQVSANKTEEKEGEKE	11.5 kDa
MKHHHHHHPMKQ..Z2-carrier...VDAGSGSGSENLYFQ`GAMEKVEKDAQVSANKTEEKEGEKE	12.9 kDa
MKHHHHHHPMSD..trx-carrier...NLGSGSGSENLYFQ`GAMEKVEKDAQVSANKTEEKEGEKE	16.96 kDa
MKHHHHHHPMKI..MBP-carrier...TNSGSGSGSENLYFQ`GAMEKVEKDAQVSANKTEEKEGEKE	45.7 kDa
MKHHHHHHPMKE..NusA-carrier...EATGSGSGSENLYFQ`GAMEKVEKDAQVSANKTEEKEGEKE	60.0 kDa

Fig. 10. Schematic representation of the His6-‘Ca’-cBASP1pep fusion proteins. His6 tag and Carrier proteins in green; TEV protease recognition site with the site of cleavage in red; cBASP1 peptide sequence (corresponding to cBASP1 residues 59-80) in blue. Identical regions are marked by grey boxes.

2. The His6-Carrier-cBASP1 peptide fusion proteins

As described in section “Expression and Purification of His6-Carrier-cBASP1 peptide fusion proteins”, the different fusion proteins were expressed in the *E.coli* strain Rosetta(DE3)pLysS and purified via Ni²⁺ affinity chromatography and optional preparative gel filtration (Fig. 11). The molecular weights of the individual His6-‘Ca’-cBASP1pep fusion

proteins as well as the apparent molecular weights at which the individual proteins are migrating on a 15% SDS polyacrylamide gel are noted in the table below.

	MW (kDa)	Apparent MW (kDa)
His6-GB1-cBASP1pep	11.5	~ 17.5 *
His6-MBP-cBASP1pep	45.7	~ 45
His6-NusA-cBASP1pep	60.0	~ 66
His6-trx-cBASP1pep	16.96	~ 18
His6-Z2-cBASP1pep	12.9	~ 16

*His6-GB1-cBASP1pep sometimes didn't migrate properly and produced long smears on a 15 % SDS-polyacrylamide gel

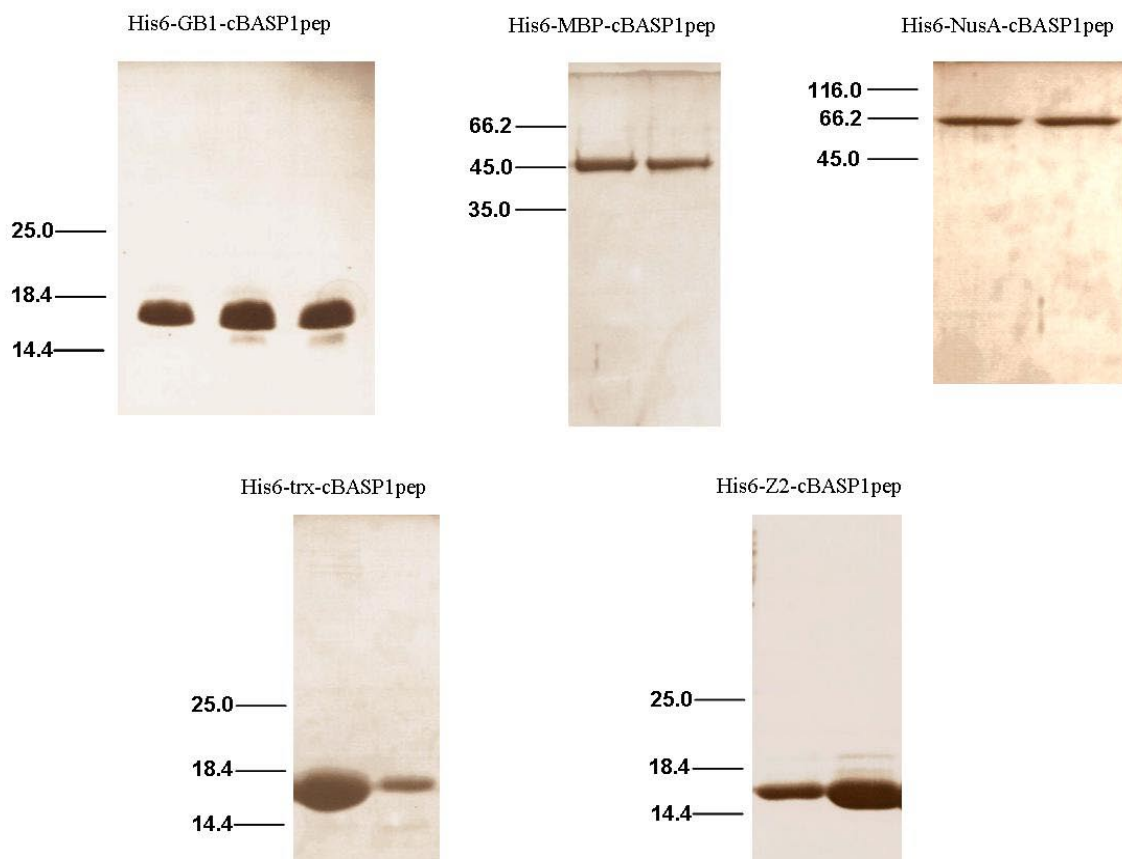


Fig. 11. Purified His6-‘Ca’-cBASP1pep fusion proteins. Coomassie stained 15% SDS-polyacrylamide gels show pure fractions of recombinant protein after Ni²⁺ affinity chromatography or after an additional preparative gel filtration step.

In order to test the possibility for cleavage with TEV protease, an initial screen for TEV protease – substrate ratio determination was performed on His6-trx-cBASP1pep as described in section “*TEV protease cleavage of proteins*”. Aliquots of the different cleavage mixtures were analyzed by SDS-PAGE (Fig. 12). Cleavage of the cBASP1 peptide from the His6-trx moiety had been in principle successful confirming the functionality of the TEV cleavage site. His6-trx-cBASP1pep (16.96 kDa) migrates at ~ 18 kDa, whereas the cleaved fragment His6-trx (14.2 kDa) migrates at ~ 14.4 kDa. The cleaved cBASP1 peptide (GAM-EKVEKDAQVSANKTEEKEGEKE) with a molecular weight of 2765 Da can't be seen on the SDS-polyacrylamide gel, as peptides smaller than 5 kDa can diffuse out of the gel during the staining procedure. Even at a ratio 1:50 of TEV protease to His6-trx-cBASP1pep only half the amount of protein was cleaved. There are different explanations for the low processing efficiency. Firstly, the sample of TEV protease is already old and therefore TEV protease activity is reduced. Also autolysis of TEV protease has been described, which renders the protease inactive [176]. Secondly, steric hindrance at the TEV cleavage site might be a reason for low activity.

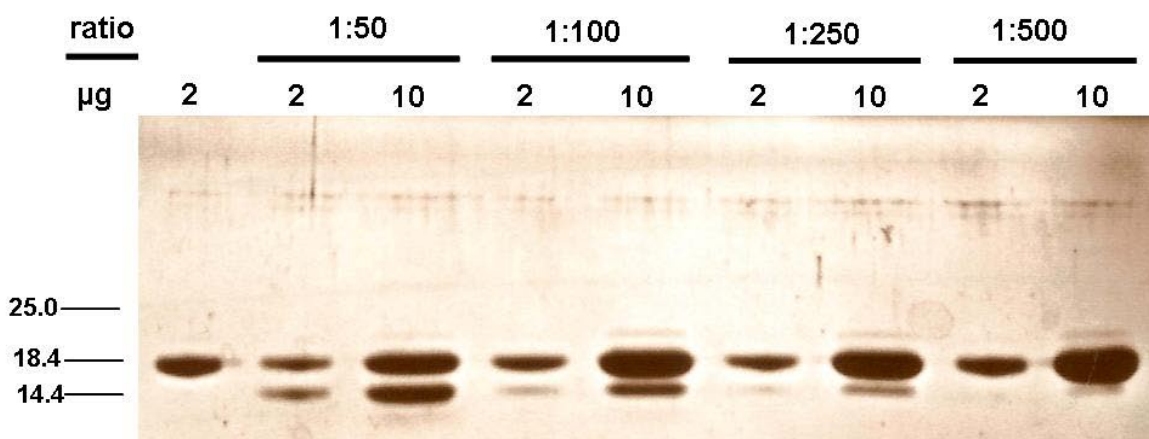


Fig. 12. TEV cleavage of His6-trx-cBASP1pep. Lanes 2-9 show different ratios of TEV protease to His6-trx-cBASP1pep and different amounts of protein applied onto the SDS polyacrylamide gel. As a control served 2 µg of full length His6-trx-cBASP1pep (lane 1). Full length His6-trx-cBASP1pep (16.96 kDa) migrates at ~ 18 kDa. Cleaved His6-trx (14.2 kDa) migrates at ~ 14.4 kDa.

3. *The MC29EB protein*

The cBASP1 peptide was hypothesized to interact with the transactivation domain of c-Myc. The MC29EB protein encoded by pET3d-MC29EB corresponds to a part of the viral Gag-Myc fusion protein, which comprises v-Myc residues 1-140 corresponding to chicken c-Myc TAD (residues 1-140) with additional 14 N-terminal residues from the viral Gag protein and 6 residues encoded by the 5' untranslated region of chicken c-Myc. Fig. 13 (A) shows a schematic representation of the MC29 retrovirus encoded Gag-Myc fusion protein, the recombinant MC29EB protein and chicken c-Myc. The term v-Myc corresponds to the part of the Gag-Myc fusion protein, which was derived from the cellular proto-oncogenic c-Myc sequence. Several substitution mutations of key residues are found in the MC29 encoded v-Myc sequence, which are noted in the table below.

	human c-Myc	chicken c-Myc		MC29 Gag-Myc
phosphorylation site and O-GlcNAc glycosylation site [78]	Thr58	Thr61	→	Met61
acetylation site [180, 181]	Lys157	Arg146	→	Gln146
phosphorylation site [182]	Ser348	Ser325	→	Leu325
phosphorylation site [183]	Ser373	Ser350	→	Arg350
not determined	Lys430	Lys407	→	Asn407

MC29EB was expressed in the *E.coli* strain Rosetta(DE3)pLysS, enriched from inclusion bodies and depending on subsequent experiments, purified via anion exchange chromatography under denaturing conditions and preparative gel filtration as described in section “*Expression and purification of the MC29EB protein*”. Preparative gel filtration was carried out after dialysis and renaturation of MC29EB in 20 mM Tris×HCl pH 7.4. MC29EB was eluted in all protein containing fractions (Fig. 13, B). A contaminating protein migrating at ~ 26 kDa was even eluted in the purest fractions after preparative gel filtration and could not be removed by gel filtration under denaturing conditions (data not shown).

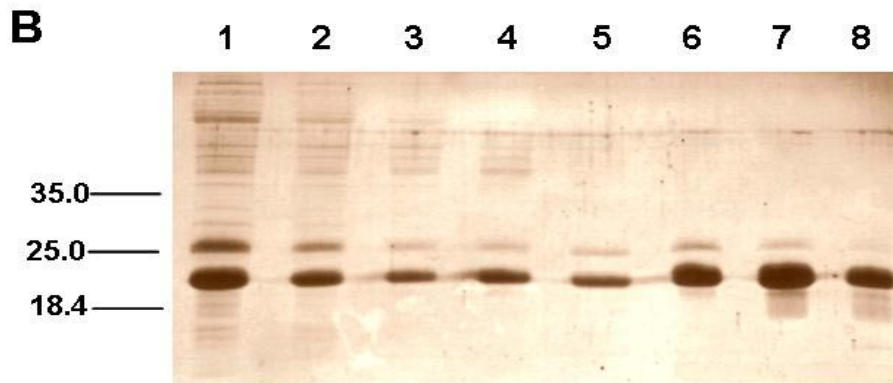
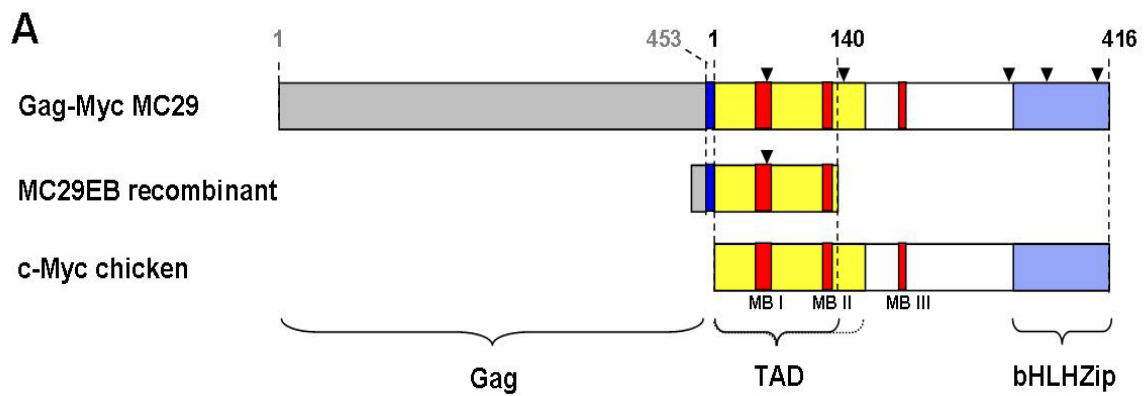
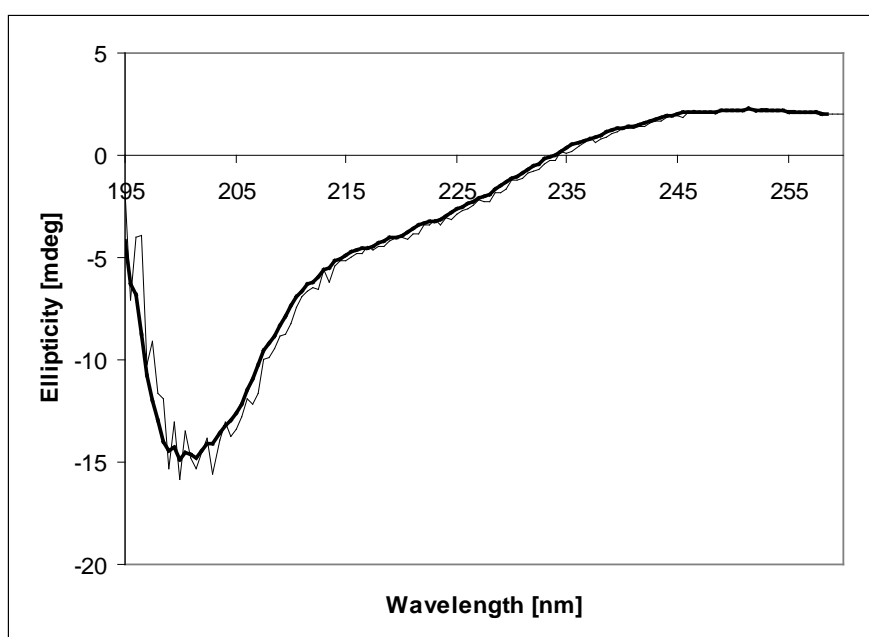


Fig. 13. MC29EB recombinant protein. (A) Schematic representation of the Gag-Myc fusion protein encoded by the MC29 retrovirus, the MC29EB recombinant protein and chicken c-Myc. Gag (grey); TAD: transactivation domain (yellow); MB I-III: Myc boxes I-III (red); bHLHZip motif (light blue); peptide encoded by the 5' untranslated region of chicken c-Myc (blue); substitution mutations (arrowheads). Grey numbers correspond to MC29 Gag protein. Black numbers correspond to chicken c-Myc. The extended bracket indicating TAD reminds for the recent finding that a C-terminally prolonged region of TAD is binding with higher affinity to interactors than the previously described "minimal region" of TAD. (B) Preparative gel filtration of MC29EB in 20 mM Tris×HCl (pH 7.4) after anion exchange chromatography under denaturing conditions. The Coomassie stained 15% SDS-polyacrylamide gel shows protein containing fractions. MC29EB (17.8 kDa) migrates at ~ 21 kDa. Compare impure fractions (lanes 1-4) with more or less pure fractions (lanes 5-8).

4. **Circular Dichroism Spectroscopy of MC29EB**

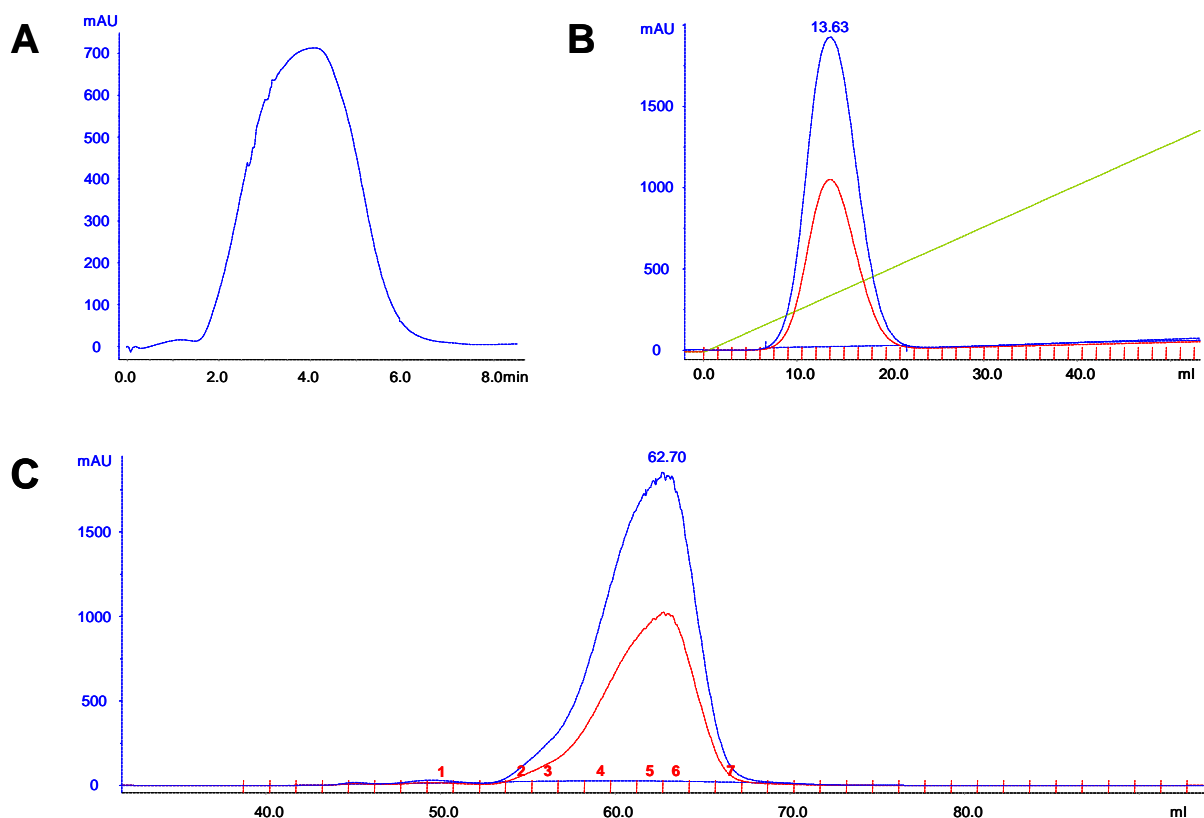
CD measurement has been performed to estimate the secondary structural content of MC29EB protein. The CD spectrum of MC29EB shows the characteristics of a random conformation with a minimum at around 200 nm (Fig. 14). Similar spectra were observed with a human c-Myc TAD polypeptide spanning residues 1-143 (human c-Myc₁₋₁₄₃) [149]. CD measurements with a slightly extended version of human c-Myc TAD (c-Myc₁₋₁₆₇) show a shift of the minimum from 200 nm towards 208 nm and an increased negative CD signal at 222 nm, which is characteristic for α -helical structures [145]. Interestingly, a similar increase in α -helical structure has been observed with c-Myc₁₋₁₄₃ after addition of the hydrophobic solvent TFE (trifluoroethanol), which favours secondary structure formation in regions which have a propensity to form an α -helix [149]. The MC29EB CD spectrum, compared with spectra observed with human c-Myc₁₋₁₄₃ before and after addition of 10% TFE [149] as well as with spectra observed with human c-Myc₁₋₁₆₇ [145], might already show some contribution of α -helical structure deduced from the slight dip in the curve at around 222 nm. As a matter of fact, MC29EB comprises residues 1-140 of chicken c-Myc and residue 140 from chicken c-Myc is equivalent to residue 151 of human c-Myc. It therefore extends further into a region, which is described to enhance α -helical structure formation.



5. ***Pull-down assay with purified His6-Carrier-cBASP1pep as bait protein and enriched MC29EB as prey protein***

We wanted to investigate the formation of a complex between a His6-‘Ca’-cBASP1pep fusion protein and MC29EB by using a pull-down methodology. In an on-column binding assay, we loaded His6-MBP-cBASP1pep onto a Ni²⁺-column, washed with low imidazole buffer and loaded MC29EB onto the His6-MBP-cBASP1pep charged Ni²⁺ column at very slow flow rates. MC29EB was eluted during the loading and the subsequent washing step. His6-MBP-cBASP1pep was eluted without bound MC29EB during the following gradient elution. Protein containing fractions after gradient elution were pooled and loaded onto a gel filtration column. Protein containing fractions after gel filtration were analyzed by SDS-PAGE.

It seems that MC29EB is not binding to His6-MBP-cBASP1pep as it is already eluted during the loading step (Fig. 15, A). SDS-PAGE of the flow-through fraction confirmed that the peak corresponds to MC29EB (data not shown). Subsequent gradient elution, gel filtration and SDS-PAGE seem to confirm that MC29EB does not bind to His6-MBP-cBASP1pep (Fig. 15, B-D).



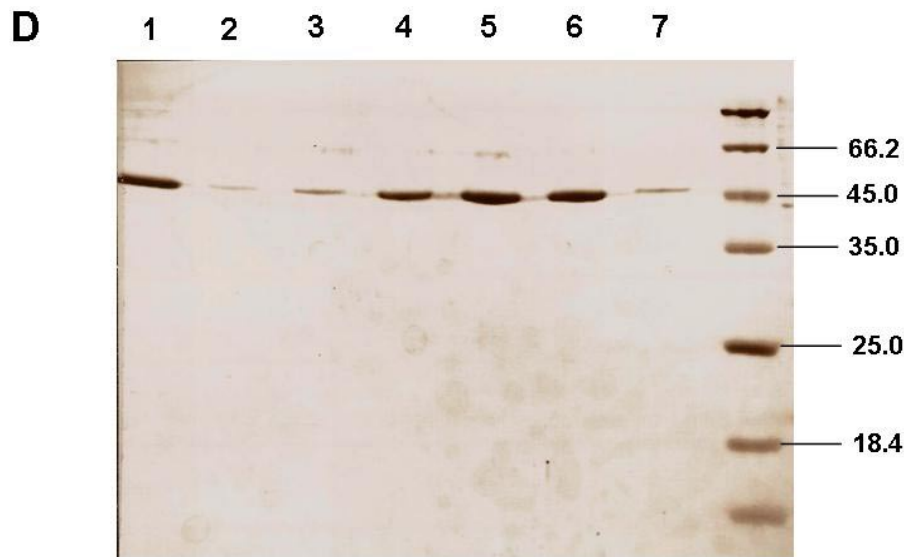


Fig. 15. On-column binding assay with His6-MBP-cBASP1pep and MC29EB. (A) Chromatogram after loading MC29EB onto the His6-MBP-cBASP1pep charged Ni^{2+} column. (B) Chromatogram of the subsequent gradient elution from 0-100% high imidazole buffer. (C) Gel filtration of protein containing fractions after gradient elution. (D) SDS-polyacrylamide gel of protein containing fractions after gel filtration. Numbering of lanes (1-7) corresponds to the fractions denoted in the chromatogram of the gel filtration step. His6-MBP-cBASP1pep migrates at ~ 45 kDa. MC29EB migrates at ~ 21 kDa.

In order to test, if the on-column binding method might be the reason for the failure of complex formation, as the continuous flow during loading and washing steps might hinder interaction between MC29EB and His6-MBP-cBASP1pep, we mixed the potential binding partners before loading them onto the Ni^{2+} column. In this experiment His6-trx-cBASP1pep was used as a bait protein. MC29EB was mixed with an excess of His6-trx-cBASP1pep and incubated for 1 h at 4°C. Afterwards the mixture was divided into 4 aliquots. The aliquots were incubated 0 min, 1 min, 5 min and 10 min at 37°C, respectively. Each mixture was loaded onto a Ni^{2+} -column. In all four pull-down assays MC29EB was eluted during the loading and washing steps (Fig. 16, compare A and B with lane 1 in D). During the subsequent gradient elution only His6-trx-cBASP1pep protein was eluted (Fig. 16, compare C with lane 2-5 in D). The flow-through fractions as well as protein containing fractions during the gradient elution were analyzed by SDS-PAGE (Fig. 16, D). The chromatograms and the SDS polyacrylamide gel are shown for the sample, which was incubated for 5 min at 37°C. The other 3 samples produced similar results (data not shown).

Hence, complex formation between the tagged cBASP1 peptide and MC29EB could not be observed with the pull-down method in combination with Ni^{2+} columns.

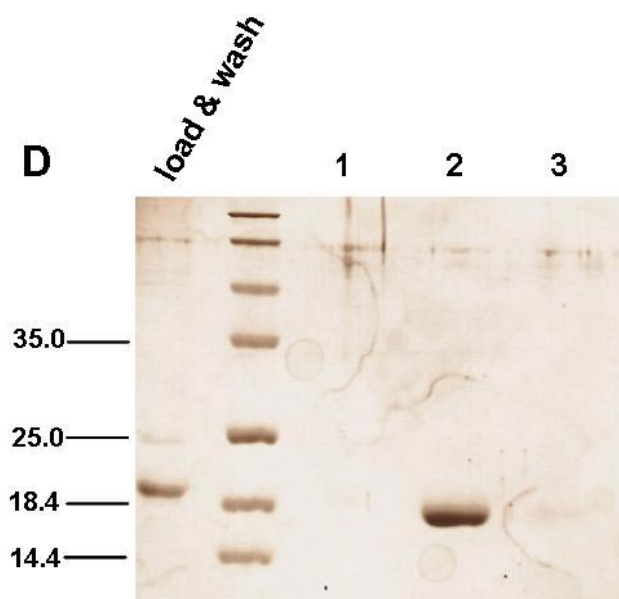
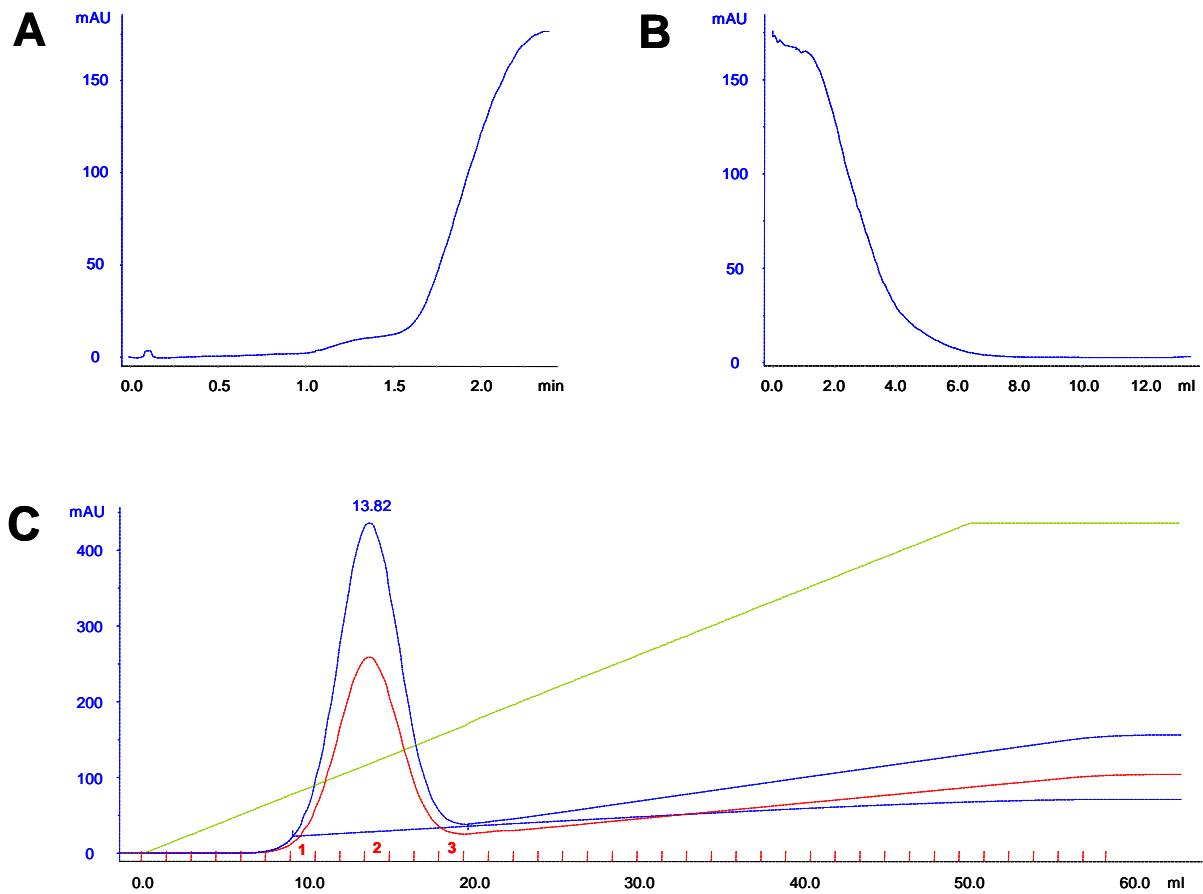


Fig. 16. Pull-down assay with His6-trx-cBASP1pep and MC29EB. (A-C) Chromatograms corresponding to different steps during the pull-down assay. (A) Loading the mixture of His6-trx-cBASP1pep and MC29EB onto the Ni²⁺ column. (B) Washing step with low imidazole buffer. (C) Gradient elution from 0-100% high imidazole buffer. (D) SDS-PAGE of protein containing fractions after gradient elution from Ni²⁺ column. Numbering of lanes 2-5 (1-3) corresponds to the fractions denoted in the chromatogram of the gradient elution step. MC29EB migrates at ~ 21 kDa. His6-trx-cBASP1pep migrates at ~ 18 kDa.

6. Binding assay between His6-Carrier-cBASP1pep and MC29EB via analytical gel filtration

Another method to investigate complex formation between proteins is analytical size exclusion chromatography (Superdex 75 10/300 GL). If two proteins form a complex, the complex can be observed at an elution volume distinct from the elution volumes of the single proteins.

In this experiment, His6-GB1-cBASP1pep was used as potential interactor. First, the single components of the potential complex were applied to analytical gel filtration with the elution volumes 9.05 ml ($K_{av} = 0.068$) for MC29EB (17.8 kDa) (Fig. 17, A) and 10.29 ml ($K_{av} = 0.147$) for His6-GB1-cBASP1pep (11.5 kDa) (Fig. 17, B). An equimolar mixture of the two proteins incubated for ~ 1 h at 4°C produced a chromatogram with two peaks at the elution volumes 8.76 ml ($K_{av} = 0.049$) and 10.16 ml ($K_{av} = 0.139$) (Fig. 17, C).

As a matter of fact no run with standard proteins was performed, so conclusions about multimeric states or the migration at the correct elution volume according to the size of the analyzed protein cannot be drawn. Despite those facts, the elution volumes of the two peaks observed during analytical gel filtration with the mixture of proteins nearly correspond to the elution volumes that were observed with the individual components. This interpretation favours the observation of no complex formation between the two proteins and is in accordance with previous results.

Another possible interpretation relies on the assumption that the peak at the elution volume of 8.76 ml does not correspond to the peak of single MC29EB at the elution volume of 9.05 ml. Accordingly, the mentioned peak at 8.76 ml would correspond to a complex between His6-GB1-cBASP1pep and MC29EB. The peak at an elution volume of 10.16 ml would then correspond to excess unbound His6-GB1-cBASP1pep protein. Contradicting this theory is the assumption that a complex between His6-GB1-cBASP1pep and MC29EB with a molecular weight of ~ 29.3 kDa would have a lower elution volume than 8.76 ml.

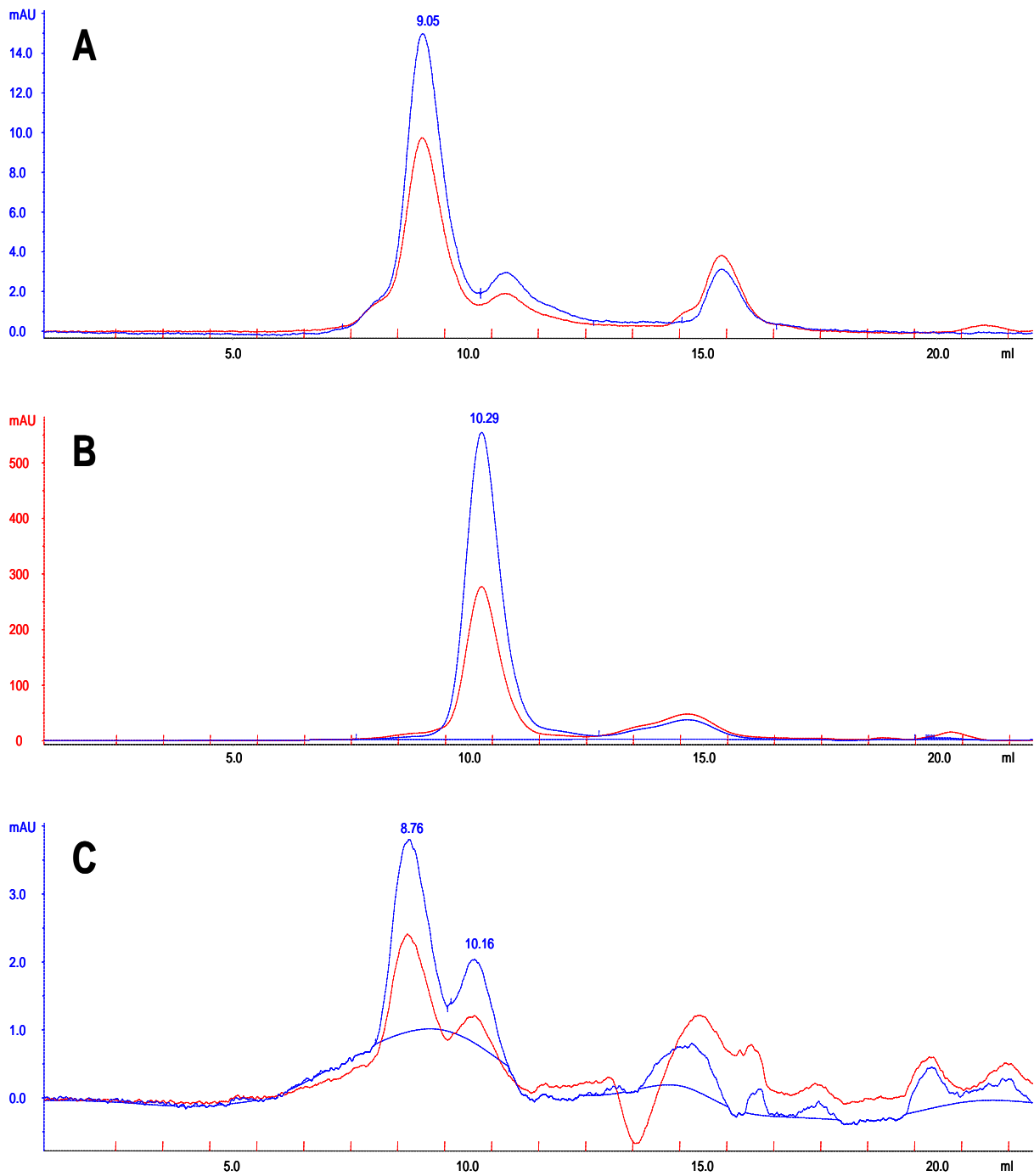


Fig. 17. Binding assay between His6-GB1-cBASP1pep and MC29EB via analytical gel filtration. (A) MC29EB alone with an elution volume of 9.05 ml. (B) His6-GB1-cBASP1pep alone with an elution volume of 10.29 ml. (C) Equimolar mixture of His6-GB1-cBASP1pep and MC29EB. Two peaks with elution volumes 8.76 ml and 10.16 ml.

Investigation of direct interaction between v-Myc and the cBASP1 interacting peptide

1. **MC29 transformed chicken embryonic fibroblasts**

Previous pull-down assays were performed with MC29EB, which is an N- and C-terminally truncated version of the MC29 Gag-Myc fusion protein (v-Myc), therefore being devoid of C-terminal regions corresponding to chicken c-Myc (residues 141-416). In order to test if full length v-Myc may bind to His6-Carrier-cBASP1pep fusion proteins, we wanted to perform a pull-down assay with His6-Carrier-cBASP1pep (bait protein) and cellular extracts from MC29 transformed chicken embryonic fibroblasts, which express oncogenic v-Myc.

Chicken embryonic fibroblasts were transformed with MC29 virus and after adopting a transformed state (visual inspection) cellular extracts were harvested and prepared for subsequent pull-down assays.

2. **Pull-down assay with purified His6-Carrier-cBASP1pep as bait protein and cellular extract from MC29 transformed CEF**

Pull-down assays with His6-trx-cBASP1pep and cellular extract from MC29 transformed CEF were performed as described in section “*Pull-Down Assay*” on HiTrap Chelating HP 1ml columns with Co^{2+} as the immobilized metal ion. Co^{2+} has been observed to be less susceptible to unspecific binding of proteins. Eluted fractions were subsequently analyzed by SDS-PAGE and western blot analysis using antibodies directed against v-Myc and antibodies directed against WS5 as a control. WS5 is a gene differentially expressed in transformed fibroblasts and is not supposed to interact with cBASP1.

Pre-clearing of the cellular extract and pull down assays were performed with buffers supplemented with 0.5 M NaCl to reduce unspecific binding of proteins to the Co^{2+} column. Nonetheless, at the pre-clearing step it can be seen that v-Myc binds unspecifically to the Co^{2+} column. It is eluted in the pre-cleared fraction as well as in the fraction containing non-specific binders (Fig. 18, compare lanes 2 and 3). Therefore, it is hard to draw conclusions regarding interaction between v-Myc and His6-trx-cBASP1pep. In the pull-down assay without pre-clearing of the cellular extract, v-Myc is mainly eluted during elution with high

imidazole but is also found in the flow through fraction (Fig. 18, compare lane 8 with lane 7). Interestingly, in the same assay even WS5, which is not supposed to bind to cBASP1, is eluted during the elution with high imidazole (Fig. 18, lane 8, lower panel). The pull-down assay performed with pre-cleared cellular extract is inconclusive as well. As before, v-Myc is found in the flow-through fraction and in the elution fraction (Fig. 18, lanes 4 and 5). Bands are less strong as compared to bands observed during the pull-down assay without pre-clearing of the cellular extract, as already a lot of v-Myc protein is lost during the pre-clearing step.

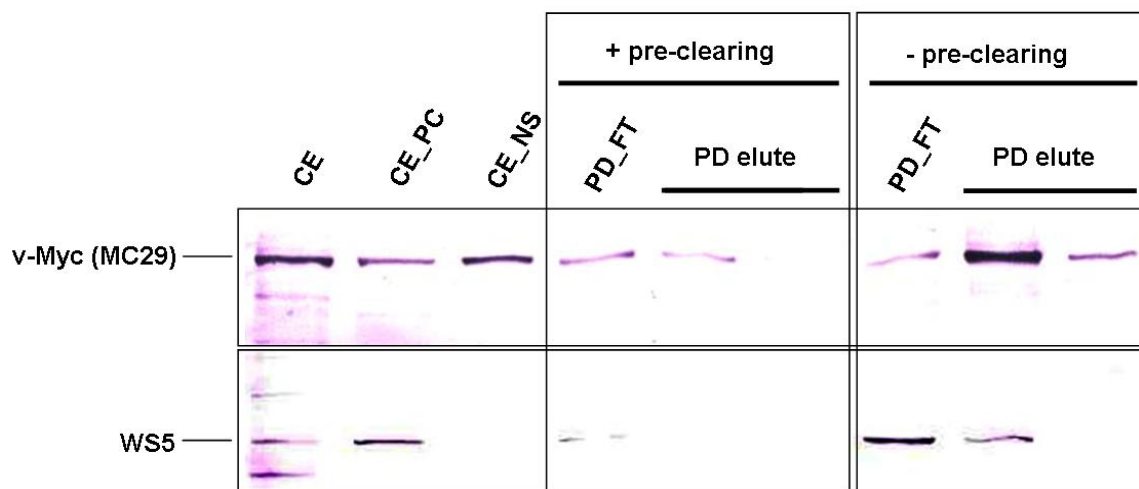


Fig. 18. Pull-down assay with His6-trx-cBASP1pep and cellular extract from MC29 transformed chicken embryonic fibroblasts (CEF) and subsequent Western blot analysis with antibodies directed against Myc (upper panel) and antibodies directed against WS5 as a control (lower panel). Pull-downs were performed either directly with cellular extract (6.2 mg) or after pre-clearing of cellular extract (6.2 mg). Samples were fractionated over a Co^{2+} column (HiTrap Chelating HP 1 ml) loaded with ~ 1 mg of His6-trx-cBASP1pep. CE (cellular extract); CE_PC (pre-cleared cellular extract); CE_NS (non-specific binders of the Co^{2+} column within the cellular extract); PD_FT (flow through fraction of the pull-down); PD elute (eluted fractions of the pull-down).

Other pull-down assays performed, included a pull-down assay with His6-trx-cBASP1pep and cellular extracts from untransformed quail embryonic fibroblasts in order to investigate direct interaction between His6-trx-cBASP1pep and endogenous c-Myc. Despite the fact that antibodies directed against chicken c-Myc also recognize quail c-Myc, the outcome of the pull-down is inconclusive. Bands corresponding to chicken c-Myc and quail c-Myc, respectively, could only be observed in lanes, where 12.4 μg of MC29 transformed CEF cell extract and 9 μg of untransformed QEF cell extract was loaded onto the SDS-polyacrylamide gel (data not shown).

A pull-down assay, intended as a control for a specific interaction of Myc, was carried out with a His6 tagged version of the Minimax protein (His6-Minimax → section: “*Expression and purification of His6-Minimax*”) and cellular extract from MC29 transformed CEF. In this experiment, pre-clearing was not performed. v-Myc is found in the flow-through fraction, what is particular disturbing as it should specifically interact with Minimax, and in the elution fractions of the pull-down (data not shown). Here has to be mentioned, that His6-Minimax behaved strangely during purification by Ni²⁺ affinity chromatography. Only about 50% of the recombinant protein was retained by the Ni²⁺ column. It might be that the ability of Max to form homodimers interferes with the ability to bind to the Ni²⁺ column. This might also serve as an explanation why v-Myc is partly found in the flow through fraction. Binding of v-Myc to His6-Minimax might interfere with binding of the His6 tag to the Co²⁺ column; consequently v-Myc would strip His6-Minimax from the Co²⁺ column.

Concluding, it is presumed that positive results of the performed pull-down assays are mainly due to unspecific binding of proteins to the Co²⁺ column. Hence, complex formation between v-Myc or c-Myc and the His6-‘Ca’-cBASP1pep fusion proteins used in this study cannot be confirmed with the pull-down method in combination with Co²⁺ or Ni²⁺ columns.

Meta-structure analysis of BASP1 and WT1

Human BASP1 has been identified as cosuppressor of human WT1 via binding to the WT1 suppression region (WT1 residues 92-101) [161]. We wanted to test, if meta-structure analysis of those proteins is in agreement with those findings. Meta-structure analysis of proteins predicts residue-based compactness and secondary structure of a protein. Meta-structural parameters are then used to predict residue-based protein interaction probabilities as well as the probable secondary structure of the interactor.

Protein alignment of human BASP1 and chicken BASP1 indicates 63.1% sequence identity between those proteins. Fig. 19 shows an alignment (ClustalW) of BASP1 from different species. The N-terminus is highly conserved in different species, highlighting its importance for BASP1 function. As a matter of fact, interaction with CaM depends on residues at the extreme N-terminus of BASP1 and the myristoyl-group, which is attached to the N-terminus of BASP1 [169]. Myristoylation is not found with BASP1 functioning as a transcriptional cosuppressor [161]. The region around chicken BASP1 residues 60-80 is less conserved between different species. Meta-structure analysis of chicken BASP1 and human BASP1 depicts a similar low degree of compactness and secondary structural content (→ “Introduction” Fig. 7) for compactness and secondary structure prediction of chicken BASP1) and more importantly, a quite similar profile concerning probability for protein interaction (Fig. 20); highest probabilities were predicted for chicken BASP1 residues 42-80 and for human BASP1 residues 42-90, despite the relatively low degree of conservation in those regions. The low probability values calculated for human BASP1 residues 68-84 are possibly due to technical reasons of the alignment algorithm used. As the N-terminal myristoyl-group is indispensable for interaction of BASP1 with CaM, the meta-structure analysis does not predict high probability for protein interaction for the N-terminus of BASP1. For chicken BASP1 the secondary structure of the interactor was predicted to be in an extended, loop or β -stranded conformation.

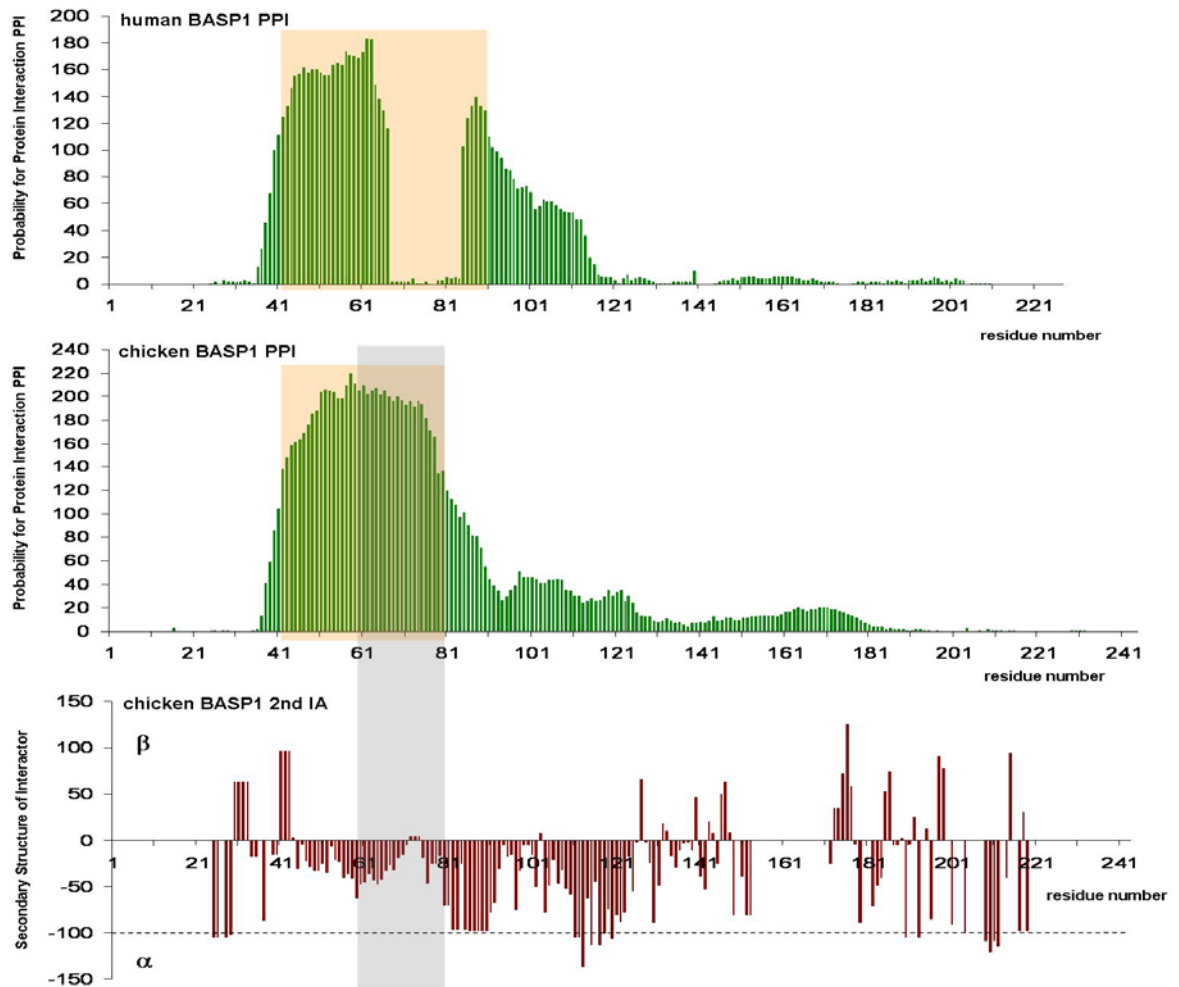


Fig. 20. Residue-based Probability for Protein Interaction (PPI) based on the meta-structure analysis of human BASP1 and chicken BASP1 as well as probable Secondary Structure of the Interactor (2nd IA) of chicken BASP1. Ad 2nd IA: Probabilities for α -helical segments are typically below -100 (dashed line); probabilities for extended conformations and β -strands are typically above -100. Regions with high probability for interaction are indicated by orange boxes. The cBASP1 peptide (residues 60-80) is indicated by a grey box.

Fig. 21 shows a protein alignment (ClustalW) of human WT1 isoform C and chicken WT1 (87.3% sequence identity). Even between chicken and humans, WT1 amino acid sequence is well conserved, especially in the C-terminus harbouring the four zinc-fingers necessary for DNA binding. Meta-structure analysis of human WT1 and chicken WT1 predicted similar values of high compactness and predominantly β -strand secondary structural elements. Fig. 22 shows compactness and secondary structure prediction for human WT1 isoform C. The N-terminal suppression region of WT1 spanning residues 92-101 (indicated by the grey box in Fig. 21 and Fig. 22) is predicted to be in a loop or β -stranded conformation. This finding is consistent with the prediction of the secondary structure of the BASP1 interactor, which was also predicted to be in a loop or β -stranded conformation.

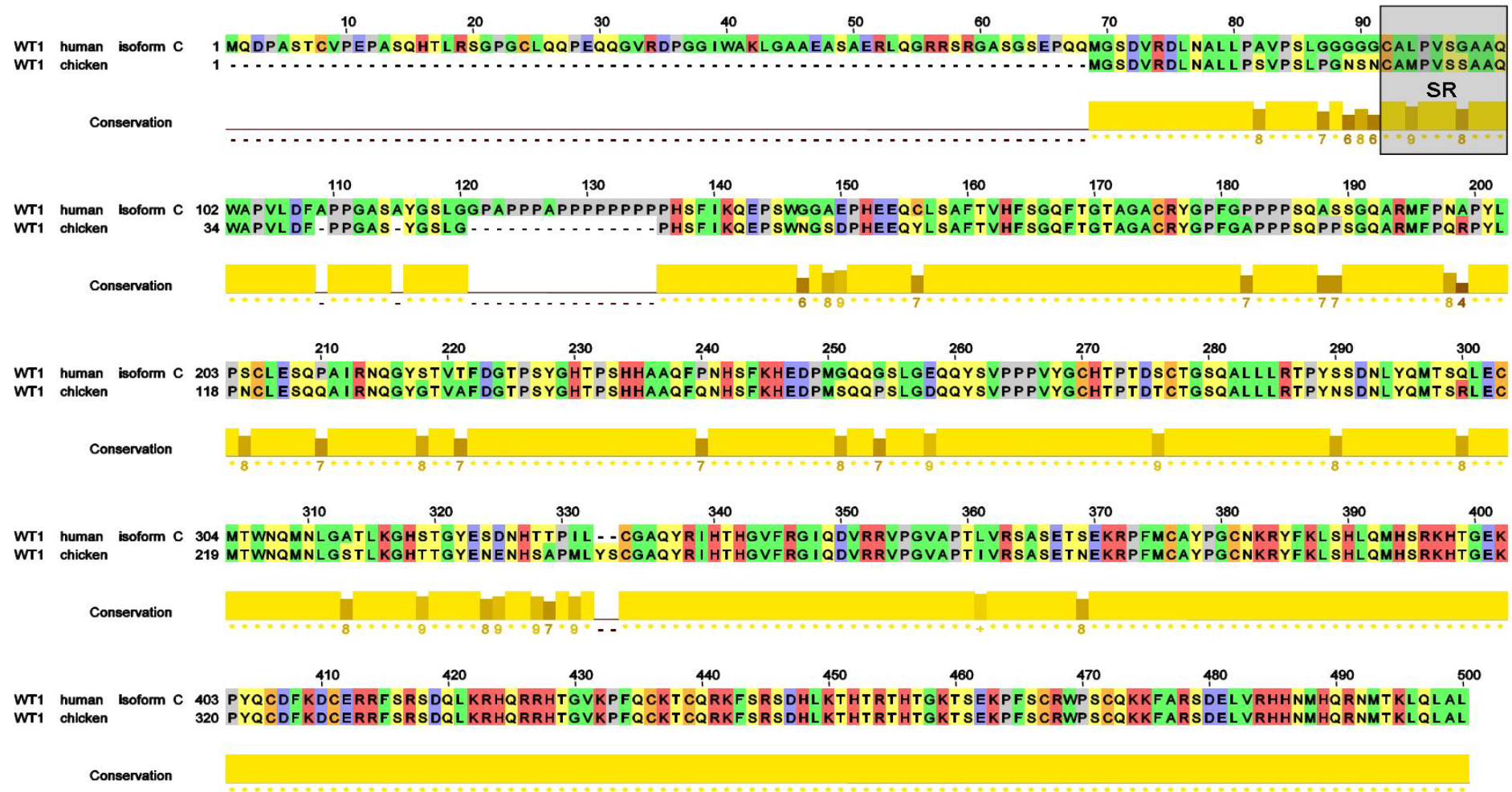


Fig. 21. Alignment of human WT1 isoform C and chicken WT1 amino acid sequences. The colour code outlines roughly amino acid properties: acidic (blue), basic (red), hydrophobic (green), polar (yellow) as well as cysteine (orange) and proline (grey). The histogram below gives a measure of conservation between the different sequences. The grey box indicates the suppression region of WT1 (human WT1 residues 92-101). Upper numbers correspond to human WT1 residue numbers.

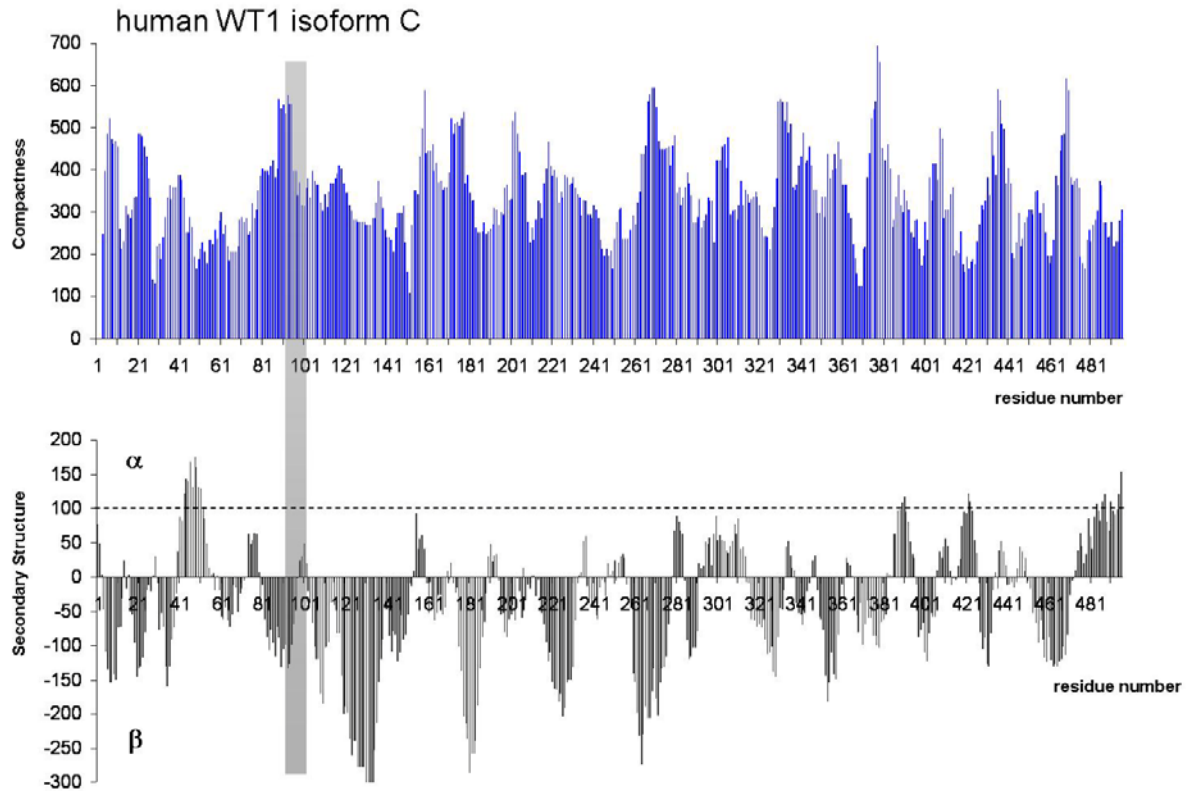


Fig. 22. Meta-structure analysis of human WT1 isoform C yielding residue-based Compactness values and Secondary Structure probabilities. Probabilities for α -helical segments are typically above 100 (dashed line); probabilities for extended conformations and β -strands are typically below 100. The N-terminal suppression region is indicated by a grey box.

Fig. 23 shows the meta-structure based analysis of probability for protein interaction and secondary structure of the interactor of human WT1, which is similar to chicken WT1. It depicts a very high probability for interaction in three large parts of the protein. An N-terminal region of high interaction probability (residues 70-106), which surrounds the suppression domain (residues 92-101), a part in the middle with high interaction probability (residues 153-245), which coincides with the transactivation domain of WT1 (residues 180-250) [161] and a C-terminal region of high interaction probability (residues 292-435), where the C-terminal zinc-fingers are located. For the suppression region the secondary structure of the interactor is predicted to be rather in a loop or β -stranded conformation.

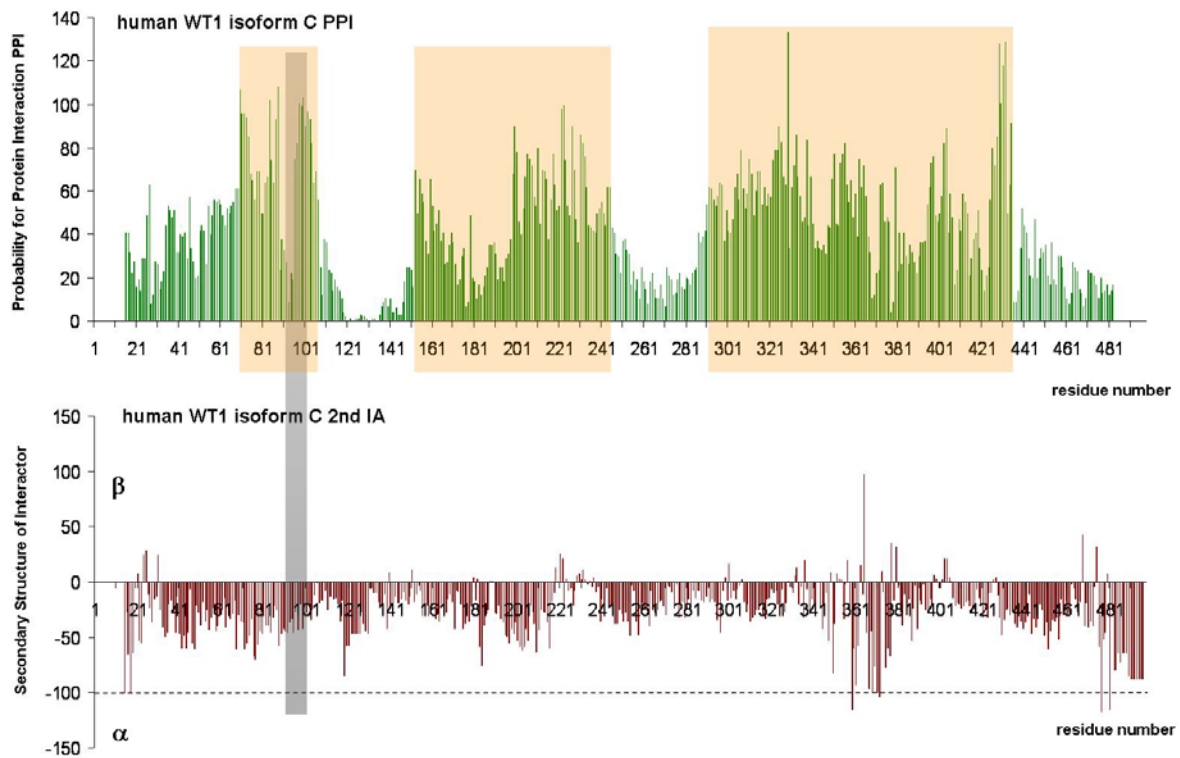


Fig. 23. Residue-based Probability for Protein Interaction (PPI) as well as probable Secondary Structure of the Interactor (2nd IA) of human WT1 isoform C based on its meta-structure analysis. Ad 2nd IA: Probabilities for α -helical segments are typically below -100 (dashed line); probabilities for extended conformations and β -strands are typically above -100. Regions with high probability for interaction are indicated by orange boxes. The WT1 suppression region is indicated by a grey box.

The finding that the interactor of the WT1 suppression region is in a rather loop or β -stranded conformation is consistent with the meta-structural data of chicken BASP1 (\rightarrow “Introduction” Fig. 7). Meta-structure analysis of human BASP1 in the region of high protein interaction probability predicts also a propensity for the formation of α -helical segments, especially the region spanning residues 73-80 (Fig. 24).

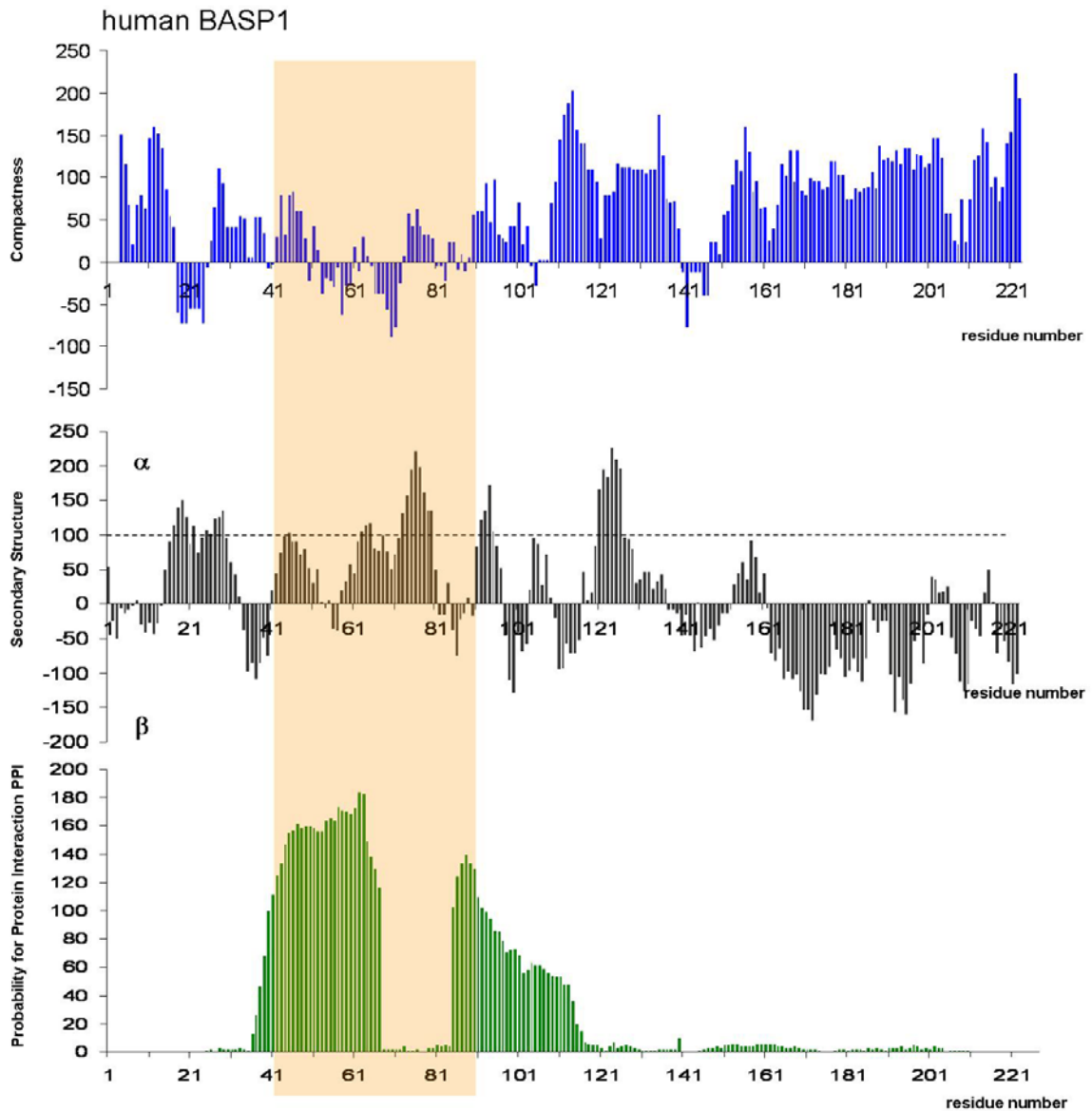


Fig. 24. Meta-structure analysis of human BASP1 yielding residue-based Compactness values and Secondary Structure probabilities as well as Probabilities for Protein Interaction (PPI). Ad Secondary Structure prediction: probabilities for α -helical segments are typically above 100 (dashed line); probabilities for extended conformations and β -strands are typically below 100. The region with highest probability for protein interaction is indicated by an orange box (residues 42-80).

Concluding, meta-structure analysis of WT1 and BASP1 supports the finding that BASP1 interacts via a region found to be highly probable for protein interaction with the suppression region of WT1.

Discussion

The Pull-down assay as a method for the investigation of protein interaction

The pull-down assay is a quite powerful tool in confirming the interaction between proteins and is comparable to immunoprecipitation techniques. But it has to be handled with great care and it cannot – as can be seen by the difficulties encountered in this study – be used as the sole experiment to verify a potential protein interaction. As a matter of fact, positive results don't mean necessarily direct interaction between two proteins. A lot of proteins may exist in multi-protein complexes and a seemingly direct interaction could also be explained by indirect interaction via adaptor proteins, which tether two proteins together. Other methods exist to validate direct interaction of proteins.

Pull-down assays are usually performed with GST tags on glutathione agarose or His6 tags in combination with immobilized bivalent metal ion matrices. GST tags should be favoured in the sense that they are less prone to unspecific binding of proteins to the affinity ligand. A lot of proteins are able to bind bivalent ions by themselves and therefore might bind unwanted to the immobilized metal ions used with the His6 methodology. Furthermore ion exchange effects are observed with IMAC columns. Therefore, especially with very acidic proteins, it is not advisable to use pull down techniques based on IMAC.

As a matter of fact, MC29EB, c-Myc and v-Myc are quite acidic proteins with theoretical pI values of 4.33, 5.28 and 5.52, respectively. Anion exchange chromatography

even is used for the purification of MC29EB. So it is not quite surprising that ion exchange effects are observed with those proteins in combination with Ni²⁺/Co²⁺ columns. On the other hand, unspecific binding to the column could not be observed during pull-down assays performed with purified MC29EB. However, in this case Coomassie Staining of polyacrylamide gels was used to detect the proteins in question, which is a highly insensitive detection method. Therefore it is possible that minimal undetectable amounts of MC29EB adhered unspecifically to the Ni²⁺ column. The immunoblotting method used for detection of v-Myc or endogenous c-Myc in cellular extracts is much more sensitive and therefore able to detect small amounts of unspecifically bound proteins.

To produce reliable results, it is important to include negative and positive controls. As positive control a protein should be used, which has been already confirmed to interact with the BASP1 protein (e.g. WT1). BASP1 was identified as cosuppressor for the Wilms' tumor suppressor protein 1 (WT1) and has been shown with the help of pull-down assays to interact with an N-terminal suppression region of WT1 [161]. Additionally, it would be advisable to test full-length BASP1 for binding to target proteins in advance. As negative control has to be used the tag alone bound to the column. In the current study the His6-'Ca' moiety without the C-terminal cBASP1 peptide would serve as a negative control.

Does BASP1 bind directly to Myc TAD?

In the current study the N-terminal transactivation domain of chicken c-Myc and v-Myc, respectively, wanted to be tested for interaction with cBASP1. Therefore, His6 tagged fusion proteins were expressed and purified, which contain a small peptide stretch of cBASP1 (residues 59 to 80). The meta-structure approach predicted this peptide to be highly probable for interaction with a supposedly loop or β -stranded part of another protein. In subsequent pull-down assays the fusion proteins were used as bait proteins and either a purified part of v-Myc containing chicken c-Myc TAD residues 1-140 (MC29EB) or full-length v-Myc (cellular lysate from MC29 transformed chicken embryonic fibroblasts) and/or endogenous c-Myc (cellular lysate from untransformed chicken embryonic fibroblasts) as potential prey proteins. There are different possibilities to explain the failure to observe direct interaction between those proteins.

First of all, we didn't test full length cBASP1 for interaction with Myc TAD. High affinity binding of cBASP1 to Myc might need a bigger portion of the protein compared to

the 20 residues peptide used in this study. Moreover, the carrier protein fused to the small cBASP1 peptide might interfere with the capacity of the peptide to bind to other proteins. A possibility to test for those factors, the already described BASP1 interactor WT1 or its suppression domain ranging from WT1 residue 92-101 [161] should be tested for interaction with the Carrier-BASP1-peptide fusion proteins. Even so, a negative result will not solve the problem, if the carrier might disturb interaction or the peptide is too short for high affinity binding.

Furthermore and worth to notice, is the recent finding that residues 1-143 of Myc TAD are less efficiently binding to Myc interacting proteins MM1 and TBP as compared to a more elongated Myc TAD (human c-Myc₁₋₁₆₇) [145]. Maybe binding of BASP1 is even not possible with the shorter version of c-Myc TAD. In the referred study a more elongated region, including Myc residues 144-167, was discovered to greatly enhance binding to the mentioned interactors [145]. Human c-Myc residues 1-143 were formerly described as being the minimal region required for neoplastic transformation of primary rat embryo cells in cooperation with oncogenic Ras [148]. Even though, nearly devoid of secondary structure – rather adopting a random coil conformation –, c-Myc₁₋₁₄₃ is still able to interact with TBP. Moreover, an induction of protein conformation could be seen with c-Myc₁₋₁₄₃ upon binding to the target factor TBP [149]. Interestingly, secondary structure prediction software predicted an amphipathic helix ranging from human c-Myc residues 140-157. As a matter of fact, CD measurements of human c-Myc₁₋₁₆₇ show a higher degree of helicity as c-Myc₁₋₁₄₃ and indicate a molten globule-like state of c-Myc₁₋₁₆₇ as compared to the random coil conformation of c-Myc₁₋₁₄₃ [145, 149]. At this point, it is notable that studies concerned with c-Myc degradation gave contradictory results, if fusion proteins were attached to the N-terminus of a c-Myc TAD 1-147 construct [184] or to the C-terminus of a c-Myc TAD 1-149 construct [185]. C-terminal fusion proteins may stabilize c-Myc TAD in the sense that they could induce protein conformation in a similar way as c-Myc residues 144-167 do, which harbour the predicted amphipathic helix. Conversely, a c-Myc TAD 1-147 construct with an N-terminal fusion protein might miss the induction of protein conformation and therefore is more prone to protein degradation.

Secondary structure prediction of human c-Myc TAD suggested α -helical as well as β -stranded parts, which are outlined in Fig. 6 in the introduction. Three β -strands were predicted covering residues 3-7, 22-24 and 114-116. Four α -helices were identified spanning residues 31-37, 47-53, 96-106 and 140-157, where the latter three are supposedly amphipathic [145]. Binding of proteins to c-Myc TAD can be quite diverse. For example, cyclin T1

binding to Myc was identified to depend on the highly conserved Myc box I, whereas cdk8 binding localized to the extreme N-terminus of the Myc TAD [186], where rather β -stranded parts were predicted. Interaction studies using B-Myc revealed that MM-1 binding to B-Myc affects Myc box I and Myc box II as well as residues found outside the conserved Myc boxes. One of those residues Phe104 of rat B-Myc (corresponding to Phe115 of human c-Myc) even lies in a supposedly β -stranded region of human c-Myc TAD (residues 114-116). Association of TBP with B-Myc influences mostly Myc box II and sequences C-terminal to this core motif [151]. Interestingly, studies elucidating the interaction mechanism of Myc TAD with TBP and MM-1, respectively, with the help of surface plasmon resonance assays employing Biacore technology as well as CD spectroscopy, revealed that the N-terminal part of c-Myc TAD alone (c-Myc₁₋₈₈) is not able to bind TBP and MM-1, whereas the C-terminal part (c-Myc₉₂₋₁₆₇) binds TBP and MM-1 but with less affinity as compared with c-Myc₁₋₁₆₇ and c-Myc₃₈₋₁₆₇. Only the full-length TAD (c-Myc₁₋₁₆₇) binds TBP and MM-1 with highest affinity. Therefore it was concluded, that N- and C-terminal halves cooperate in binding to target proteins. The kinetic data of interaction between Myc and TBP or MM-1 was found to fit a conformational change model, where binding to interactors enhances helicity indicating a possible folding-upon-binding mechanism. The additional stretch of residues 144-167 is needed for stabilizing secondary structures and for high affinity binding to interactors [145].

BASP1 has been predicted by the meta-structure approach to bind to a rather loop or β -stranded entity of a protein. As binding of proteins to Myc TAD can involve quite different parts of the transactivation domain, it might be possible that binding of BASP1 to Myc TAD depends strongly on the predicted α -helical stretch reaching from human c-Myc residues 140-157 to induce protein conformation and thereby establishing the interaction platform for BASP1. In our study we used the recombinant protein MC29EB as a potential interactor of chicken BASP1 (cBASP1). MC29EB harbours residues 1-140 of chicken c-Myc TAD, which correspond to residues 1-151 of human c-Myc. Therefore MC29EB ends in the middle of the region predicted to form an amphipathic α -helix. Hence, it's quite possible that MC29EB is not able to form this C-terminal helix. CD measurements of MC29EB seem to support this view, as the spectra indicate a rather random coil conformation of MC29EB. Maybe BASP1 needs a better folded part to be able to interact with Myc TAD.

Another possibility is that BASP1 binds to the C-terminal bHLHZip domain of Myc. As a matter of fact, this region has been shown to be involved not only in dimer or possibly tetramer formation but also interacts with other proteins that regulate Myc function as CBP

and p300 [112]. On the other hand, the C-terminus of c-Myc consists almost entirely of α -helices and therefore is rather unlikely to interact with BASP1.

The mutual suppression of Myc and BASP1

Ectopic expression of BASP1 hinders transformation by v-Myc

We wanted to investigate direct binding between Myc and BASP1 based on the observations outlined in the “Results”-section.

Ectopic expression of cBASP1 in chicken embryonic fibroblasts hinders transformation by v-Myc (unpublished data). Direct binding between Myc and cBASP1 can be the reason for the inability of v-Myc to exert its oncogenic function in cBASP1 overexpressing cells. cBASP1 might hinder v-Myc in exerting its function as a transcriptional activator by obstructing its ability to bind to its target genes. Nevertheless, this scenario is rather improbable as it would involve interaction of cBASP1 with the C-terminus of Myc. Another possibility involving direct interaction might be that BASP1 acts as a cosuppressor of Myc by binding to its transactivation domain, subsequently switching Myc function from an activating to a repressing state. Similarly, WT1 was discovered as a transcriptional activator, but represses transcription when in complex with BASP1 [161].

Direct binding between Myc and BASP1 is only one possibility to explain the mutual suppression found with those two proteins. As quoted before, BASP1 is able to interact with WT1 and thereby leads to the repression of WT1 target genes. WT1 is a transcription factor that plays an essential role in urogenital development and it is overexpressed in a variety of human cancers. WT1 can bind via its four zinc fingers to GC-rich Egr1 sites (5'-GNGNGGGNG-3') [187], to WTE sites (5'-GCGTGGGAGT-3') [188] and to the (TCC)_n motif [189] and either enhances or represses transcription. Target genes of WT1 comprise growth factor genes, growth factor repressor genes, transcription factor and other genes, including *N-myc* and *c-myc* [35, 190-192]. As a matter of fact, *c-myc* possesses WT1 binding sites in its promoter region and the four major isoforms of WT1 could enhance expression of *c-myc* promoter::luciferase reporter constructs in human breast cancer and leukemia cells. The WT1-enhancing activity could be attributed solely to a WT1 binding site upstream of the P2 transcription start site of the *c-myc* promoter, between nucleotides -107 and +36 [35].

Moreover, an enhanced expression of N-myc in Wilms' tumor cells has been observed [193]. Interestingly, there are disparate results concerning the function of WT1, as some studies identify it as a tumor-suppressor gene and others as an oncogene. It seems that whether *c-myc* is positively or negatively regulated by WT1 is dependent on the cellular context.

The discovery of BASP1 as a cosuppressor of WT1 might explain those contradictory results. BASP1 binds to an N-terminal suppression region of WT1 spanning WT1 residues 92-101 and thereby regulates its transcriptional activation domain ranging from WT1 residues 180-250. Meta-structure analysis of BASP1 and WT1 (chicken and human) as well as meta-structure based prediction of protein interaction probability and secondary structure of the interactor is consistent with the hypothesis that the small stretch of chicken BASP1 residues 60-80 would bind to the suppression region of WT1 (residues 92-101). BASP1 confers WT1 cosuppressor activity in transfection assays and elimination of endogenous BASP1 expression augments transcriptional activation by WT1. As BASP1 can modulate the function of WT1 via binding to its suppression domain, it was proposed that in a specific cellular context, the WT1-BASP1 interaction may be disrupted or BASP1 may be downregulated to release the transcriptional activation function of WT1. Moreover, the cellular localization of BASP1 might be a possibility to regulate WT1 function [161]. This hypothesis is substantiated by the recent finding, that human BASP1 was found to be cleaved and subsequently translocated from the nucleus to the cytoplasm of HeLa cells upon induction of apoptosis [162].

c-myc is a target gene of WT1. Therefore, it might be transcriptionally enhanced by WT1 or repressed when in complex with BASP1. It would be interesting to test MC29-transformed as well as untransformed chicken embryonic fibroblasts (CEF) for WT1 expression and if chicken BASP1 overexpression reduces endogenous c-Myc expression in untransformed CEF.

The fact that WT1 regulates the transcription of *c-myc* via binding to its promoter region cannot explain the fact that BASP1 hinders transformation by v-Myc as the gene *v-myc* encoded by the MC29 proviral genome lacks *c-myc* promoter regions. It would be interesting to test, if WT1 is able to bind to viral promoter regions and thereby influences *v-myc* transcription.

Another possibility assuming the involvement of WT1 in the hindrance of v-Myc based transformation is that WT1 in complex with BASP1 leads to the repression of cellular genes that might be required for transformation. It has been shown that an elevated expression of c-Myc alone is not sufficient for transformation and neoplastic tumor formation and requires the deregulation of proteins from distinct pathways (e.g. Ras signaling) [131-133].

Maybe WT1-BASP1 mediated repression of a multitude of target genes and subsequent alteration of many different signaling pathways influencing cell behaviour is counteracting transformation by v-Myc.

Transformation by v-Myc leads to BASP1 repression

Chicken *BASP1* has been found to be repressed already at the transcriptional level after transformation by oncogenic v-Myc (unpublished data). Myc proteins bind to a lot of different promoters – either directly via E-box DNA sequences or indirectly via the recruitment by other transcription factors (e.g. Miz1) – and can enhance as well as repress transcription of target genes. It would be interesting to search for E-box sequences in regulatory regions of *cBASP1* to see if Myc proteins would be able to directly bind and influence the *cBASP1* transcription. Moreover, it would be advisable to search for binding sites of other transcription factors that are able to recruit Myc proteins to their target genes. For example, one mechanism of Myc-dependent repression involves the recruitment of Myc by the normally positive acting factor Miz-1 to initiator elements (INR) in core promoters lacking E-box DNA sequences [102, 103]. Moreover, several other factors have been suggested to recruit Myc to their cognate DNA binding site (e.g. Sp1, NF-Y, TFII-I and yingyang-1 [106-109]).

References

1. Reddy, E.P., et al., *Nucleotide sequence analysis of the proviral genome of avian myelocytomatosis virus (MC29)*. Proc Natl Acad Sci U S A, 1983. **80**(9): p. 2500-4.
2. Konrat, R., *The Meta-Structure Concept*.
3. Vecchio, G., *Oncogenes of DNA and RNA tumor viruses and the origin of cellular oncogenes*. History and philosophy of the life sciences, 1993. **15**(1): p. 59-74.
4. Stehelin, D., et al., *Detection and enumeration of transformation-defective strains of avian sarcoma virus with molecular hybridization*. Virology, 1977. **76**(2): p. 675-84.
5. Mladenov, Z., et al., *Strain MC29 avian leukosis virus. Myelocytoma, endothelioma, and renal growths: pathomorphological and ultrastructural aspects*. J Natl Cancer Inst, 1967. **38**(3): p. 251-85.
6. Bister, K., M.J. Hayman, and P.K. Vogt, *Defectiveness of avian myelocytomatosis virus MC29: isolation of long-term nonproducer cultures and analysis of virus-specific polypeptide synthesis*. Virology, 1977. **82**(2): p. 431-48.
7. Duesberg, P.H., K. Bister, and P.K. Vogt, *The RNA of avian acute leukemia virus MC29*. PNAS, 1977. **74**: p. 4320-4324.
8. Shih, T.Y., et al., *Identification of a sarcoma virus-coded phosphoprotein in nonproducer cells transformed by Kirsten or Harvey murine sarcoma virus*. Virology, 1979. **96**(1): p. 64-79.
9. Chang, H.W., et al., *Molecular cloning of the Harvey sarcoma virus circular DNA intermediates. II. Further structural analyses*. J Virol, 1980. **33**(2): p. 845-55.
10. Maki, Y., et al., *Avian sarcoma virus 17 carries the jun oncogene*. Proc Natl Acad Sci U S A, 1987. **84**(9): p. 2848-52.
11. Ivanov, X., et al., *Bull. Inst. Pathol. Comp. Anim.*, 1964. **10**: p. 5 - 38.
12. Bishop, J.M., *Retroviruses and cancer genes*. Adv Cancer Res, 1982. **37**: p. 1-32.
13. Bister, K. and H.W. Jansen, *Oncogenes in retroviruses and cells: biochemistry and molecular genetics*. Adv Cancer Res, 1986. **47**: p. 99-188.
14. Lee, C.M. and E.P. Reddy, *The v-myc oncogene*. Oncogene, 1999. **18**(19): p. 2997-3003.
15. Bister, K., et al., *OK10, an avian acute leukemia virus of the MC 29 subgroup with a unique genetic structure*. Proc Natl Acad Sci U S A, 1980. **77**(12): p. 7142-6.
16. Doggett, D.L., et al., *Structure, origin, and transforming activity of feline leukemia virus-myc recombinant provirus FTT*. J Virol, 1989. **63**(5): p. 2108-17.
17. Hayflick, J., et al., *Nucleotide sequence of two overlapping myc-related genes in avian carcinoma virus OK10 and their relation to the myc genes of other viruses and the cell*. Proc Natl Acad Sci U S A, 1985. **82**(9): p. 2718-22.
18. Kan, N.C., et al., *Nucleotide sequence of avian carcinoma virus MH2: two potential onc genes, one related to avian virus MC29 and the other related to murine sarcoma virus 3611*. Proc Natl Acad Sci U S A, 1984. **81**(10): p. 3000-4.
19. Walther, N., et al., *Molecular cloning of proviral DNA and structural analysis of the transduced myc oncogene of avian oncovirus CMII*. J Virol, 1985. **54**(2): p. 576-85.
20. Sheiness, D., L. Fanshier, and J.M. Bishop, *Identification of nucleotide sequences which may encode the oncogenic capacity of avian retrovirus MC29*. J Virol, 1978. **28**(2): p. 600-10.
21. Robins, T., et al., *Structural relationship between a normal chicken DNA locus and the transforming gene of the avian acute leukemia virus MC29*. J Virol, 1982. **41**(2): p. 635-42.
22. Xu, L., et al., *Role of first exon/intron sequences in the regulation of myc family oncogenic potency*. Oncogene, 1993. **8**(9): p. 2547-53.
23. Sugiyama, A., et al., *Isolation and characterization of s-myc, a member of the rat myc gene family*. Proc Natl Acad Sci U S A, 1989. **86**(23): p. 9144-8.
24. DePinho, R.A., N. Schreiber-Agus, and F.W. Alt, *myc family oncogenes in the development of normal and neoplastic cells*. Adv Cancer Res, 1991. **57**: p. 1-46.
25. Wierstra, I. and J. Alves, *The c-myc promoter: still Mystery and challenge*. Adv Cancer Res, 2008. **99**: p. 113-333.
26. Watt, R., et al., *The structure and nucleotide sequence of the 5' end of the human c-myc oncogene*. Proc Natl Acad Sci U S A, 1983. **80**(20): p. 6307-11.
27. Strieder, V. and W. Lutz, *Regulation of N-myc expression in development and disease*. Cancer Lett, 2002. **180**(2): p. 107-19.
28. Yagi, K., et al., *c-myc is a downstream target of the Smad pathway*. J Biol Chem, 2002. **277**(1): p. 854-61.
29. Chen, C.R., Y. Kang, and J. Massague, *Defective repression of c-myc in breast cancer cells: A loss at the core of the transforming growth factor beta growth arrest program*. Proc Natl Acad Sci U S A, 2001. **98**(3): p. 992-9.
30. Bossone, S.A., et al., *MAZ, a zinc finger protein, binds to c-MYC and C2 gene sequences regulating transcriptional initiation and termination*. Proc Natl Acad Sci U S A, 1992. **89**(16): p. 7452-6.
31. Dufort, D. and A. Nepveu, *The human cut homeodomain protein represses transcription from the c-myc promoter*. Mol Cell Biol, 1994. **14**(6): p. 4251-7.
32. Pirc, J.J., K.H. Moberg, and D.J. Hall, *Isolation of a novel cDNA encoding a zinc-finger protein that binds to two sites within the c-myc promoter*. Biochemistry, 1992. **31**(16): p. 4102-10.
33. Duyao, M.P., et al., *Transactivation of the c-myc promoter by human T cell leukemia virus type 1 tax is mediated by NF kappa B*. J Biol Chem, 1992. **267**(23): p. 16288-91.

34. Li, J., et al., *Novel NEMO/IkappaB kinase and NF-kappa B target genes at the pre-B to immature B cell transition.* J Biol Chem, 2001. **276**(21): p. 18579-90.
35. Han, Y., et al., *Transcriptional activation of c-myc proto-oncogene by WT1 protein.* Oncogene, 2004. **23**(41): p. 6933-41.
36. Hewitt, S.M., et al., *Regulation of the proto-oncogenes bcl-2 and c-myc by the Wilms' tumor suppressor gene WT1.* Cancer Res, 1995. **55**(22): p. 5386-9.
37. Barone, M.V. and S.A. Courtneidge, *Myc but not Fos rescue of PDGF signalling block caused by kinase-inactive Src.* Nature, 1995. **378**(6556): p. 509-12.
38. Chiariello, M., M.J. Marinissen, and J.S. Gutkind, *Regulation of c-myc expression by PDGF through Rho GTPases.* Nat Cell Biol, 2001. **3**(6): p. 580-6.
39. Cleveland, J.L., et al., *Tyrosine kinase oncogenes abrogate interleukin-3 dependence of murine myeloid cells through signaling pathways involving c-myc: conditional regulation of c-myc transcription by temperature-sensitive v-abl.* Mol Cell Biol, 1989. **9**(12): p. 5685-95.
40. Zou, X., et al., *Induction of c-myc transcription by the v-Abl tyrosine kinase requires Ras, Raf1, and cyclin-dependent kinases.* Genes Dev, 1997. **11**(5): p. 654-62.
41. Pietenpol, J.A., et al., *TGF-beta 1 inhibition of c-myc transcription and growth in keratinocytes is abrogated by viral transforming proteins with pRB binding domains.* Cell, 1990. **61**(5): p. 777-85.
42. Coffey, R.J., Jr., et al., *Selective inhibition of growth-related gene expression in murine keratinocytes by transforming growth factor beta.* Mol Cell Biol, 1988. **8**(8): p. 3088-93.
43. He, T.C., et al., *Identification of c-MYC as a target of the APC pathway.* Science, 1998. **281**(5382): p. 1509-12.
44. Rhee, K., T. Ma, and E.A. Thompson, *The macromolecular state of the transcription factor E2F and glucocorticoid regulation of c-myc transcription.* J Biol Chem, 1994. **269**(25): p. 17035-42.
45. Ramana, C.V., et al., *Regulation of c-myc expression by IFN-gamma through Stat1-dependent and -independent pathways.* Embo J, 2000. **19**(2): p. 263-72.
46. Michelotti, E.F., et al., *Cellular nucleic acid binding protein regulates the CT element of the human c-myc protooncogene.* J Biol Chem, 1995. **270**(16): p. 9494-9.
47. Siddiqui-Jain, A., et al., *Direct evidence for a G-quadruplex in a promoter region and its targeting with a small molecule to repress c-MYC transcription.* Proc Natl Acad Sci U S A, 2002. **99**(18): p. 11593-8.
48. Yang, D. and L.H. Hurley, *Structure of the biologically relevant G-quadruplex in the c-MYC promoter.* Nucleosides Nucleotides Nucleic Acids, 2006. **25**(8): p. 951-68.
49. Huppert, J.L. and S. Balasubramanian, *G-quadruplexes in promoters throughout the human genome.* Nucleic Acids Res, 2007. **35**(2): p. 406-13.
50. Eddy, J. and N. Maizels, *Gene function correlates with potential for G4 DNA formation in the human genome.* Nucleic Acids Res, 2006. **34**(14): p. 3887-96.
51. Maizels, N., *Dynamic roles for G4 DNA in the biology of eukaryotic cells.* Nat Struct Mol Biol, 2006. **13**(12): p. 1055-9.
52. Oganessian, L. and T.M. Bryan, *Physiological relevance of telomeric G-quadruplex formation: a potential drug target.* Bioessays, 2007. **29**(2): p. 155-65.
53. Fry, M., *Tetraplex DNA and its interacting proteins.* Front Biosci, 2007. **12**: p. 4336-51.
54. Cooney, M., et al., *Site-specific oligonucleotide binding represses transcription of the human c-myc gene in vitro.* Science, 1988. **241**(4864): p. 456-9.
55. Avigan, M.I., B. Strober, and D. Levens, *A far upstream element stimulates c-myc expression in undifferentiated leukemia cells.* J Biol Chem, 1990. **265**(30): p. 18538-45.
56. Liu, J., et al., *Defective interplay of activators and repressors with TFIH in xeroderma pigmentosum.* Cell, 2001. **104**(3): p. 353-63.
57. Liu, J., et al., *The FBP interacting repressor targets TFIH to inhibit activated transcription.* Mol Cell, 2000. **5**(2): p. 331-41.
58. Kim, M.J., et al., *Downregulation of FUSE-binding protein and c-myc by tRNA synthetase cofactor p38 is required for lung cell differentiation.* Nat Genet, 2003. **34**(3): p. 330-6.
59. Chung, H.J. and D. Levens, *c-myc expression: keep the noise down!* Mol Cells, 2005. **20**(2): p. 157-66.
60. Kouzine, F., et al., *The dynamic response of upstream DNA to transcription-generated torsional stress.* Nat Struct Mol Biol, 2004. **11**(11): p. 1092-100.
61. Schwab, M., et al., *Amplified DNA with limited homology to myc cellular oncogene is shared by human neuroblastoma cell lines and a neuroblastoma tumour.* Nature, 1983. **305**(5931): p. 245-8.
62. Nau, M.M., et al., *L-myc, a new myc-related gene amplified and expressed in human small cell lung cancer.* Nature, 1985. **318**(6041): p. 69-73.
63. Kohl, N.E., et al., *Transposition and amplification of oncogene-related sequences in human neuroblastomas.* Cell, 1983. **35**(2 Pt 1): p. 359-67.
64. Oster, S.K., et al., *The myc oncogene: Marvelously Complex.* Adv Cancer Res, 2002. **84**: p. 81-154.
65. Pelengaris, S., M. Khan, and G.I. Evan, *Suppression of Myc-induced apoptosis in beta cells exposes multiple oncogenic properties of Myc and triggers carcinogenic progression.* Cell, 2002. **109**(3): p. 321-34.
66. Eilers, M., S. Schirm, and J.M. Bishop, *The MYC protein activates transcription of the alpha-prothymosin gene.* Embo J, 1991. **10**(1): p. 133-41.
67. Freytag, S.O. and T.J. Geddes, *Reciprocal regulation of adipogenesis by Myc and C/EBP alpha.* Science, 1992. **256**(5055): p. 379-82.
68. Iritani, B.M. and R.N. Eisenman, *c-Myc enhances protein synthesis and cell size during B lymphocyte development.* Proc Natl Acad Sci U S A, 1999. **96**(23): p. 13180-5.
69. Johnston, L.A., et al., *Drosophila myc regulates cellular growth during development.* Cell, 1999. **98**(6): p. 779-90.

70. Baudino, T.A., et al., *c-Myc is essential for vasculogenesis and angiogenesis during development and tumor progression*. Genes Dev, 2002. **16**(19): p. 2530-43.
71. Arnold, I. and F.M. Watt, *c-Myc activation in transgenic mouse epidermis results in mobilization of stem cells and differentiation of their progeny*. Curr Biol, 2001. **11**(8): p. 558-68.
72. Frye, M., et al., *Evidence that Myc activation depletes the epidermal stem cell compartment by modulating adhesive interactions with the local microenvironment*. Development, 2003. **130**(12): p. 2793-808.
73. Felsher, D.W. and J.M. Bishop, *Transient excess of MYC activity can elicit genomic instability and tumorigenesis*. Proc Natl Acad Sci U S A, 1999. **96**(7): p. 3940-4.
74. Raffeld, M., et al., *Clustered mutations in the transcriptional activation domain of Myc in 8q24 translocated lymphomas and their functional consequences*. Curr Top Microbiol Immunol, 1995. **194**: p. 265-72.
75. Bahram, F., et al., *c-Myc hot spot mutations in lymphomas result in inefficient ubiquitination and decreased proteasome-mediated turnover*. Blood, 2000. **95**(6): p. 2104-10.
76. Frykberg, L., T. Graf, and B. Vennstrom, *The transforming activity of the chicken c-myc gene can be potentiated by mutations*. Oncogene, 1987. **1**(4): p. 415-22.
77. Papas, T.S. and J.A. Lautenberger, *Sequence curiosity in v-myc oncogene*. Nature, 1985. **318**(6043): p. 237.
78. Chou, T.Y., G.W. Hart, and C.V. Dang, *c-Myc is glycosylated at threonine 58, a known phosphorylation site and a mutational hot spot in lymphomas*. J Biol Chem, 1995. **270**(32): p. 18961-5.
79. Albert, T., et al., *Ongoing mutations in the N-terminal domain of c-Myc affect transactivation in Burkitt's lymphoma cell lines*. Oncogene, 1984. **9**: p. 759 - 763.
80. Kawagoe, H., et al., *Overexpression of N-Myc rapidly causes acute myeloid leukemia in mice*. Cancer Res, 2007. **67**(22): p. 10677-85.
81. Grandori, C., et al., *The Myc/Max/Mad network and the transcriptional control of cell behavior*. Annu Rev Cell Dev Biol, 2000. **16**: p. 653-99.
82. Henriksson, M. and B. Luscher, *Proteins of the Myc network: essential regulators of cell growth and differentiation*. Adv Cancer Res, 1996. **68**: p. 109-82.
83. Hurlin, P.J., C. Queva, and R.N. Eisenman, *Mnt: a novel Max-interacting protein and Myc antagonist*. Curr Top Microbiol Immunol, 1997. **224**: p. 115-21.
84. Hurlin, P.J., et al., *Mga, a dual-specificity transcription factor that interacts with Max and contains a T-domain DNA-binding motif*. Embo J, 1999. **18**(24): p. 7019-28.
85. Knoepfler, P.S. and R.N. Eisenman, *Sin meets NuRD and other tails of repression*. Cell, 1999. **99**(5): p. 447-50.
86. Kiermaier, A. and M. Eilers, *Transcriptional control: calling in histone deacetylase*. Curr Biol, 1997. **7**(8): p. R505-7.
87. Schreiber-Agus, N. and R.A. DePinho, *Repression by the Mad(Mxi1)-Sin3 complex*. Bioessays, 1998. **20**(10): p. 808-18.
88. Billin, A.N., et al., *Mlx, a novel Max-like BHLHZip protein that interacts with the Max network of transcription factors*. J Biol Chem, 1999. **274**(51): p. 36344-50.
89. Meroni, G., et al., *Mlx, a new Max-like bHLHZip family member: the center stage of a novel transcription factors regulatory pathway?* Oncogene, 2000. **19**(29): p. 3266-77.
90. Billin, A.N., et al., *MondoA, a novel basic helix-loop-helix-leucine zipper transcriptional activator that constitutes a positive branch of a max-like network*. Mol Cell Biol, 2000. **20**(23): p. 8845-54.
91. Cairo, S., et al., *WBSCR14, a gene mapping to the Williams--Beuren syndrome deleted region, is a new member of the Mlx transcription factor network*. Hum Mol Genet, 2001. **10**(6): p. 617-27.
92. Blackwell, T.K., et al., *Sequence-specific DNA binding by the c-Myc protein*. Science, 1990. **250**(4984): p. 1149-51.
93. Blackwell, T.K., et al., *Binding of myc proteins to canonical and noncanonical DNA sequences*. Mol Cell Biol, 1993. **13**(9): p. 5216-24.
94. McMahon, S.B., et al., *The novel ATM-related protein TRRAP is an essential cofactor for the c-Myc and E2F oncoproteins*. Cell, 1998. **94**(3): p. 363-74.
95. Bouchard, C., et al., *Regulation of cyclin D2 gene expression by the Myc/Max/Mad network: Myc-dependent TRRAP recruitment and histone acetylation at the cyclin D2 promoter*. Genes Dev, 2001. **15**(16): p. 2042-7.
96. Frank, S.R., et al., *Binding of c-Myc to chromatin mediates mitogen-induced acetylation of histone H4 and gene activation*. Genes Dev, 2001. **15**(16): p. 2069-82.
97. Kusch, T., et al., *Acetylation by Tip60 is required for selective histone variant exchange at DNA lesions*. Science, 2004. **306**(5704): p. 2084-7.
98. Kobor, M.S., et al., *A protein complex containing the conserved Swi2/Snf2-related ATPase Swr1p deposits histone variant H2A.Z into euchromatin*. PLoS Biol, 2004. **2**(5): p. E131.
99. Herold, S., et al., *Negative regulation of the mammalian UV response by Myc through association with Miz-1*. Mol Cell, 2002. **10**(3): p. 509-21.
100. Mao, D.Y., et al., *Analysis of Myc bound loci identified by CpG island arrays shows that Max is essential for Myc-dependent repression*. Curr Biol, 2003. **13**(10): p. 882-6.
101. Peukert, K., et al., *An alternative pathway for gene regulation by Myc*. Embo J, 1997. **16**(18): p. 5672-86.
102. Staller, P., et al., *Repression of p15INK4b expression by Myc through association with Miz-1*. Nat Cell Biol, 2001. **3**(4): p. 392-9.
103. Seoane, J., et al., *TGFbeta influences Myc, Miz-1 and Smad to control the CDK inhibitor p15INK4b*. Nat Cell Biol, 2001. **3**(4): p. 400-8.
104. Seoane, J., H.V. Le, and J. Massague, *Myc suppression of the p21(Cip1) Cdk inhibitor influences the outcome of the p53 response to DNA damage*. Nature, 2002. **419**(6908): p. 729-34.
105. Barsyte-Lovejoy, D., D.Y. Mao, and L.Z. Penn, *c-Myc represses the proximal promoters of GADD45a and GADD153 by a post-RNA polymerase II recruitment mechanism*. Oncogene, 2004. **23**(19): p. 3481-6.

106. Gartel, A.L., et al., *Myc represses the p21(WAF1/CIP1) promoter and interacts with Sp1/Sp3*. Proc Natl Acad Sci U S A, 2001. **98**(8): p. 4510-5.
107. Izumi, H., et al., *Mechanism for the transcriptional repression by c-Myc on PDGF beta-receptor*. J Cell Sci, 2001. **114**(Pt 8): p. 1533-44.
108. Roy, A.L., et al., *Direct role for Myc in transcription initiation mediated by interactions with TFII-I*. Nature, 1993. **365**(6444): p. 359-61.
109. Shrivastava, A., et al., *Inhibition of transcriptional regulator Yin-Yang-1 by association with c-Myc*. Science, 1993. **262**(5141): p. 1889-92.
110. Qi, Y., et al., *p19ARF directly and differentially controls the functions of c-Myc independently of p53*. Nature, 2004. **431**(7009): p. 712-7.
111. Datta, A., et al., *Myc-ARF (alternate reading frame) interaction inhibits the functions of Myc*. J Biol Chem, 2004. **279**(35): p. 36698-707.
112. Vervoorts, J., et al., *Stimulation of c-MYC transcriptional activity and acetylation by recruitment of the cofactor CBP*. EMBO Rep, 2003. **4**(5): p. 484-90.
113. Brenner, C., et al., *Myc represses transcription through recruitment of DNA methyltransferase corepressor*. Embo J, 2005. **24**(2): p. 336-46.
114. Knoepfler, P.S., P.F. Cheng, and R.N. Eisenman, *N-myc is essential during neurogenesis for the rapid expansion of progenitor cell populations and the inhibition of neuronal differentiation*. Genes Dev, 2002. **16**(20): p. 2699-712.
115. Kenney, A.M., M.D. Cole, and D.H. Rowitch, *Nmyc upregulation by sonic hedgehog signaling promotes proliferation in developing cerebellar granule neuron precursors*. Development, 2003. **130**(1): p. 15-28.
116. Warner, B.J., et al., *Myc downregulation by transforming growth factor beta required for activation of the p15(Ink4b) G(1) arrest pathway*. Mol Cell Biol, 1999. **19**(9): p. 5913-22.
117. Shim, H., et al., *c-Myc transactivation of LDH-A: implications for tumor metabolism and growth*. Proc Natl Acad Sci U S A, 1997. **94**(13): p. 6658-63.
118. Dang, C.V., *c-Myc target genes involved in cell growth, apoptosis, and metabolism*. Mol Cell Biol, 1999. **19**(1): p. 1-11.
119. Semenza, G.L., et al., *'The metabolism of tumours': 70 years later*. Novartis Found Symp, 2001. **240**: p. 251-60; discussion 260-4.
120. Bowen, H., et al., *c-Myc represses and Miz-1 activates the murine natural resistance-associated protein 1 promoter*. J Biol Chem, 2002. **277**(38): p. 34997-5006.
121. Wu, K.J., A. Polack, and R. Dalla-Favera, *Coordinated regulation of iron-controlling genes, H-ferritin and IRP2, by c-MYC*. Science, 1999. **283**(5402): p. 676-9.
122. Nikiforov, M.A., et al., *A functional screen for Myc-responsive genes reveals serine hydroxymethyltransferase, a major source of the one-carbon unit for cell metabolism*. Mol Cell Biol, 2002. **22**(16): p. 5793-800.
123. Boon, K., et al., *N-myc enhances the expression of a large set of genes functioning in ribosome biogenesis and protein synthesis*. Embo J, 2001. **20**(6): p. 1383-93.
124. Rosenwald, I.B., et al., *Increased expression of eukaryotic translation initiation factors eIF-4E and eIF-2 alpha in response to growth induction by c-myc*. Proc Natl Acad Sci U S A, 1993. **90**(13): p. 6175-8.
125. Greasley, P.J., C. Bonnard, and B. Amati, *Myc induces the nucleolin and BN51 genes: possible implications in ribosome biogenesis*. Nucleic Acids Res, 2000. **28**(2): p. 446-53.
126. Menssen, A. and H. Hermeking, *Characterization of the c-MYC-regulated transcriptome by SAGE: identification and analysis of c-MYC target genes*. Proc Natl Acad Sci U S A, 2002. **99**(9): p. 6274-9.
127. Grewal, S.S., et al., *Myc-dependent regulation of ribosomal RNA synthesis during Drosophila development*. Nat Cell Biol, 2005. **7**(3): p. 295-302.
128. Grandori, C., et al., *c-Myc binds to human ribosomal DNA and stimulates transcription of rRNA genes by RNA polymerase I*. Nat Cell Biol, 2005. **7**(3): p. 311-8.
129. Arabi, A., et al., *c-Myc associates with ribosomal DNA and activates RNA polymerase I transcription*. Nat Cell Biol, 2005. **7**(3): p. 303-10.
130. Adhikary, S. and M. Eilers, *Transcriptional regulation and transformation by Myc proteins*. Nature Reviews Molecular Cell Biology, 2005. **6**(8): p. 635-45.
131. Land, H., L.F. Parada, and R.A. Weinberg, *Tumorigenic conversion of primary embryo fibroblasts requires at least two cooperating oncogenes*. Nature, 1983. **304**(5927): p. 596-602.
132. Drayton, S., et al., *Tumor suppressor p16INK4a determines sensitivity of human cells to transformation by cooperating cellular oncogenes*. Cancer Cell, 2003. **4**(4): p. 301-10.
133. Wei, W., et al., *Abolition of cyclin-dependent kinase inhibitor p16Ink4a and p21Cip1/Waf1 functions permits Ras-induced anchorage-independent growth in telomerase-immortalized human fibroblasts*. Mol Cell Biol, 2003. **23**(8): p. 2859-70.
134. Sears, R., et al., *Multiple Ras-dependent phosphorylation pathways regulate Myc protein stability*. Genes Dev, 2000. **14**(19): p. 2501-14.
135. Yeh, E., et al., *A signalling pathway controlling c-Myc degradation that impacts oncogenic transformation of human cells*. Nat Cell Biol, 2004. **6**(4): p. 308-18.
136. Gregory, M.A., Y. Qi, and S.R. Hann, *Phosphorylation by glycogen synthase kinase-3 controls c-myc proteolysis and subnuclear localization*. J Biol Chem, 2003. **278**(51): p. 51606-12.
137. Bouchard, C., et al., *Myc-induced proliferation and transformation require Akt-mediated phosphorylation of FoxO proteins*. Embo J, 2004. **23**(14): p. 2830-40.
138. Wanzel, M., et al., *Akt and I4-3-3eta regulate Miz1 to control cell-cycle arrest after DNA damage*. Nat Cell Biol, 2005. **7**(1): p. 30-41.

139. Watnick, R.S., et al., *Ras modulates Myc activity to repress thrombospondin-1 expression and increase tumor angiogenesis*. *Cancer Cell*, 2003. **3**(3): p. 219-31.
140. Nair, S.K. and S.K. Burley, *X-ray structures of Myc-Max and Mad-Max recognizing DNA. Molecular bases of regulation by proto-oncogenic transcription factors*. *Cell*, 2003. **112**(2): p. 193-205.
141. Fieber, W., et al., *Structure, function, and dynamics of the dimerization and DNA-binding domain of oncogenic transcription factor v-Myc*. *J Mol Biol*, 2001. **307**(5): p. 1395-410.
142. Brownlie, P., et al., *The crystal structure of an intact human Max-DNA complex: new insights into mechanisms of transcriptional control*. *Structure*, 1997. **5**(4): p. 509-20.
143. Saiz, L. and J.M. Vilar, *DNA looping: the consequences and its control*. *Curr Opin Struct Biol*, 2006. **16**(3): p. 344-50.
144. Facchini, L.M. and L.Z. Penn, *The molecular role of Myc in growth and transformation: recent discoveries lead to new insights*. *Faseb J*, 1998. **12**(9): p. 633-51.
145. Fladvad, M., et al., *N and C-terminal sub-regions in the c-Myc transactivation region and their joint role in creating versatility in folding and binding*. *J Mol Biol*, 2005. **346**(1): p. 175-89.
146. Herbst, A., et al., *Multiple cell-type-specific elements regulate Myc protein stability*. *Oncogene*, 2004. **23**(21): p. 3863-71.
147. Herbst, A., et al., *A conserved element in Myc that negatively regulates its proapoptotic activity*. *EMBO Rep*, 2005. **6**(2): p. 177-83.
148. Kato, G.J., et al., *An amino-terminal c-myc domain required for neoplastic transformation activates transcription*. *Mol Cell Biol*, 1990. **10**(11): p. 5914-20.
149. McEwan, I.J., et al., *Functional interaction of the c-Myc transactivation domain with the TATA binding protein: evidence for an induced fit model of transactivation domain folding*. *Biochemistry*, 1996. **35**(29): p. 9584-93.
150. Hermann, S., K.D. Berndt, and A.P. Wright, *How transcriptional activators bind target proteins*. *J Biol Chem*, 2001. **276**(43): p. 40127-32.
151. Burton, R.A., et al., *B-myc: N-terminal recognition of myc binding proteins*. *Biochemistry*, 2006. **45**(32): p. 9857-65.
152. Juo, Z.S., et al., *How proteins recognize the TATA box*. *J Mol Biol*, 1996. **261**(2): p. 239-54.
153. Mori, K., et al., *MM-1, a novel c-Myc-associating protein that represses transcriptional activity of c-Myc*. *J Biol Chem*, 1998. **273**(45): p. 29794-800.
154. Dyson, H.J. and P.E. Wright, *Intrinsically unstructured proteins and their functions*. *Nat Rev Mol Cell Biol*, 2005. **6**(3): p. 197-208.
155. Tompa, P., *Intrinsically unstructured proteins*. *Trends Biochem Sci*, 2002. **27**(10): p. 527-33.
156. Uversky, V.N., *Natively unfolded proteins: a point where biology waits for physics*. *Protein Sci*, 2002. **11**(4): p. 739-56.
157. Uversky, V.N., J.R. Gillespie, and A.L. Fink, *Why are "natively unfolded" proteins unstructured under physiologic conditions?* *Proteins*, 2000. **41**(3): p. 415-27.
158. Epand, R.M., et al., *Cholesterol-dependent partitioning of PtdIns(4,5)P2 into membrane domains by the N-terminal fragment of NAP-22 (neuronal axonal myristoylated membrane protein of 22 kDa)*. *Biochem J*, 2004. **379**(Pt 3): p. 527-32.
159. Korshunova, I., et al., *Characterization of BASP1-mediated neurite outgrowth*. *J Neurosci Res*, 2008. **86**(10): p. 2201-13.
160. Shaw, J.E., et al., *Tracking peptide-membrane interactions: insights from in situ coupled confocal-atomic force microscopy imaging of NAP-22 peptide insertion and assembly*. *J Struct Biol*, 2006. **155**(3): p. 458-69.
161. Carpenter, B., et al., *BASP1 is a transcriptional cosuppressor for the Wilms' tumor suppressor protein WT1*. *Mol Cell Biol*, 2004. **24**(2): p. 537-49.
162. Ohsawa, S., et al., *Novel antibody to human BASP1 labels apoptotic cells post-caspase activation*. *Biochem Biophys Res Commun*, 2008. **371**(4): p. 639-43.
163. Widmer, F. and P. Caroni, *Identification, localization, and primary structure of CAP-23, a particle-bound cytosolic protein of early development*. *J Cell Biol*, 1990. **111**(6 Pt 2): p. 3035-47.
164. Maekawa, S., et al., *Purification and molecular cloning of a novel acidic calmodulin binding protein from rat brain*. *J Biol Chem*, 1993. **268**(18): p. 13703-9.
165. Mosevitsky, M.I., et al., *Neuronal protein GAP-43 is a member of novel group of brain acid-soluble proteins (BASP)s*. *Neurosci Res*, 1994. **19**(2): p. 223-8.
166. Mosevitsky, M.I., et al., *The BASP1 family of myristoylated proteins abundant in axonal termini. Primary structure analysis and physico-chemical properties*. *Biochimie*, 1997. **79**(6): p. 373-84.
167. Maekawa, S., H. Murofushi, and S. Nakamura, *Inhibitory effect of calmodulin on phosphorylation of NAP-22 with protein kinase C*. *J Biol Chem*, 1994. **269**(30): p. 19462-5.
168. Takasaki, A., et al., *Identification of the calmodulin-binding domain of neuron-specific protein kinase C substrate protein CAP-22/NAP-22. Direct involvement of protein myristoylation in calmodulin-target protein interaction*. *J Biol Chem*, 1999. **274**(17): p. 11848-53.
169. Matsubara, M., et al., *Crystal structure of a myristoylated CAP-23/NAP-22 N-terminal domain complexed with Ca²⁺/calmodulin*. *Embo J*, 2004. **23**(4): p. 712-8.
170. Zakharov, V.V., et al., *Natural N-terminal fragments of brain abundant myristoylated protein BASP1*. *Biochim Biophys Acta*, 2003. **1622**(1): p. 14-9.
171. Golub, T., S. Wacha, and P. Caroni, *Spatial and temporal control of signaling through lipid rafts*. *Curr Opin Neurobiol*, 2004. **14**(5): p. 542-50.
172. Janmey, P.A. and U. Lindberg, *Cytoskeletal regulation: rich in lipids*. *Nat Rev Mol Cell Biol*, 2004. **5**(8): p. 658-66.

173. Sakisaka, T., et al., *Phosphatidylinositol 4,5-bisphosphate phosphatase regulates the rearrangement of actin filaments*. Mol Cell Biol, 1997. **17**(7): p. 3841-9.
174. Shibasaki, Y., et al., *Massive actin polymerization induced by phosphatidylinositol-4-phosphate 5-kinase in vivo*. J Biol Chem, 1997. **272**(12): p. 7578-81.
175. Hanahan, D., *Studies on transformation of Escherichia coli with plasmids*. J Mol Biol, 1983. **166**(4): p. 557-80.
176. Waugh, D.S. *TEV Protease FAQ*. [cited; Available from: http://mc11.ncifcrf.gov/waugh_tech/faq/tev.pdf].
177. Laemmli, U.K., *Cleavage of structural proteins during the assembly of the head of bacteriophage T4*. Nature, 1970. **227**(5259): p. 680-5.
178. Ornstein, L., *Disc Electrophoresis. I. Background and Theory*. Ann N Y Acad Sci, 1964. **121**: p. 321-49.
179. Davis, B.J., *Disc Electrophoresis. II. Method and Application to Human Serum Proteins*. Ann N Y Acad Sci, 1964. **121**: p. 404-27.
180. Faiola, F., et al., *Dual regulation of c-Myc by p300 via acetylation-dependent control of Myc protein turnover and coactivation of Myc-induced transcription*, in Mol Cell Biol. 2005. p. 10220-34.
181. Zhang, K., F. Faiola, and E. Martinez, *Six lysine residues on c-Myc are direct substrates for acetylation by p300*. Biochem Biophys Res Commun, 2005. **336**(1): p. 274-80.
182. Luscher, B., et al., *Myc oncoproteins are phosphorylated by casein kinase II*. Embo J, 1989. **8**(4): p. 1111-9.
183. Huang, Z., J.A. Traugh, and J.M. Bishop, *Negative control of the Myc protein by the stress-responsive kinase Pak2*. Mol Cell Biol, 2004. **24**(4): p. 1582-94.
184. Salghetti, S.E., S.Y. Kim, and W.P. Tansey, *Destruction of Myc by ubiquitin-mediated proteolysis: cancer-associated and transforming mutations stabilize Myc*. Embo J, 1999. **18**(3): p. 717-26.
185. Flinn, E.M., C.M. Busch, and A.P. Wright, *myc boxes, which are conserved in myc family proteins, are signals for protein degradation via the proteasome*. Mol Cell Biol, 1998. **18**(10): p. 5961-9.
186. Eberhardy, S.R. and P.J. Farnham, *Myc recruits P-TEFb to mediate the final step in the transcriptional activation of the cad promoter*. J Biol Chem, 2002. **277**(42): p. 40156-62.
187. Rauscher, F.J., 3rd, *Tumor suppressor genes which encode transcriptional repressors: studies on the EGR and Wilms' tumor (WT1) gene products*. Adv Exp Med Biol, 1993. **348**: p. 23-9.
188. Nakagama, H., et al., *Sequence and structural requirements for high-affinity DNA binding by the WT1 gene product*. Mol Cell Biol, 1995. **15**(3): p. 1489-98.
189. Wang, Z.Y., et al., *A second transcriptionally active DNA-binding site for the Wilms tumor gene product, WT1*. Proc Natl Acad Sci U S A, 1993. **90**(19): p. 8896-900.
190. Li, R.S., et al., *Ornithine decarboxylase is a transcriptional target of tumor suppressor WT1*. Exp Cell Res, 1999. **247**(1): p. 257-66.
191. Loeb, D.M., et al., *Cyclin E is a target of WT1 transcriptional repression*. J Biol Chem, 2002. **277**(22): p. 19627-32.
192. Scharnhorst, V., A.J. van der Eb, and A.G. Jochemsen, *WT1 proteins: functions in growth and differentiation*. Gene, 2001. **273**(2): p. 141-61.
193. Nisen, P.D., et al., *Enhanced expression of the N-myc gene in Wilms' tumors*. Cancer Res, 1986. **46**(12 Pt 1): p. 6217-22.

„Ich habe mich bemüht, sämtliche Inhaber der Bildrechte ausfindig zu machen und ihre Zustimmung zur Verwendung der Bilder in dieser Arbeit eingeholt. Sollte dennoch eine Urheberrechtsverletzung bekannt werden, ersuche ich um Meldung bei mir.“

Curriculum Vitae

Name: Leonhard Geist

Adresse: Breiteneicherstr. 5 / 3250 Wieselburg

Geburtsdatum: 25.12.1981

Geburtsort: Wien

Staatsbürgerschaft: Österreich

1988-1992: Volksschule Wieselburg/Erlauf

1992-2000: Bundesrealgymnasium Wieselburg/Erlauf

2000-2001: Präsenzdienst: Sanitäter

2001-2008: Studium der Molekularen Biologie an der Universität Wien mit den Schwerpunktsfächern Strukturbiologie, Genetik und Molekulare Medizin.

Okt 2004-Juni 2005: Praktikum am Centre de Biologie du Développement an der Université Paul Sabatier in Toulouse (Frankreich) in der Gruppe von Marc Haenlin.